ADAPTIVE GROUND IMPLEMENTED PHASED ARRAY

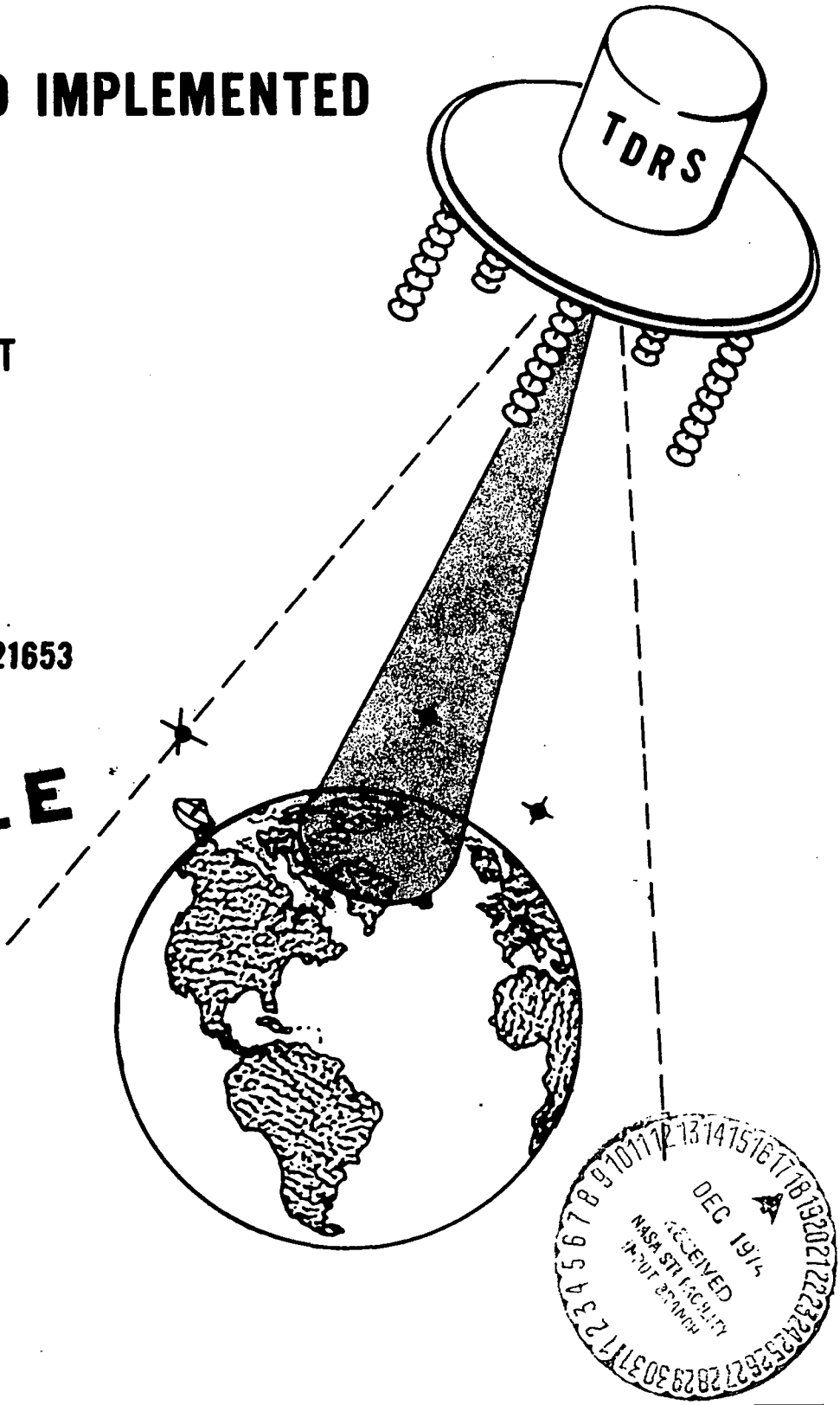

FINAL REPORT

February 1973
Contract No. NAS 5-21653

Prepared for
NATIONAL AERONAUTICS AND SPACE ADMINISTRATION
Goddard Space Flight Center
Greenbelt, Maryland

AIL a division of CUTLER-HAMMER
DEER PARK, LONG ISLAND, NEW YORK 11729

ADAPTIVE GROUND IMPLEMENTED PHASED ARRAY

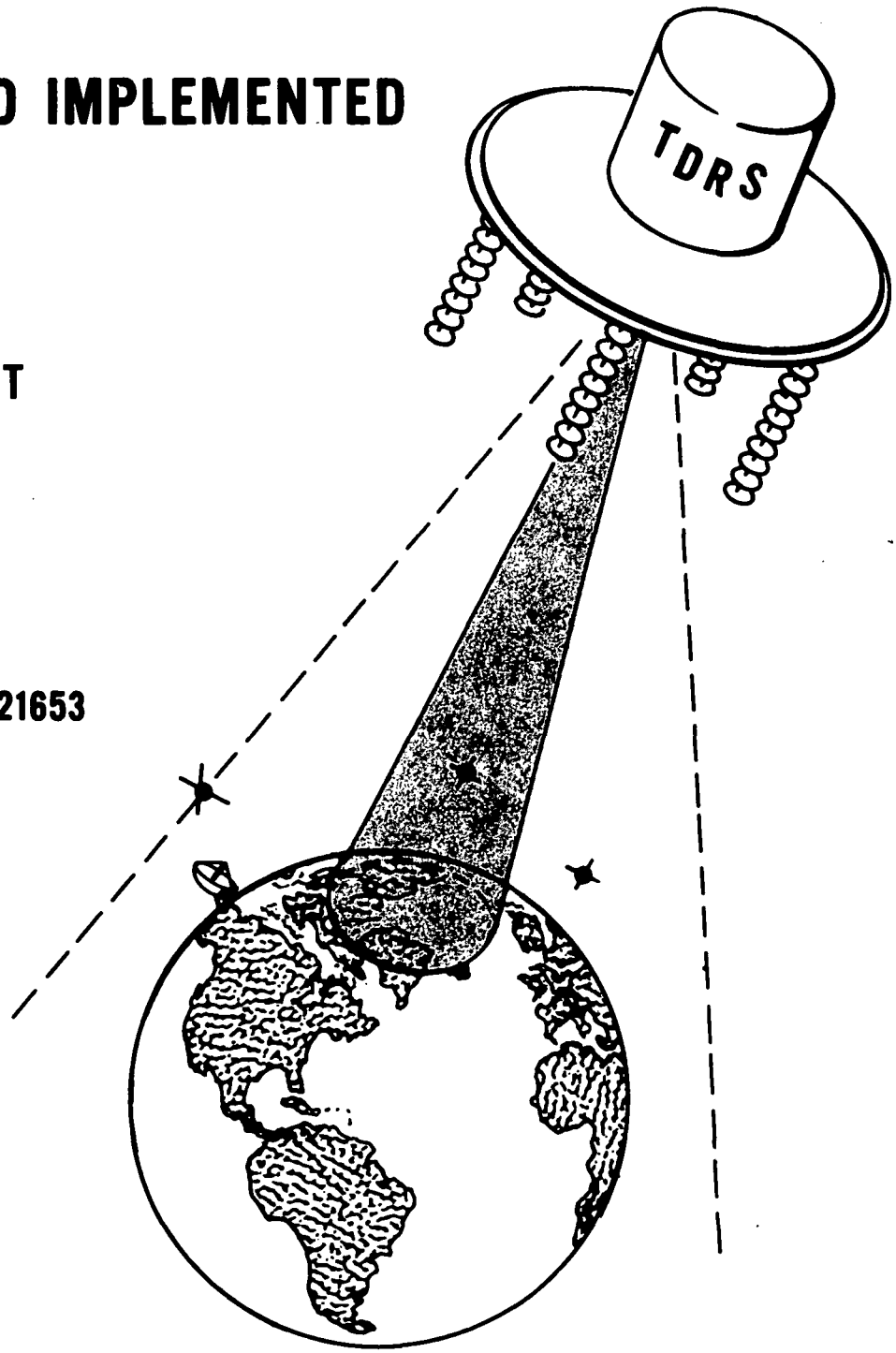

FINAL REPORT

February 1973
Contract No. NAS 5-21653

Prepared for
NATIONAL AERONAUTICS AND SPACE ADMINISTRATION
Goddard Space Flight Center
Greenbelt, Maryland

AIL a division of CUTLER-HAMMER
DEER PARK, LONG ISLAND, NEW YORK 11729

ABSTRACT

This is the final report of NASA Contract NAS 5-21653. It describes an Adaptive Ground Implemented Phased Array (AGIPA) feasibility demonstration model designed, developed, fabricated, and tested by AIL to confirm the ability of an adaptive array to overcome the limitations of the severely RFI limited low data rate TDRS VHF link.

In particular, the testing of the demonstration model adaptive array is described and compared against the alternative Fixed Field-of-View (F-FOV) system. The results of the tests tabulated in this report clearly show the advantages of the adaptive array system over that of the alternative F-FOV system.

NOTE

(September 1973)

In accordance with modification number two to NASA Contract Number NAS 5-21653, the results of the additional testing program have been included within this AGIPA final report as Appendix C.

PREFACE

This final report is being submitted to the National Aeronautics and Space Administration by AIL, a division of Cutler-Hammer as required under Contract NAS 5-21653. This report covers work performed between August 1971 and February 1973.

Report Prepared by: James M. Smith — J. M. Smith — 2/8/73 — Date

Report Approved by: L. Schwartz — L. Schwartz — 2/8/73 — Date

TABLE OF CONTENTS

LIST OF ILLUSTRATIONS

1.0 INTRODUCTION AND SUMMARY

This is the final report under NASA Contract NAS-5-21653. The primary purpose of this contract was to confirm the feasibility of employing an Adaptive Ground Implemented Phased Array (AGIPA) to overcome the limitations of the RFI limited low data rate TDRS VHF return link. Under the contract, a feasibility demonstration model of a single user channel AGIPA system was designed, developed, fabricated, and tested by AIL. By scaling the frequency and aperture geometry from VHF to S-band, the system performance was more easily demonstrated in the controlled environment of an anechoic chamber. The primary emphasis of this report is given to the performance recorded during a 4-month testing period of the AGIPA system. Previous reports on the hardware design[1] and forward link analyses[2] were performed as part of the overall study[3]. The 4-month testing program was designed to realistically evaluate the performance of a system which optimizes the signal-to-interference (S/I) ratio by employing both spatial filtering and polarization discrimination to enhance the desired signal as well as to combat undesired interference signals. The technique employs an AGIPA in which received signals from each element of the array are processed on the ground to form an adaptive, independent, computer controlled beam for each user.

---

[1] Design Analysis AGIPA, AIL, a division of Cutler-Hammer, Contract No. NAS-5-21653, November 1971.

[2] Design Analysis AGIPA Addendum, AIL, a division of Cutler-Hammer, Contract No. NAS-5-21653, November 1972.

[3] Test Procedure AGIPA, AIL, a division of Cutler-Hammer, Contract No. NAS-5-21653, June 1972.

A key objective of the test program was to compare the performance of the AGIPA system versus that of the alternative F-FOV antenna system in a controlled environment. Toward this end, a major portion of the 4 month test program was devoted to comparisons of the alternative F-FOV system versus AGIPA. All of the tests described in this report were conducted in a specially designed anechoic chamber constructed by AIL for the AGIPA test program.

The results of the test program show that the AGIPA system significantly and consistently outperforms the alternative F-FOV antenna system. In addition, the tests showed that performance predictions by the AIL computer simulations used to evaluate the AGIPA concept for TDRS[4] are within 1 to 2 dB of those obtained with the feasibility hardware.

The time expended by the feasibility demonstration model in achieving the optimum S/I ratio depends on the location of the signal and jammers relative to the initial beam location when acquisition commences. However, at no time during the 4-month test period did the acquisition time for any scenario ever require more than fractions of 1 minute.

Although no effort was expended by AIL during the span of this contract to reduce the time for the array to adapt to an optimum S/I ratio, there was a great deal of effort expended in decreasing the number of steps necessary to achieve this goal. The means of reducing step computation time itself is quite straightforward and is discussed in paragraph 3.1.6. The projected step computation time of 50 milliseconds is considered as operationally satisfactory for any possible environmental confrontation.

---

[4] Tracking and Data Relay Satellite System Configuration and Tradeoff Study, Part I Final Report, Vol III Telecommunication Service System, NAR for NASA/GSFC, NAS-5-21705, September 1972.

Although implementation of the steps necessary to decrease the computation time of the AGIPA array might conceivably be the next step to pursue in refining the array for its final deployment, it is believed that it would be more beneficial to the TDRS program to investigate unexplored areas, that could possibly affect the adaptive array's performance. Since the testing of the AGIPA feasibility model has been of such a highly favorable nature, it is recommended that future work in this area concern itself first with the problems associated with application of the concept of a ground implemented adaptive array, and second with those refinements considered necessary to the existing feasibility model. To help define the effects of the inevitable cross-channel interference of the proposed FDM-FM TDRS/GS link upon the AGIPA array performance, it is felt that such a link should be developed and tested in conjunction with the existing feasibility model. The development of this hardware and the hardware to both make acquisition of the pseudorandom coding and remove the effects of the anticipated Doppler, would help to define and specify, from a systems viewpoint, the entire AGIPA concept.

The remainder of this final report is divided into three major sections. Section 2.0 (System Description) discusses the basic implementation and major features of the AGIPA system as well as the test facility and methods employed to simulate the operational TDRS VHF environment. Included in this section are block diagrams, photographs, and descriptions of the AGIPA system, the simulated user, and the AGIPA test facility.

Section 3.0 (AGIPA System Test Results) describes and tabulates the testing of the AGIPA system. The individual features of the adaptive array and how they were evaluated as well as a description and the tabulation of the results of the parallel testing of the F-FOV antenna system and the AGIPA array are also included.

Section 4.0 specifies the minimum requirements of the TDRS to ground station link as well as the estimated per user cost and ground-based equipment size.

Two Appendixes are included to describe tradeoff analysis and the efficient use of minicomputers in conjunction with a multichannel (up to 40) AGIPA system.

2.0 SYSTEM DESCRIPTION

One of the more significant problems facing the designers of the Tracking and Data Relay Satellite (TDRS) is that of establishing consistently reliable VHF communications for the return link of the low data rate (LDR) user.

The VHF-band, because of its heavy worldwide usage presents the TDRS designers with a potentially interference (both unintentional RFI emitters as well as intentional in-band other user signals-referred to herein as RFI) limited spectrum which precludes normal means and methods of establishing communications. In the face of this expected high level of RFI, the TDRS requirements for the LDR link maintain that the relay satellite must establish reliable relay communications (error rates of 1×10^{-5} or better) for up to as many as 20 potential LDR users. To provide rejection of RFI and increase VHF antenna gain, AIL has developed a phased array concept which adapts a custom beam for each user, such that spatial filtering is employed to maintain the desired signal to RFI ratio at a maximum. The actual beam forming of this adaptive array system is implemented at the ground station, thus, minimizing the complexity of the on-board satellite system. An AGIPA can provide significant improvement in the quality of communications, where the normal means of establishing communications have not been effective against intentional or unintentional interference signals. The overall TDRS system employing the AGIPA concept for both the forward and return LDR links is shown in Figure 2-1.

Signals originating from up to as many as 20 low-altitude user satellites are received at the TDRS by the five-element VHF ring array. The signals received at the horizontal and vertical polarized output port of each element of the array are multiplexed and relayed to the ground station

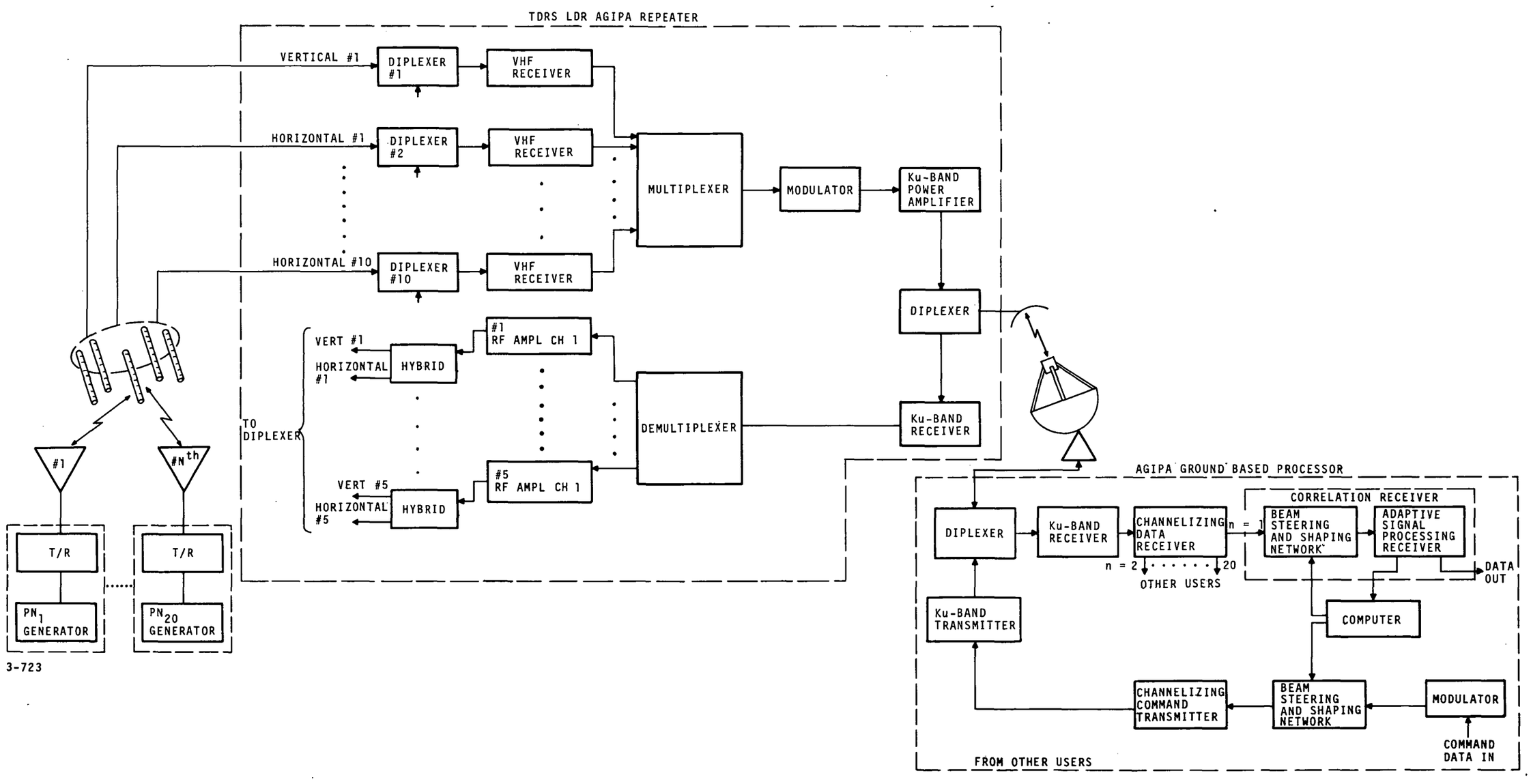

3-723

FIGURE 2-1. OVERALL AGIPA SYSTEM FOR TDRS NETWORK, BLOCK DIAGRAM

FIGURE 2-1

via a K_u-band transmission link. Thus, 10 individual channels, one for the vertical output and one for the horizontal output of each antenna element, are multiplexed and transmitted to the ground.

On the ground, the unique pseudorandom code assigned to each LDR user separates the different received signals into 20 channels, one for each user. The unique code for each channel also separates the desired signal from its cochannel interference. Thus, the contribution from each array element, in terms of both desired signal and interference, is made available for each user. This enables the computer controlled adaptive receiver to synthesize a custom beam which maximizes the S/I ratio for that channel.

Similarly, for the forward link, beam forming can be ground implemented as shown in Figure 2-1. The TDRS requires[5] two simultaneous forward link channels, each capable of transmitting either voice or 1 KBPS data. Previous study of the transmit problem[6] indicated that the requirement for only two channels makes the ground implemented versus satellite implemented beam steering a standoff in terms of on-board power and weight.

The hardware constructed to evaluate the feasibility of the AGIPA concept was directed toward an investigation of the receiving or return link segment of the system. This approach was used so that the adaptive portion of the system could be evaluated in a simulated RFI environment. The feasibility hardware is described in the following paragraph.

2.1 AGIPA FEASIBILITY MODEL

For the AGIPA feasibility demonstration program conducted by AIL, the single channel AGIPA system shown in Figure 2-2 was fabricated.

---

[5] TDRS Statement of Work, GSFC [the requirement for two simultaneous forward links was reduced to only one in the subsequent Part II phase of the TDRS study program (ibid 4)].

[6] AGIPA Design Analysis Addendum, NAS-5-21653, AIL for GSFC/NASA, November 1972.

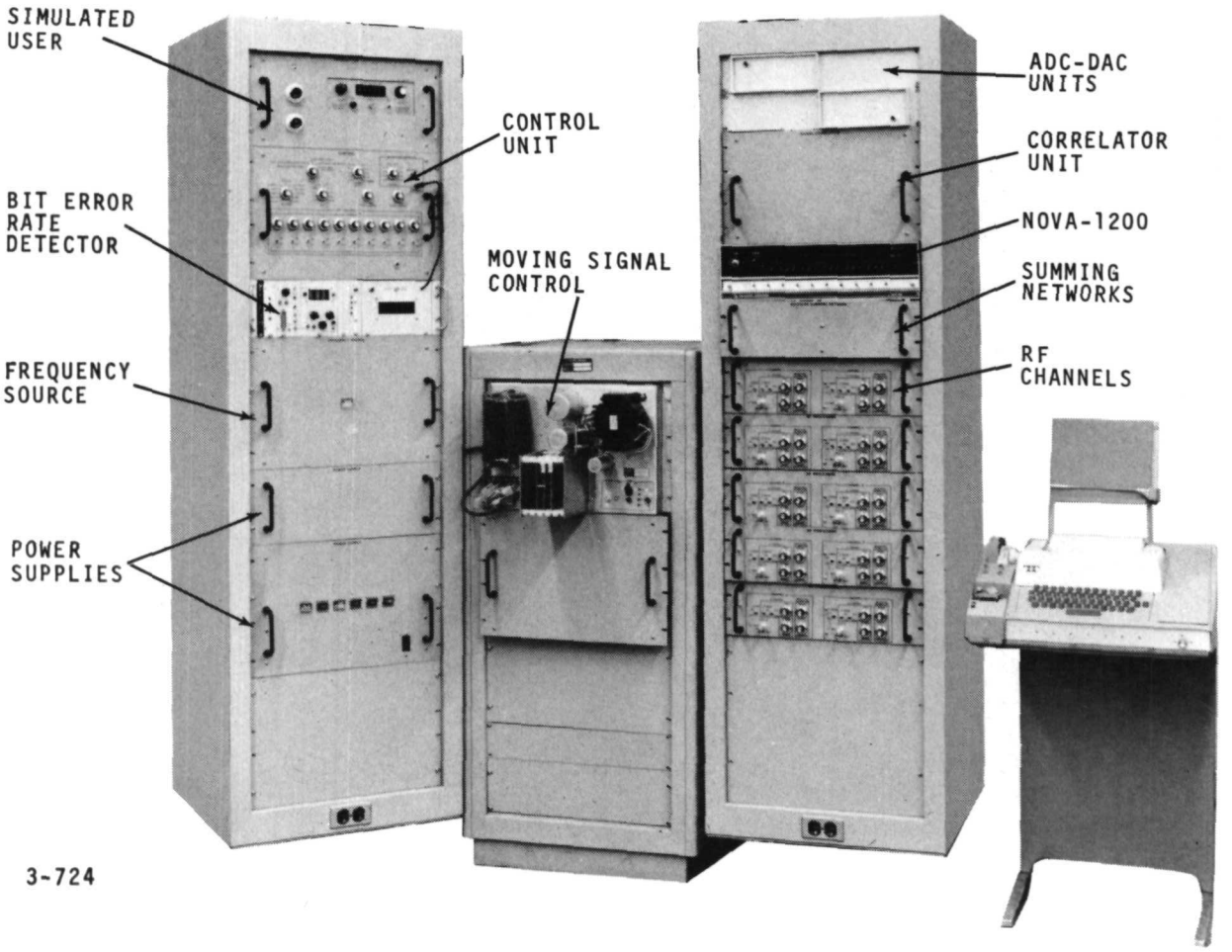

FIGURE 2-2. AGIPA FEASIBILITY SYSTEM

The system RF frequency was scaled from VHF to S-band to facilitate testing of the adaptive array within the controlled environment of an anechoic chamber. The K_u-band TDRS to ground station link was eliminated and direct interface (coaxial cable) between the array element outputs, both horizontal and vertical, and the adaptive processing receiver was made. A simplified block diagram of the AGIPA feasibility demonstration model is shown in Figure 2-3.

The 10 output, five-element array is in the upper left hand portion of the block diagram. The 10 outputs of the array are directed to 10 RF processing units, which include both the S-band receiver and the computer-controlled channel weighting network. Front panel and top view photographs of the two channel-per-drawer RF processing units are shown in Figures 2-4 and 2-5, respectively. The S-band unit, which converts the received 2298 MHz S-band signal to 137 MHz, as well as its companion 137 MHz IF amplifier, can be seen in Figure 2-5. The channel weighting network also is shown in one of the exposed RF processing drawers. The output of each S-band receiver, as well as being passed through its companion weighting network, is sampled sequentially by the correlator network. The portion of the S-band receiver output that continues through the channel weighting network is summed with the outputs of the remaining nine channels and applied to the correlator network. Prior to actual cross-correlation of the weighted summed output with the unweighted sampled outputs of the S-band receiver, the signal and its cochannel interference must be separated. Separation of these two components is accomplished by the matched set of signal band-pass and signal band reject filters in conjunction with the inputs to the two correlators (Figure 2-3). This method of separation is possible only after the unique pseudorandom code common to the user has been employed to simultaneously spread the undesired or RFI signals and despread or collapse the originally spread user signal to its data bandwidth. The accomplishment of this task is achieved through the use of a like reference code and a product detector.

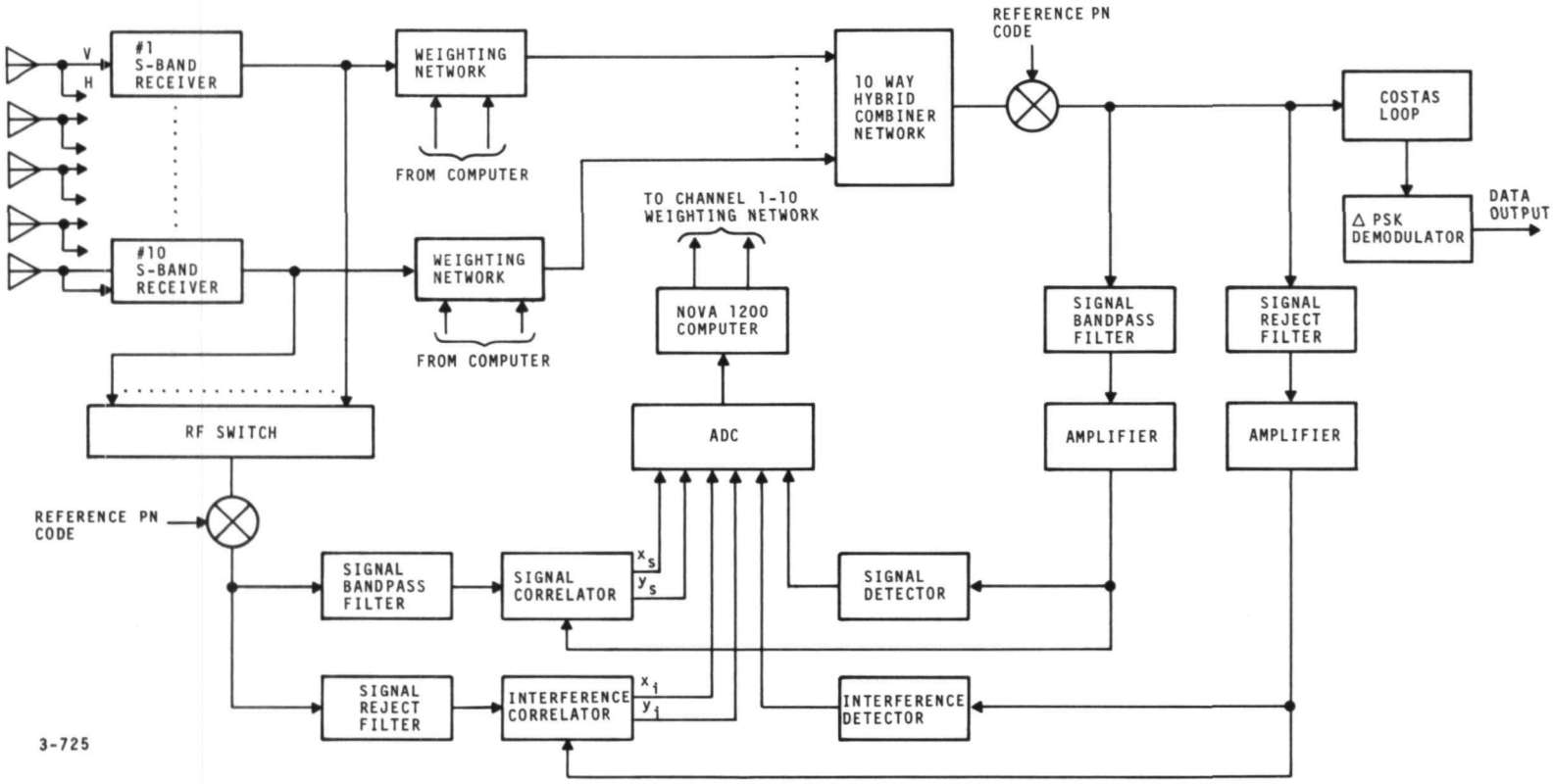

FIGURE 2-3. SIMPLIFIED AGIPA BLOCK DIAGRAM

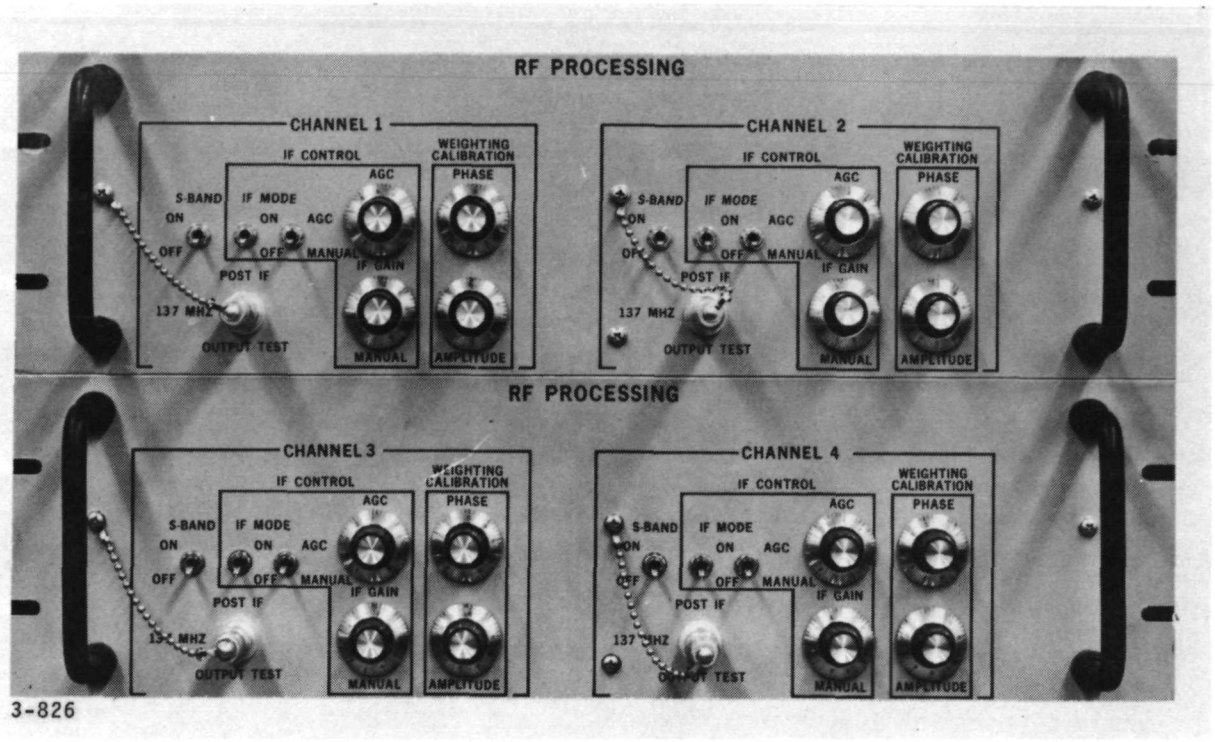

FIGURE 2-4. RF PROCESSING DRAWERS, FRONT PANEL

The four outputs of the two correlators the real and imaginary components of the two cross-correlation vectors along with the magnitude of the signal and interference components are fed to the computer through the system AD converter. Based on the value of these 42 inputs to the computer (that is, four each of the 10-array channels and the two detected signals) the algorithmic processing routine stored in the computer calculates a set of weights and directs the individual weighting network to change in a direction that improves the signal to interference ratio.

Figure 2-3 also shows the means by which the digital data is obtained from the system. At the output of the 10-way hybrid combiner, after the array output has been multiplied by the PN code, the Δ-PSK data is demodulated using a Costas loop. These units are contained in the Signal Correlation drawer shown in Figure 2-2.

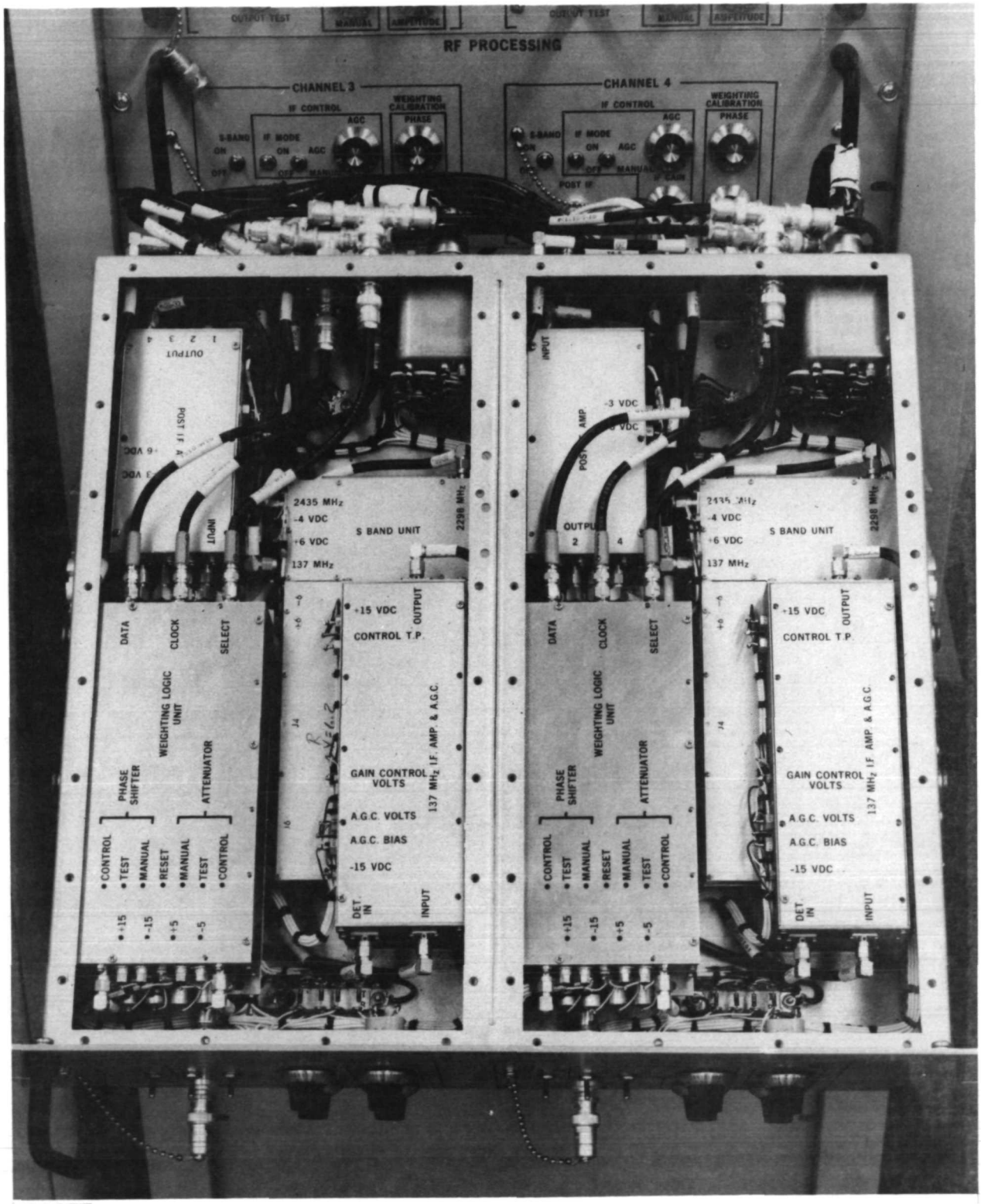

FIGURE 2-5. RF PROCESSING DRAWERS, TOP VIEW

The additional equipment shown in Figure 2-2 consists of RFI and user simulation equipment for the purpose of implementing the test function.

2.2 USER SIMULATION

The user signal, which in the case of the TDRS program is assumed to be a low altitude orbiting satellite, is simulated in the AGIPA test chamber by emissions from a cavity mounted dipole antenna. The antenna is affixed to a chain driven track and the linear movement of the antenna simulates the orbital path of the user satellite. The simulated user antenna is obtained from the transmitter unit shown in Figure 2-6. The transmitter unit encodes an artificial "data" stream, generated for test purposes, and employs the composite encoded signal to Δ-PSK modulate (0^{o}, 180^{o}) an S-band carrier for transmission. The encoding of the "data" by the transmitter is accomplished by means of a 2 Mb/s pseudorandom Gold code. The 1-kb/s artificial "data" stream is supplied by the bit error rate detector. The bit error rate detector shown in Figure 2-7 generates a 1-kb/s pseudorandom code of selectable length (63, 127, ..., 32767), and in conjunction with the Control Unit, "round-robins" the data through the system to measure AGIPA's performance.

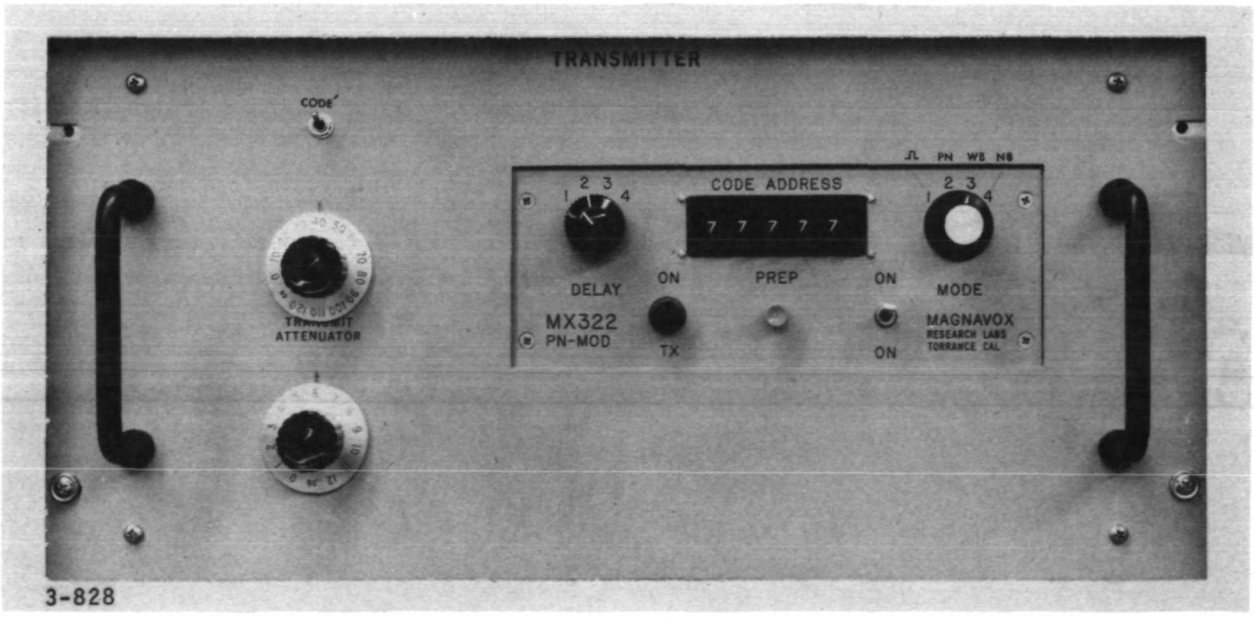

FIGURE 2-6. SIMULATED TRANSMITTER UNIT

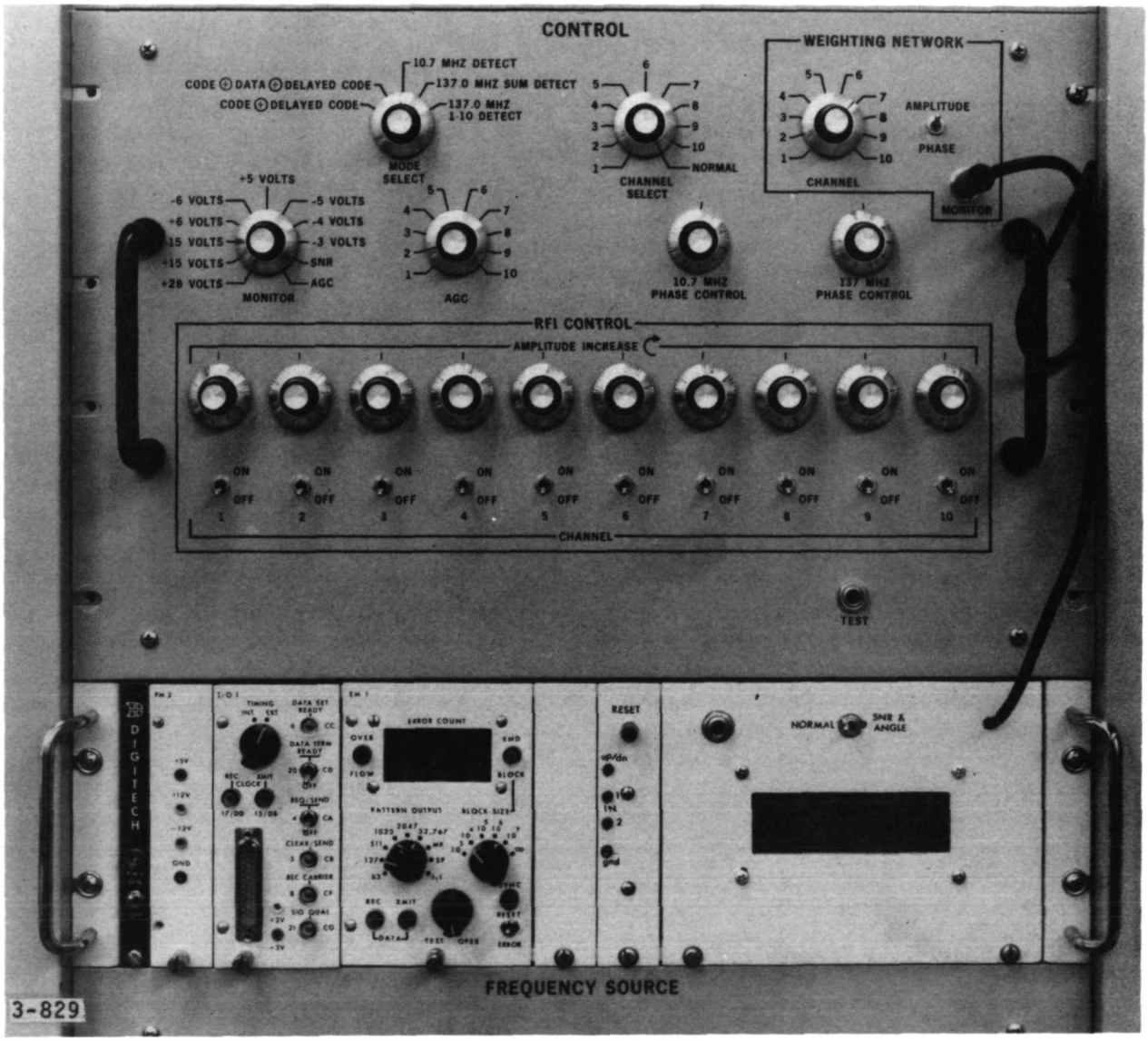

FIGURE 2-7. CONTROL AND BIT ERROR RATE DETECTOR

The performance of the AGIPA system is measured as a function of the improvement by the system in the error rate in the presence of multiple RFI jammers. The control unit controls both the activation and amplitude of the RFI jammers. The control unit also allows for the monitoring of system performance at various points in the AGIPA system.

2.3 TEST FACILITIES

The AGIPA test facilities at AIL's Deer Park, New York plant were constructed primarily to meet the needs of the AGIPA test program The test facilities center around a specially constructed 12 by 18 foot anechoic chamber. A cut away view of this test facility is depicted in Figure 2-8. The five element AGIPA array, representing the TDRS at synchronous orbit, is mounted at one end of the test chamber. A photograph of the AGIPA array installed in the chamber is shown in Figure 2-9. The test chamber wall opposite the AGIPA array mounts the simulated RFI and user source antennas. A photograph of the globe, scaled to the proper size for a synchronous orbit TDRS, is affixed to this wall to aid in simulating the actual environment. The user signal source (Figure 2-10) is mounted on a track built into the wall and can be moved ±16 degrees about boresight at speeds up to a maximum of 10 degrees per minute. The TDRS scenario requires that the signal source move at a rate of 1 degree per minute across a 31-degree field of view. These requirements are well within the above mentioned test facility capabilities.

Also note in Figure 2-10 that both the RFI and the signal sources have a dark strip marking on the face of their respective antennas. These antennas are linearly polarized and the dark strip identifies the polarization configuration of each RFI source with respect to the signal source. Varied polarization of the RFI or signal scenario is achieved by rotating the respective antennas.

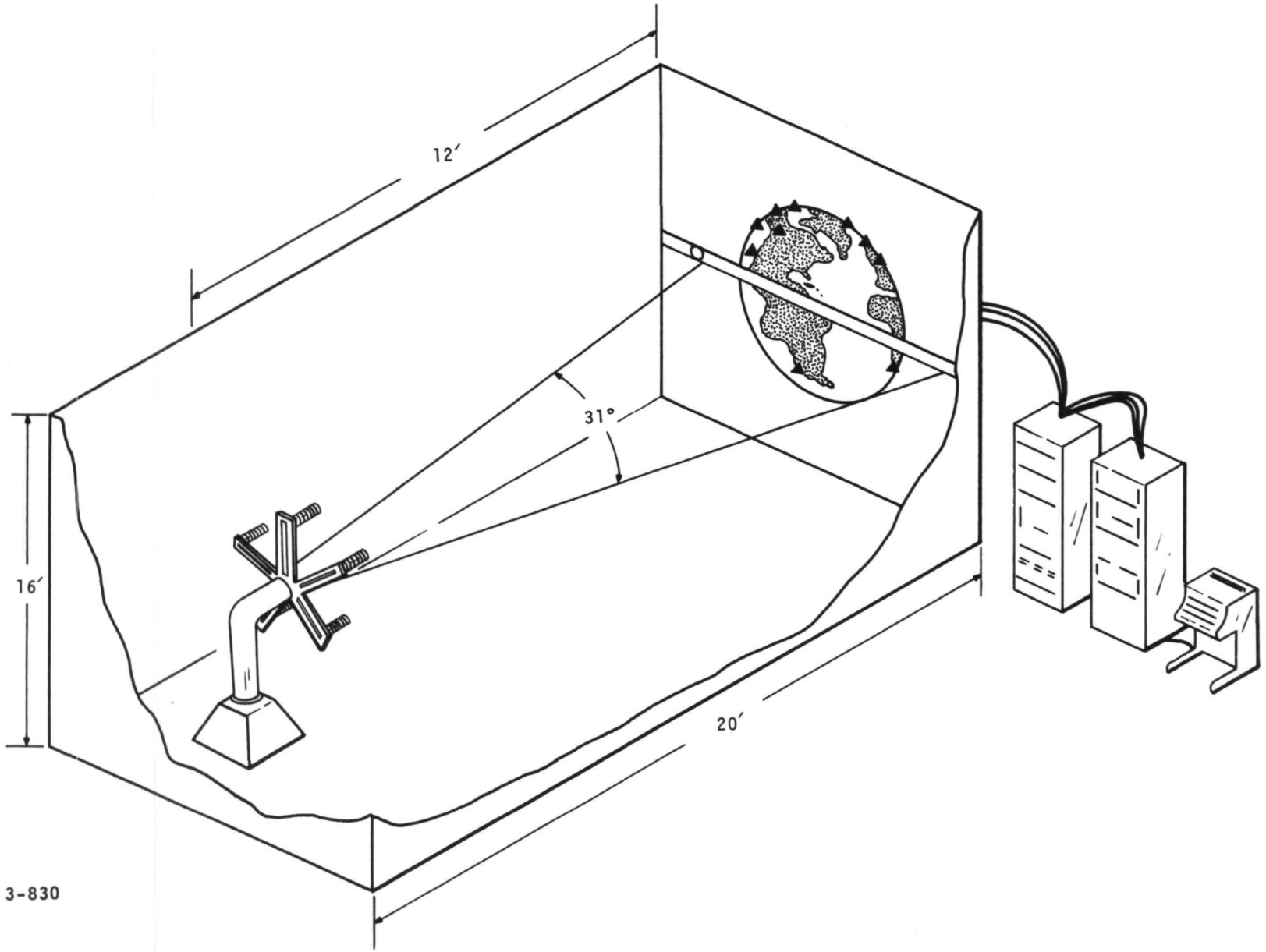

FIGURE 2-8. AGIPA TEST FACILITIES

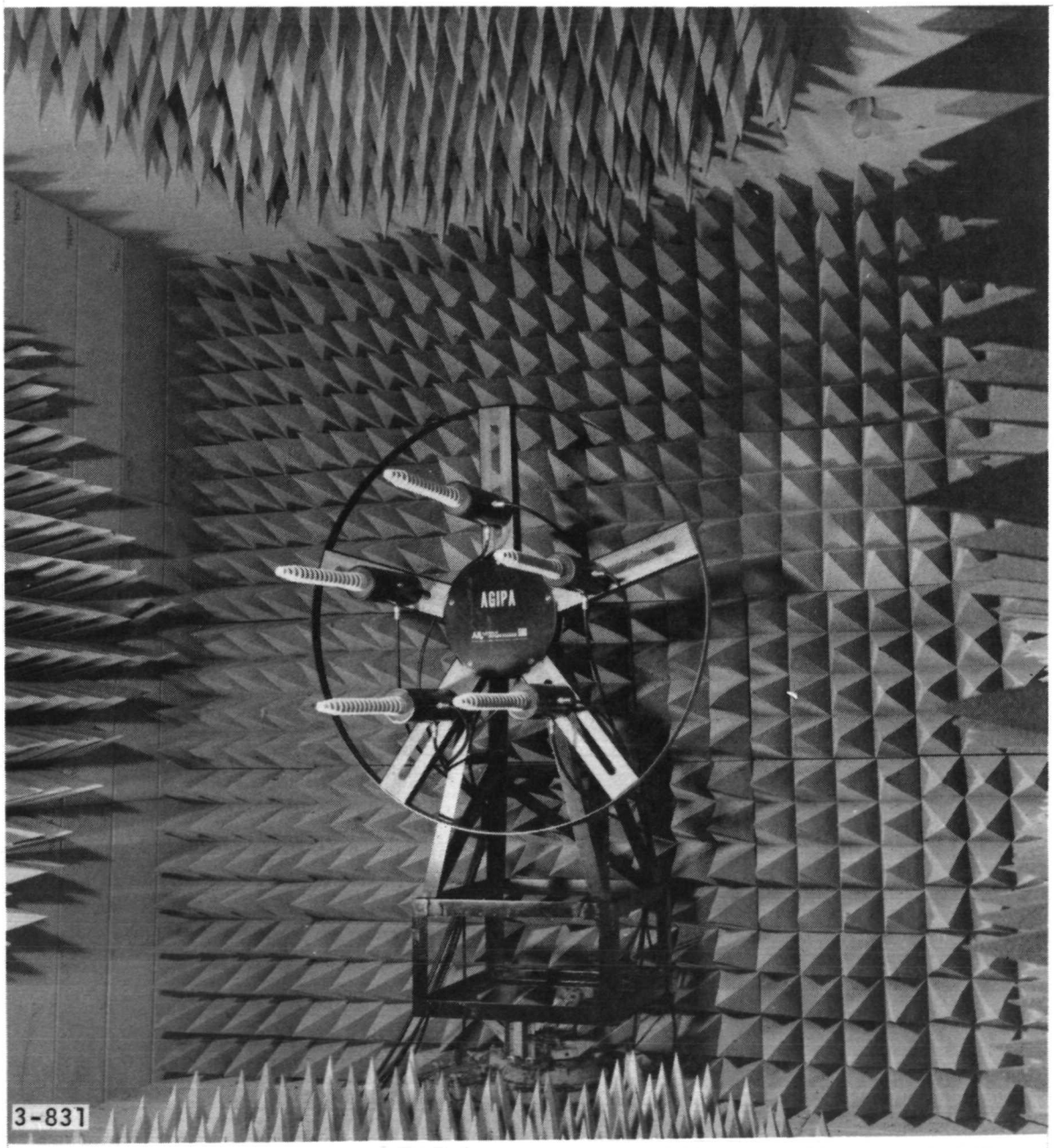

FIGURE 2-9. AGIPA ARRAY MOUNTED IN CHAMBER

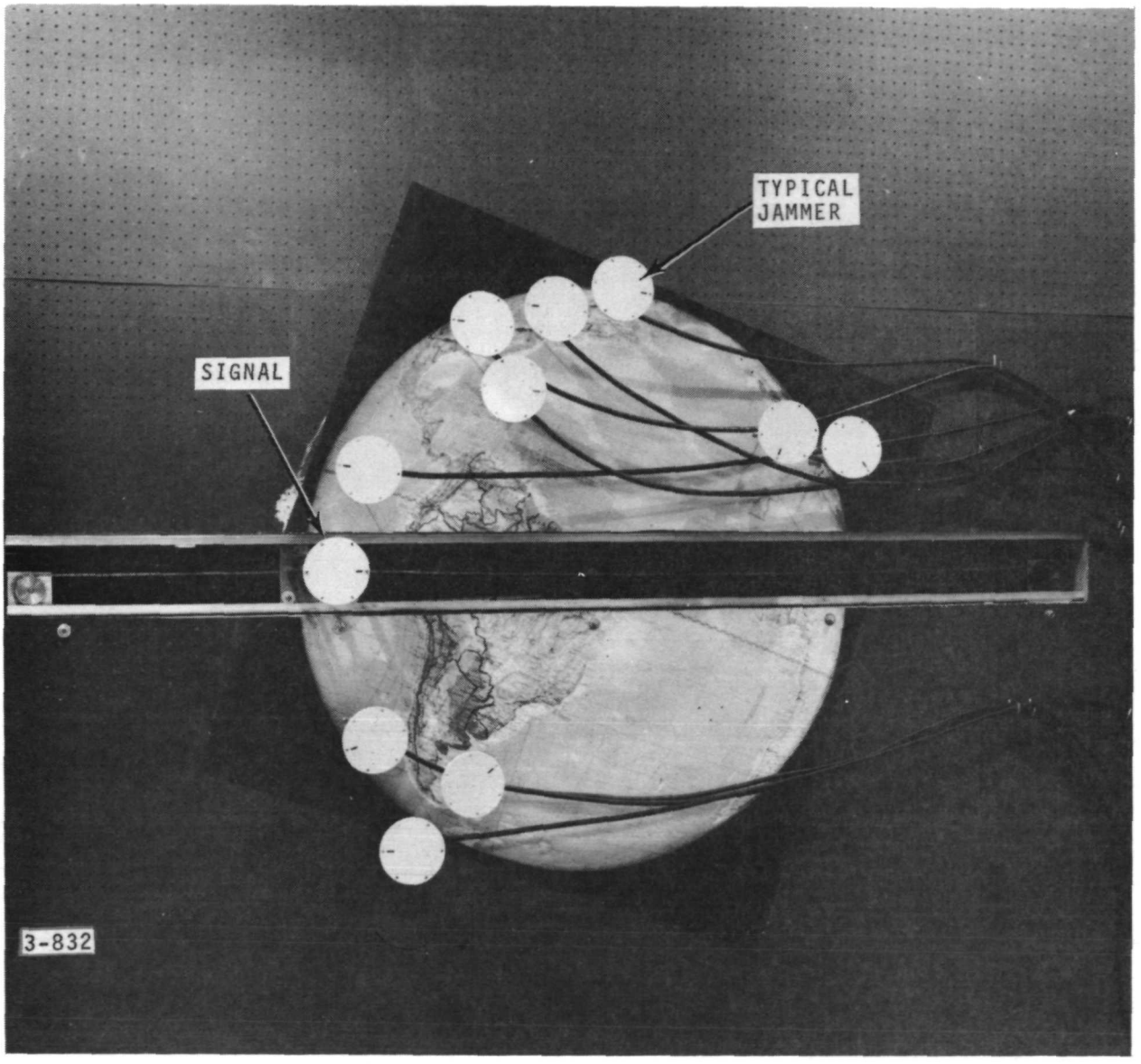

FIGURE 2-10. 10 RFI SOURCES AND MOVING USER

3.0 AGIPA SYSTEM TEST RESULTS

This section describes and documents a test program which was designed to evaluate the performance of a system which enhances S/I ratio using spatial filtering and polarization discrimination to adaptively form ground controlled beams for each low altitude user satellite.[7] The technique employs an Adaptive Ground Implemented Phased Array (AGIPA) in which received signals from each element of the array are processed on the ground to form independent computer controlled beams.

A key objective of the test program was to simulate the RFI environment which would be seen from synchronous altitude in order to demonstrate the advantages offered by the AGIPA system. Toward this end, the alternative utilizing a F-FOV antenna system is used as the basis for comparison. The F-FOV system provides a 31-degree field of view at the receive frequency, which would statically receive signals from the twenty TDRS users in addition to the RFI. This F-FOV system is simulated by a single element of the five element AGIPA array.

The AGIPA testing, which was conducted over a four-month period, required setting the system up in an anechoic chamber constructed especially for testing the AGIPA performance. The tests conducted in the chamber were designed to simulate the actual radiated RFI and signal environment seen from synchronous altitude by the AGIPA system. The chamber tests are scaled to S-band to simulate the VHF operating frequency. The setup includes ten RFI signal sources and a desired signal at one end of the chamber simulating the low altitude satellite and earth based emitters. The desired signal was on a moving track to test the

---

[7] A complete description of the test requirements can be found in; "Test Procedure, Adaptive Ground Implemented Phased Array," NAS-5-21653, AIL for NASA/GSFC, June 1972.

AGIPA tracking capability in a changing geometric situation. Tests were performed to determine S/I improvement, acquisition time, effects of antenna element spacing and number of elements. The following paragraphs describe the test procedures in detail and document the recorded data for the various test setups.

3.1 AGIPA TEST PROCEDURE RESULTS

3.1.1 OPTIMIZATION

In order to demonstrate AGIPA's optimization ability to maximize the S/I ratio, it is necessary for comparison purposes to determine for any given set of conditions what is truly optimum.

With the desired signal source fixed at an arbitrary location and polarization and all of the RFI sources off, a manual adjustment of each of the ten channels weighting network was made to increase the measured signal-to-noise ratio. When the maximum value was obtained, the signal-to-noise ratio for this manually optimized setting was recorded in Table 3-1.

At this time, arbitrary weights were set into each of the channel weighting networks from the teletype control. These weights, although arbitrary in their selection, were required to effect a decrease in the measured signal-to-noise ratio by not less than 6 dB. The signal-to-noise ratio at this quasi-arbitrary setting was recorded. At this time, the AGIPA adaptive program was activated and the resultant signal-to-noise ratio was recorded in the appropriate column of Table 3-1. The difference between the signal-to-noise ratio found manually and the signal-to-noise ratio found adaptively is a measure of the optimization of the AGIPA system.

TABLE 3-1. AGIPA ADAPTIVE OPTIMIZATION ABILITY

Signal		Signal-to-Noise Ratio (dB)		
Horizontal Location (degrees)	Polarization (degrees)	Manually Optimized	Arbitrary Setting	Adaptively Optimized
0	0	+8	-12	+8
+4	0	+8	+ 1	+8
-8	+90	+6	- 4	+6
-6	+30	+6	- 4	+6

NOTE: S/N measured in 100 kHz IF Bandwidth on AIL 707 Spectrum Analyzer

The results of these tests for four different initial conditions (different physical location or antenna polarization of the desired signal source) are recorded in Table 3-1. The recorded results show that the adaptively arrived setting of the channel weights, due to the AGIPA system processing of the received signal, achieved performance substantially the same as that acquired manually by an intelligent operator in the absence of RFI jammer signals.

3.1.2 TRACKING

In order to demonstrate the ability of the AGIPA system to track a moving signal source, a signal tracking test was performed. It is expected that the maximum required tracking speed that the operational TDRS system will require is one degree per minute. The signal tracking test demonstrated at AIL's test chamber was performed on a continuous basis with the desired signal source traveling at a rate of three degrees per minute.

With the signal set at boresight, the system was allowed to adapt and optimize. The system was allowed to continuously adapt as the desired signal source antenna was swept across the full 31-degree (±15.5 degrees from boresight) field of view. Monitoring the measured signal-to-noise ratio for various locations of the signal provided the data recorded in Table 3-2. The results of the tracking test are somewhat weighted by the unsymmetrical electromagnetic response of the anechoic chamber, that is, interfering reflections from the walls as the desired signal approaches the scan limit. The results, however, show that the AGIPA system, which was tested at a rate three times faster than the expected TDRS tracking requirements, can successfully track a moving signal source across a full 31-degree field of view.

TABLE 3-2. TRACKING TEST

Signal Location (degrees horizontal)	S/N Tracking at 3 Degrees/Minute (dB)
-15.5	+5
-12	+5
- 8	+6
0	+8
+ 5	+6
+ 8	+5
+12	+4
+15.5	+3

NOTE: S/N measured in 100-kHz IF Bandwidth on AIL 707 Spectrum Analyzer

3.1.3 ADAPTIVITY

Adaptivity is a measurement of the improvement in signal-to-interference power at the output of the AGIPA system due strictly to its adaptive techniques. AGIPA employs two powerful adaptive techniques: null steering, where the interfering signals are placed in antenna pattern nulls, and polarization discrimination. Polarization discrimination allows the array to discriminate against those interfering signals whose vertical or horizontal polarization differs from that of the desired signal.

Tests were performed to measure the adaptivity of the AGIPA system both with and without polarization discrimination. Two basic RFI location scenarios were selected for the tests. The two scenarios were dubbed "Atlantic" and "Pacific" in an attempt to closely simulate the two views seen from a synchronous orbit. Figures 3-1 and 3-2 illustrate the two selected RFI scenarios.

The results of the AGIPA adaptivity tests are listed in Table 3-3. In each instance, unless otherwise noted, the signal was originally set in an array null and the signal-to-interference ratio measured. After adaption, the signal-to-interference ratio was again measured and recorded in Table 3-3. The difference computed between these two successive measurements yielded the AGIPA adaptivity improvement. The effects of polarization discrimination upon total AGIPA adaptivity is illustrated clearly in the results of tests number one and two. With all other aspects of the test maintained constant, the polarization of the RFI jammers has been shifted from coincidental with the desired signal in test number one to orthogonal with the desired signal in test number two. The impact of this change in RFI polarization upon the final adapted signal-to-interference ratio has been recorded as a significant 5 dB further improvement.

TABLE 3-3. AGIPA ADAPTIVITY AND POLARIZATION DISCRIMINATION

Signal		RFI Environment		Initial	Adapted	Improvement
Location (degrees horizontal)	Polarization (degrees)	Number	Polarization	S/I (dB)	S/I (dB)	Δ S/I (dB)
		(Atlantic Scenario)				
0	90	10	90	-20	+14	34
0	90	10	0	-22	+19	41
0	90	10	Random	-21	+17	38
- 7	90	10	Random	-12	+12	24
0	0	10	Random	-12	+18	30
0	30	10	Random	- 5	+17	22
+ 8	30	10	Random	0	+10	10
- 7	30	10	Random	- 9	+ 8	17
		(Pacific Scenario)				
0	0	8	0	-12	+13	25
- 8	0	8	0	- 4	+ 9.5	13.5
- 8	30	8	Random	-22	+17	39
-12	30	8	Random	0	+14	14
- 4	30	8	Random	+ 9	+16	7
0	30	8	Random	- 9	+19	26
+ 8	30	8	Random	- 3	+17	20

NOTES: All RFI at -91 dBm. Signal at -107 dBm.

All S/I measured in 1-kHz data bandwidth.

All "Initial" positions chosen to place signal in a null.

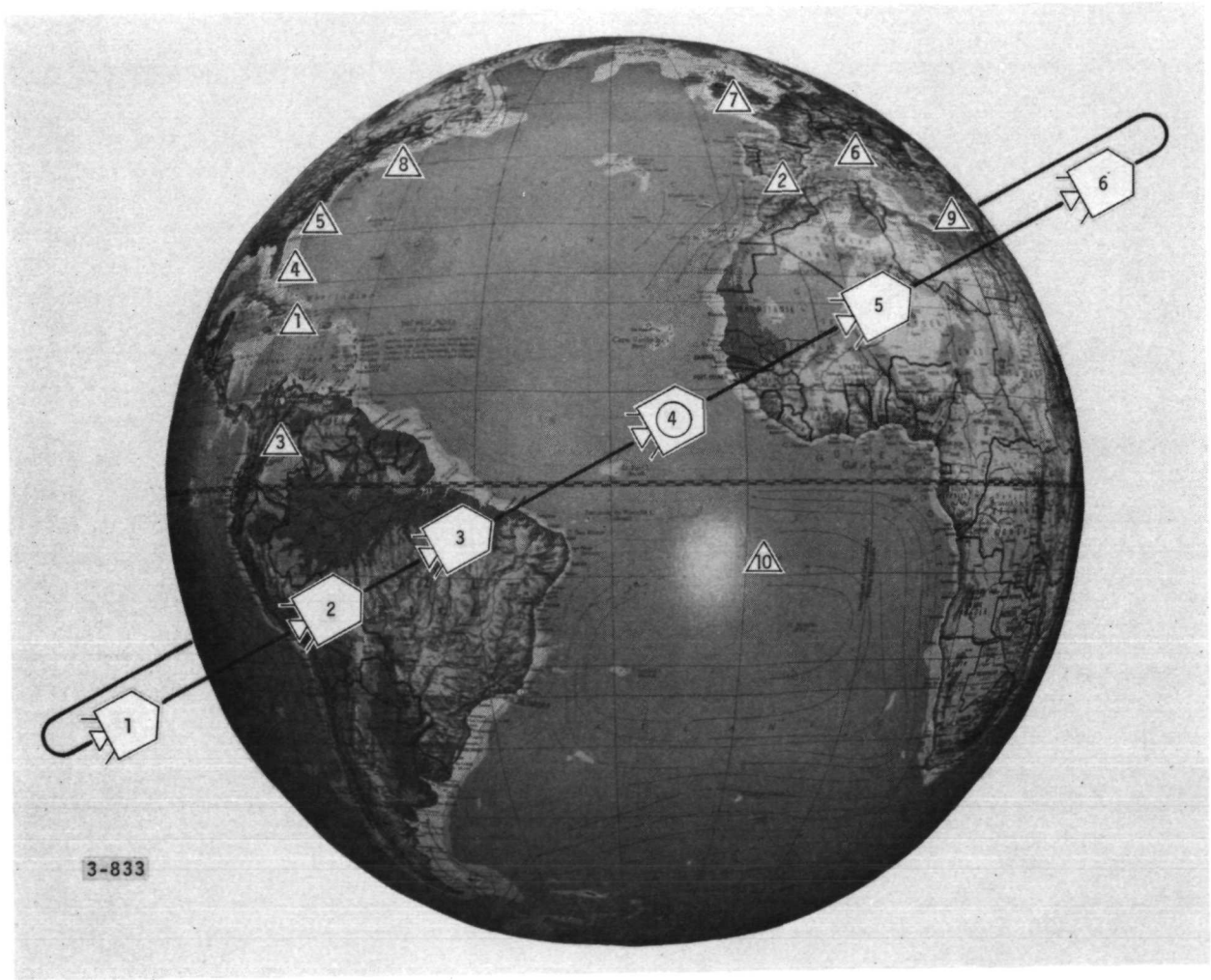

FIGURE 3-1. ATLANTIC SCENARIO

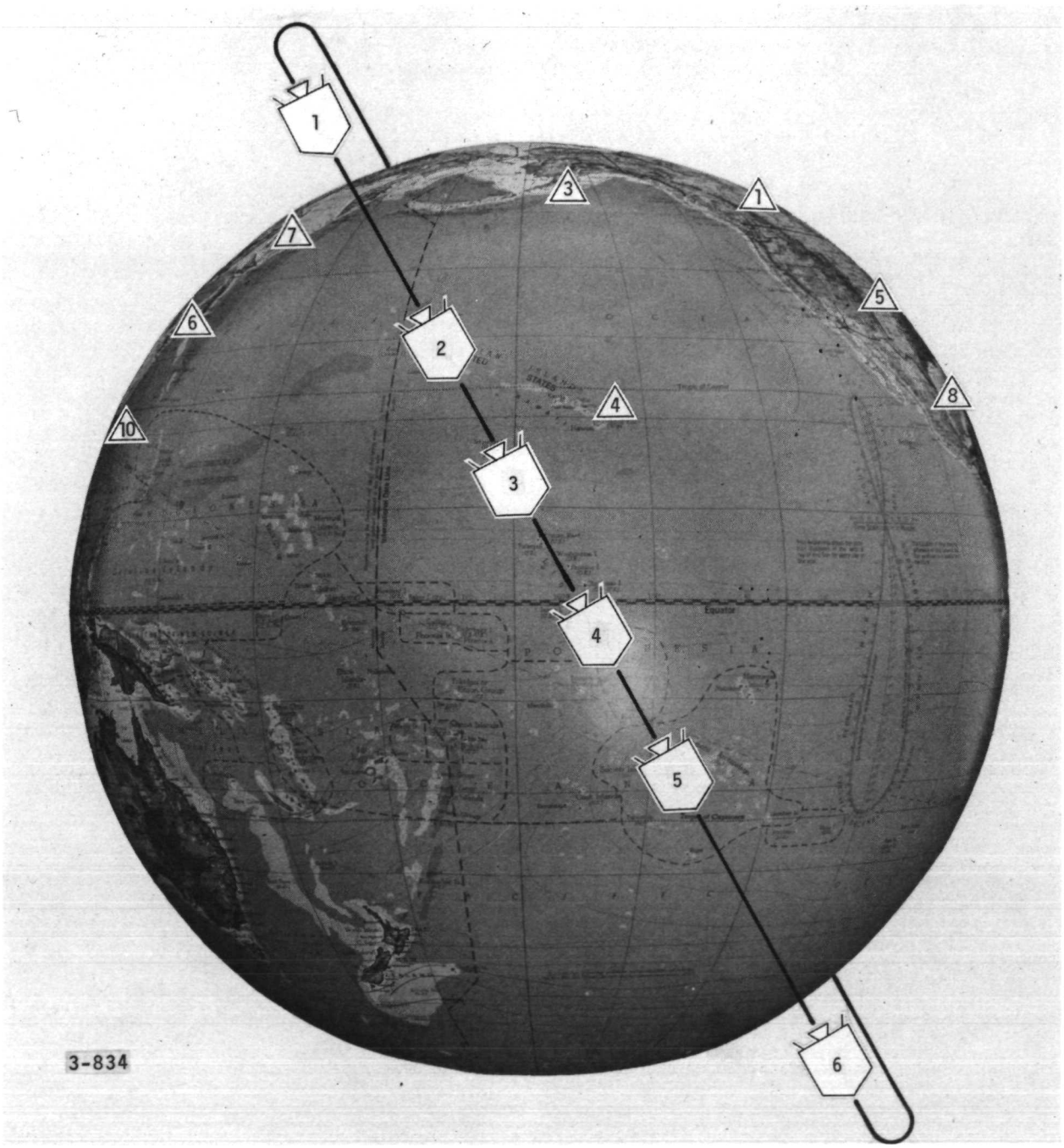

FIGURE 3-2. PACIFIC SCENARIO

The remaining tests show the adaptive ability of the AGIPA system for varied locations and polarizations of the desired signal and the RFI sources. The results for the "Altantic" and "Pacific" scenarios are listed separately in Table 3-3. The term "random" for the RFI polarization implies only that, to the extent possible, the RFI sources polarization was varied in an attempt to appear "random". The range of adaptive improvement of signal-to-interference ratio varied from a minimum of 7 dB to a maximum of 41 dB for the complete set of tests. The minimum 7-dB improvement represents a situation where the desired signal was partially illuminated by the main beam of the array initially and, therefore, the test began with an already moderate signal-to-interference ratio. The maximum 41-dB improvement illustrates the ideal situation where all of the RFI sources polarizations are orthogonal to the desired signal and the full adaptive abilities of the AGIPA system, both null steering and polarization discrimination, may be utilized to obtain the maximum signal-to-interference ratio.

3.1.4 POLARIZATION DISCRIMINATION

To effectively illustrate the concept of polarization discrimination as it pertains to the adaptibility of the AGIPA array, a test was devised to clearly demonstrate its unique features. With the desired signal centered at boresight and its radiated power split evenly between the two planes of polarization (that is, the antenna polarization set at an odd multiple of 45 degrees), the five-element array was allowed to adapt. An antenna pattern plot of a horizontal slice through the field of view is shown in Figure 3-3. As shown, the main beam of the array is as expected-located about boresight with the first array nulls located at approximately six to seven degrees either side of boresight. This plot is the resultant array pattern of combining the horizontal and vertical components of the array. At this time, two equal amplitude jammers of orthogonal polarization were activated. Although the two jammer antennas were of orthogonal polarization, each was coincidental

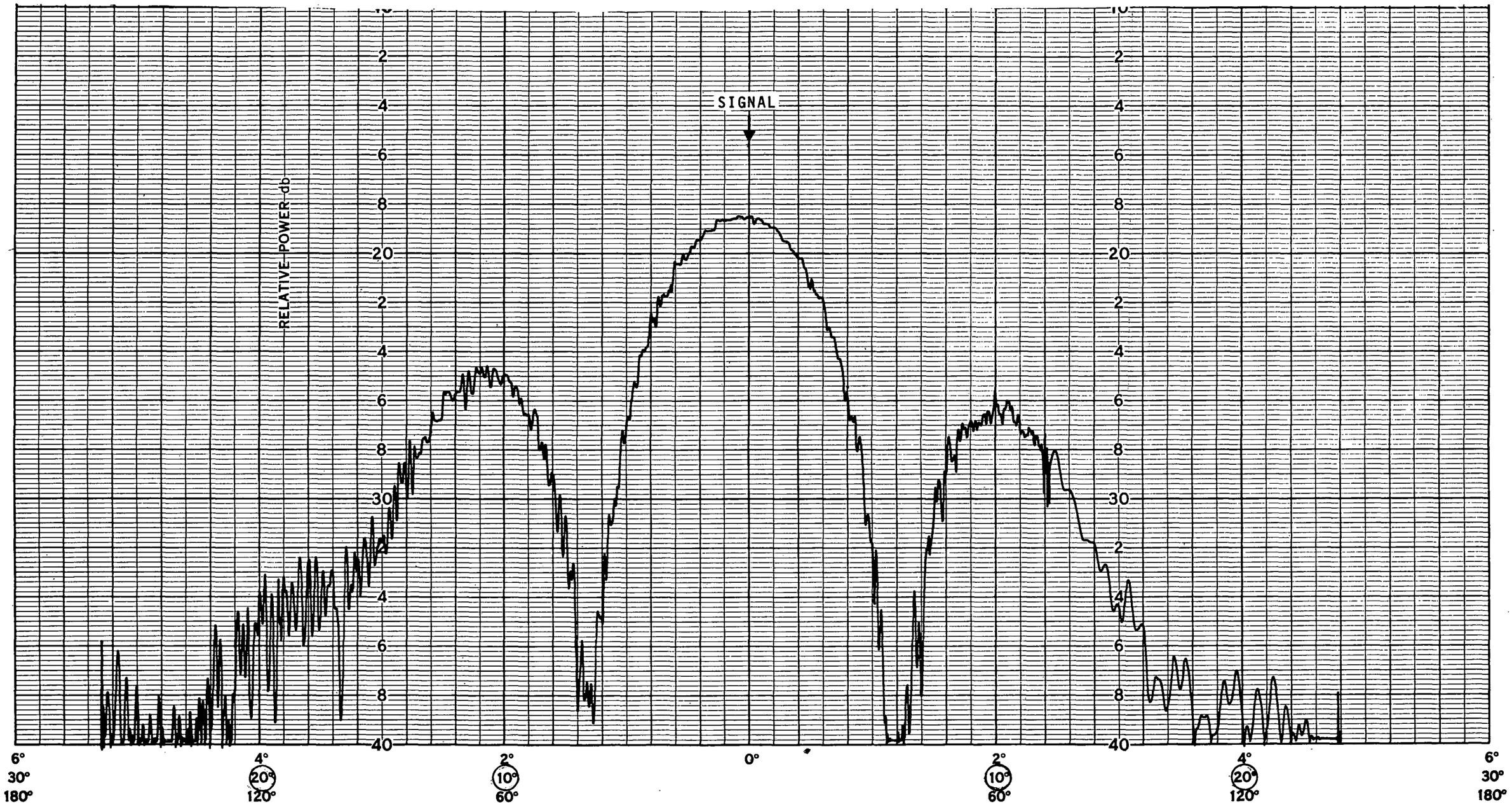

3-835

FIGURE 3-3. ARRAY PATTERN--SIGNAL AT BORESIGHT (NO JAMMING)

to a plane of polarization. The horizontally polarized jammer was located at +5 degrees horizontal and the vertically polarized jammer was located 4 degrees away at +9 degrees horizontal. The AGIPA system was allowed to adapt and antenna pattern plots, similar to the one above, were taken for the resultant horizontal and vertical components of the adapted array. Figures 3-4 and 3-5 depict these two antenna pattern plots. The horizontal component of the array pattern, shown in Figure 3-4, has a null placed on the location of the jammer whose polarization was coincidental to that plane of polarization. Simultaneously, the vertical component of the array pattern, as depicted in Figure 3-5, has placed an array null on the jammer coincidental to its plane of polarization. Two nulls on two independent jammers in two different planes of polarization are arrived at simultaneously by the adaptive abilities of the AGIPA array.

These antenna pattern plots show that the horizontally and vertically polarized array beams, although formed simultaneously, are independent of each other and give the AGIPA system an extra adaptive feature to discriminate interference signals beyond conventional null steering techniques.

3.1.5 DEPTH OF NULL

To determine the maximum "depth of null" possible against a single RFI source, a test was performed where the desired signal and the interference signal were of the same polarization, but separated physically by approximately 9 degrees. The results of this test may be seen in Figures 3-6 and 3-7 where photographs of the spectrum of the RFI jammer were taken before and after adaption. The photographs show that the adaptive AGIPA system has placed the undesired RFI signal into a 40-dB null.

If the RFI source antenna polarization has been different from that of the desired signal, further nulling of the RFI signal would have occurred. The further nulling, of course, would be due to the ability of the

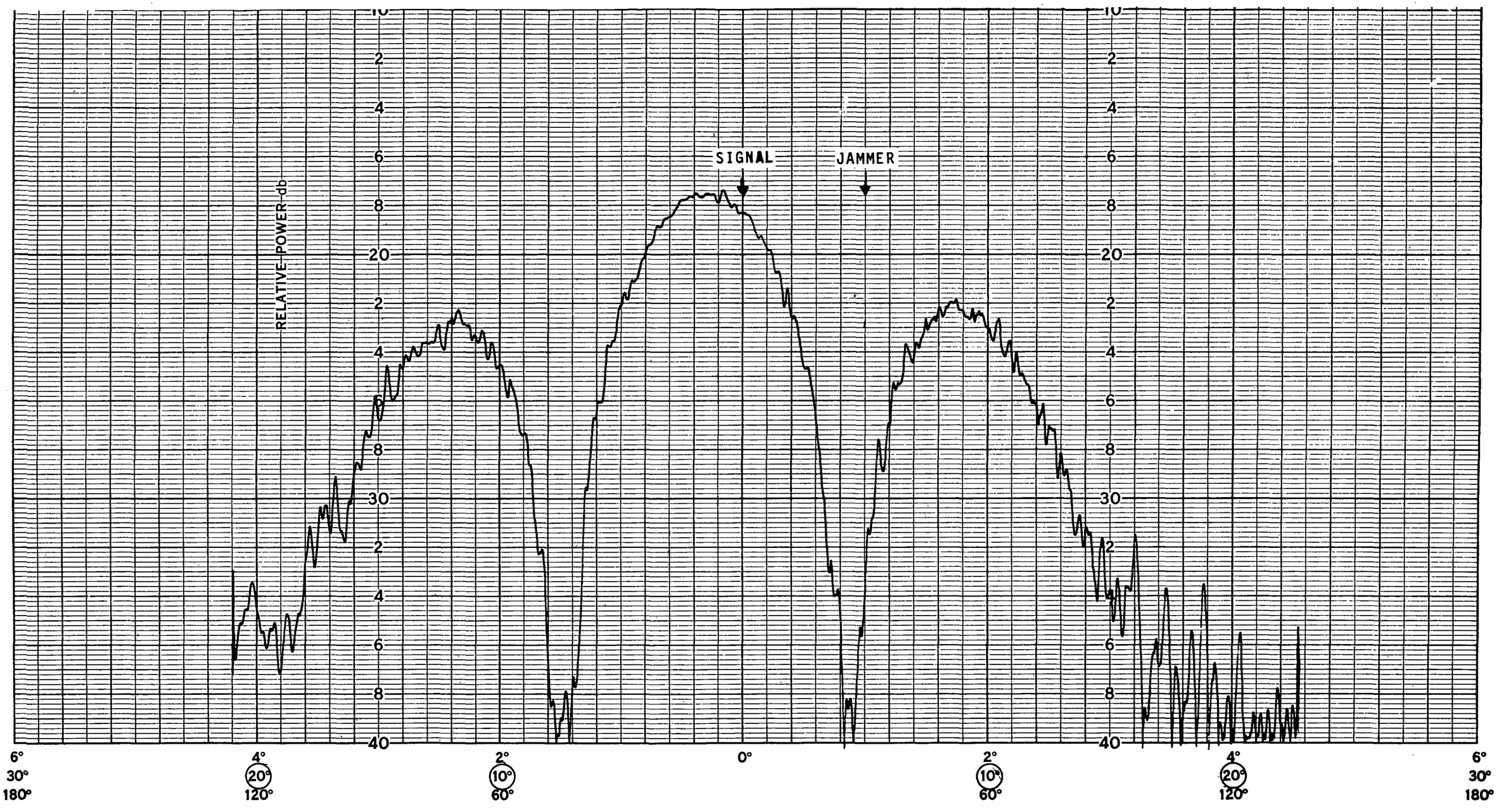

3-836

FIGURE 3-4. HORIZONTAL ARRAY PATTERN--SIGNAL AT BORESIGHT (HORIZONTALLY POLARIZED JAMMER IS AT 5 DEGREES HORIZONTAL)

FIGURE 3-4

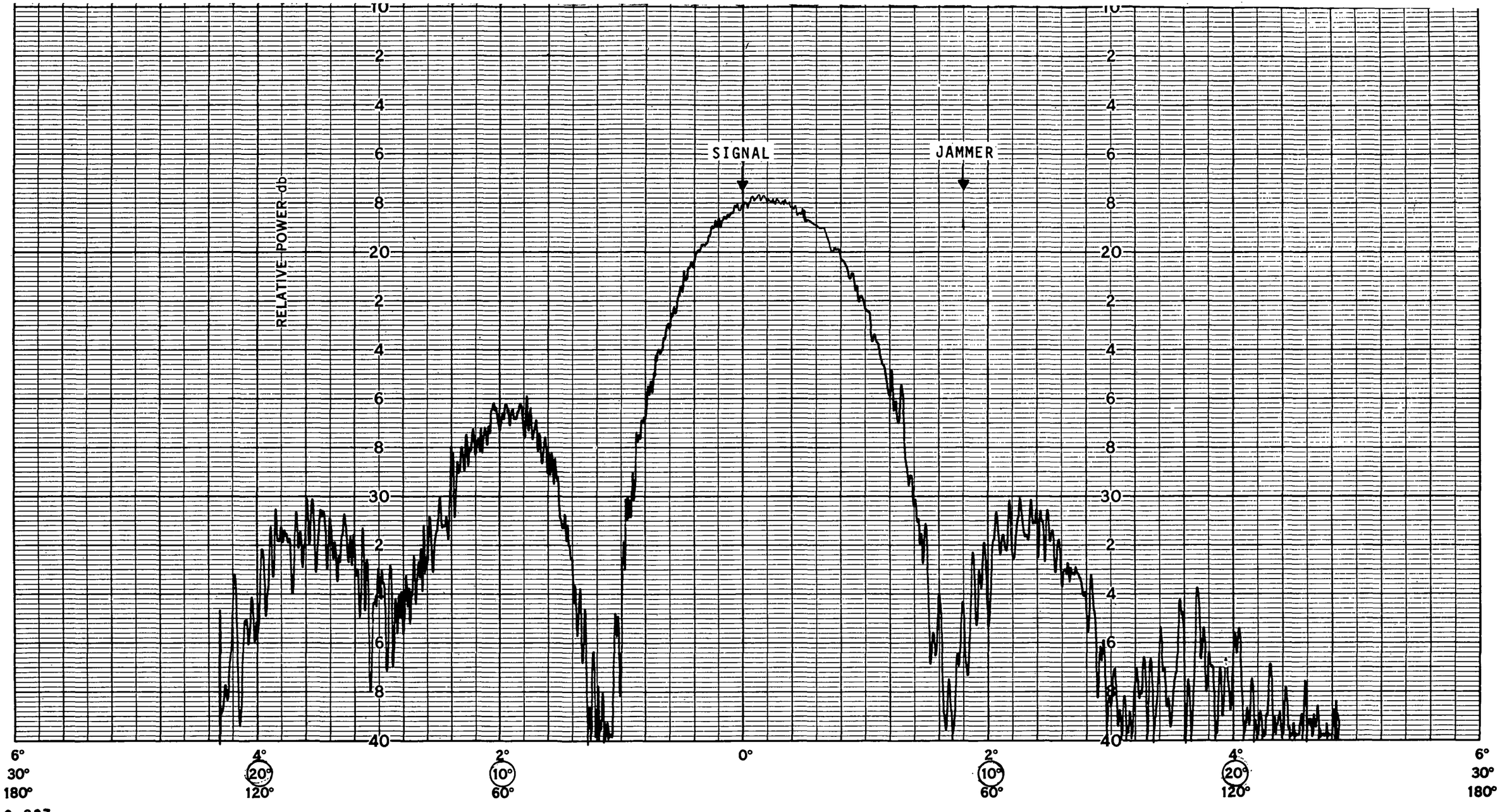

FIGURE 3-5. VERTICAL ARRAY PATTERN--SIGNAL AT BORESIGHT (VERTICALLY POLARIZED JAMMER IS AT 9 DEGREES HORIZONTAL)

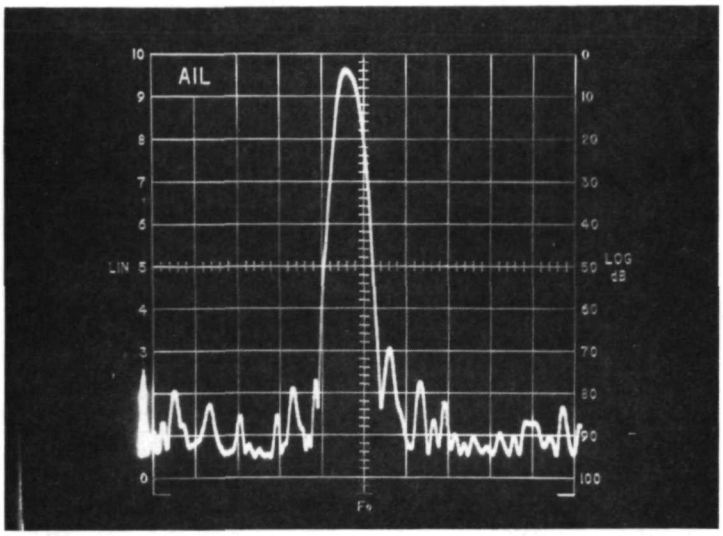

3-838

FIGURE 3-6. JAMMER BEFORE NULLING

V = 5 dB/cm

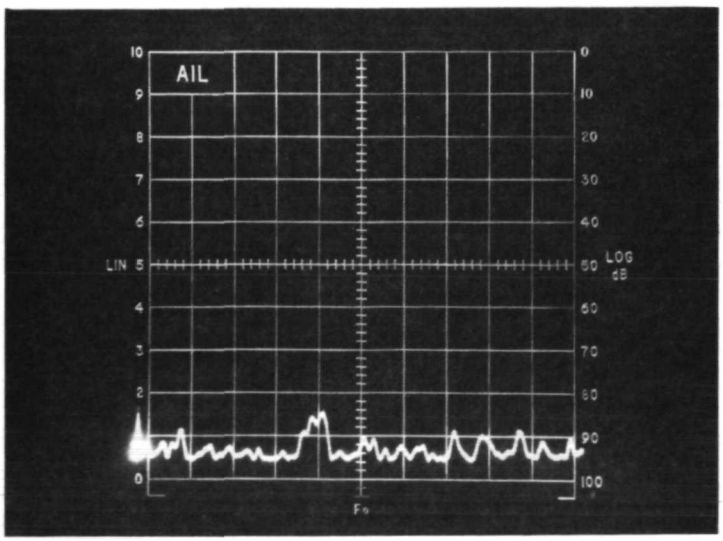

3-839

FIGURE 3-7. JAMMER NULLED 40 dB BY AGIPA

system to discriminate against signals of different polarizations. The test illustrates the ability of the adaptive system to combat a particularly strong jammer of identical polarization by directing an array null whose depth is in the order of 40 dB in the direction of the offending jammer.

3.1.6 ACQUISITION TIME

The total time needed for AGIPA to adapt to an RFI environment is equal to the product of the number of steps needed and the time required to take each step. The development effort to data has been concerned with only the number of steps needed to reach the optimum signal-to-noise ratio. No effort has been expended to reduce the time required for each step.

Two representative tests were performed to measure acquisition time for the AGIPA feasibility mode. Acquisition time for these tests was defined as the time required for the adaptive system to move the array output from a minimum signal-to-interference ratio to a point where further adaption of the array no longer yielded any measurable improvement in the signal-to-interference ratio. Initially, the signal in both tests was placed in the arrays first null and adaption begun.

The first test was performed with the signal at boresight and nine RFI jammers of the "Atlantic" scenario activated. The RFI jammers polarization was set as random as possible and each jammer was set for equal power output. The optimum signal-to-interference ratio was achieved in fourteen steps, with the most improvement occurring in the first three steps. In the second test, a single strong jammer was activated (that is, signal/jammer = -30 dB for any one element) and the number of steps required to adapt to the optimum measured. The number of steps measured was nine steps with the greatest improvement again occurring in the first three steps.

Presently, measurement and computation time consume approximately 2.5 seconds per step. The following measures are proposed to reduce processing time:

a. Building 10 pairs of correlators (a pair for each channel) rather than sharing one pair will eliminate the sequential sampling and the long waiting times now required.

b. Adding Floating Point Hardware to the computer will speed most of the calculations by a factor of 50 or more. This hardware is available from the computer manufacturer.

c. Software changes, such as the use of look-up tables for converting input and output data to replace formula evaluation, will speed computing time.

We realistically expect a processing time of 50 milliseconds per step if these three improvements are made. Assuming the 50-millisecond processing time, the elapsed acquisition time to reach the optimal signal-to-interference ratio would have been 0.7 second (that is, 14×50 ms = 0.7 second) for the nine jammer case and 0.45 second for the single jammer case. For both cases, the most improvement would have occurred in the first 0.15 second. When this speed is combined with the techniques already developed to minimize the number of steps needed to adapt, AGIPA should be extremely effective against any operationally possible RFI environment.

3.2 AGIPA VERSUS F-FOV

In order to properly evaluate the adaptive abilities of the AGIPA array in improving an RFI limited communications link, a series of tests were performed where the AGIPA array performance was compared to that of a F-FOV antenna system. The F-FOV antenna system is designed so that its "fixed-view" encompasses an entire area of possible interest. That is, for the TDRS application where the area of possible interest includes a 31-degree field of view, the F-FOV system would always view the entire area encompassed by this 31-degree field of view. Because of this fixed

wide-view, the F-FOV system, unlike an adaptive array which forms custom narrow beams to service each user, must contend with all of the RFI jammers.

To insure that the tests performed were pertinent to the TDRS application, every attempt was made to closely simulate the operational TDRS environment. The operational parameters for a TDRS F-FOV antenna system have been computed and tabulated in Table 3-4. Because of the limitations of the feasibility model and although the parameters listed in Table 3-4 for the simulated F-FOV system differ from that of the operational TDRS F-FOV system, note that the relative post-processing carrier-to-jammer ratios have remained the same. The carrier-to-jammer ratio for the AGIPA array is of course a function of the adaptive ability of the system and, thus, ranges in value from small improvement over the F-FOV system to a complete suppression of the RFI jammers.

TABLE 3-4. AGIPA VERSUS F-FOV: SIGNAL AND RFI POWER LEVELS
(RFI DENSITY = -160 dBm/Hz)

Parameter	TDRS F-FOV	Simulated F-FOV	Simulated AGIPA
T_s dB/K	31.8	43.6	43.6
P_n dBm	-105.0	- 89.5	- 89.5
P_{RFI} dBm	- 95.2	- 79.7	- 79.7
P_s dBm	-115.3	-102.8	-119.6 to -102.8*
Processing Gain (dB)	30	33	33

for C/N = 9.9 dB

*Signal level required is a function of adaptive performance.

To help underline the difference in system approach between the F-FOV and adaptive array system, Figures 3-8 and 3-9 are instructive. Figure 3-8 depicts the output from a F-FOV system. The desired signal is located in the center of the spectrum and eight similarily polarized, spatially separated, in-band RFI jammers have been activated. For clarity on the spectrum display, the signal and jammers are all clockwise. Figure 3-9 illustrates the effects of an adaptive array under the identical conditions. The AGIPA array has, through its adaptive abilities, enhanced the signal power and simultaneously reduced RFI jammer levels to a point where they are no longer visible on the spectrum. To the system designer, the differences between these two techniques are formidable. With the F-FOV approach, the system designer must formulate a technique that "lives" with the RFI jammers through complex coding or error control techniques. Employing the AGIPA array allows the system designer additional freedom from the full degradation of link capabilities due to RFI power. How much freedom can the system designer reasonably expect is the criterion for the following comparison tests.

Employing the two previously described "Atlantic" and "Pacific" scenarios (Figures 3-1 and 3-2) and randomly polarized RFI jammers, comparison tests of the signal-to-interference (S/I) ratio in the 1-kilobit data bandwidth for the F-FOV antenna system versus the AGIPA adaptive array were performed. These tests were performed with the desired signal encoded with a 2-megabit chip rate pseudorandom code. Decoding this spread-spectrum transmission necessitates accepting some portion of the power of all of the RFI jammers activated. (All jammers during these tests fall within the 2-MHz RF bandwidth of the receiver.) It is the final S/I ratio for both the F-FOV and AGIPA systems that has been recorded in Table 3-5. The desired signal has been driven along its track (paragraph 2-3) to various locations and the signal-to-interference ratio measured

for the two techniques. The results of Table 3-5 clearly show the advantageous capabilities of the AGIPA array. Figures 3-10 and 3-11 compare these results with those obtained through computer simulation. The two figures clearly depict the validity of the computer simulations done by AIL.

TABLE 3-5. AGIPA VERSUS F-FOV COMPARISON

Signal Location (degrees horizontal)	RFI Model	F-FOV S/I (dB)	AGIPA Adaptive S/I (dB)	Improvement (Δ dB)
-8	Atlantic	+0.7	+11.7	11.0
-4	Atlantic	+1.2	+15.0	13.8
0	Atlantic	+1.5	+18.0	16.5
+4	Atlantic	+0.7	+13.1	12.4
+8	Atlantic	-1.0	+10.2	11.2
-8	Pacific	+0.9	+16.2	15.3
0	Pacific	+1.7	+18.7	17.0
+6	Pacific	+0.2	+17.1	16.9

NOTE: AGIPA array diameter = 5 λ

For the F-FOV antenna system, the signal-to-interference ratios are near unity, whereas, for the adapted null steering array, strong signal-to-interference ratios ranging from 10.2 to 18.7 dB are recorded. The improvements in S/I ratio for the adapted array of anywhere from 11.0 to 17.0 dB have transformed the F-FOV RFI limited, low capacity communications link, to a reliable, low error rate, high quality data link.

3.3 VARIABLE APERTURE AGIPA

A test to measure the effects of varying the aperture of the AGIPA five-element ring array upon adaptive performance was also conducted by AIL. An "Atlantic" scenario was assumed for the tests, and with

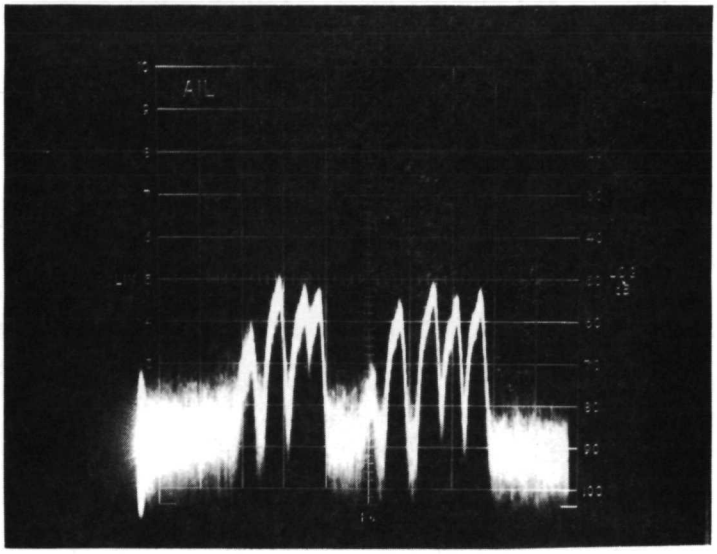

3-840

FIGURE 3-8. FIXED FIELD OF VIEW

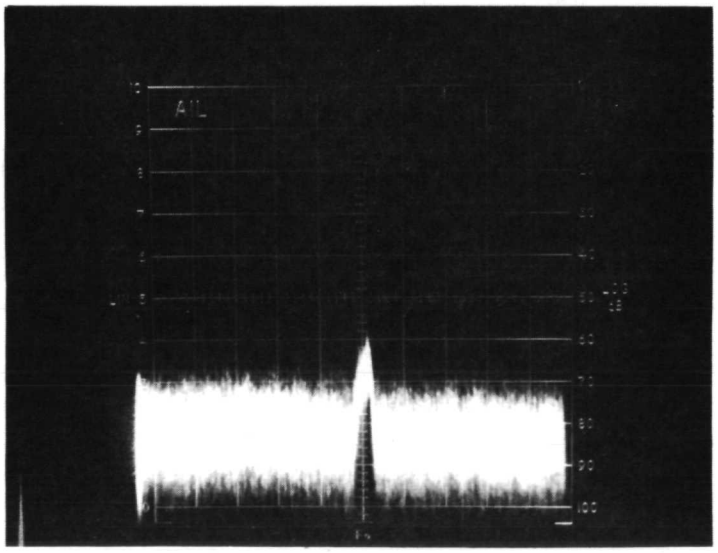

2-4961

FIGURE 3-9. ADAPTIVE GROUND IMPLEMENTED ARRAY

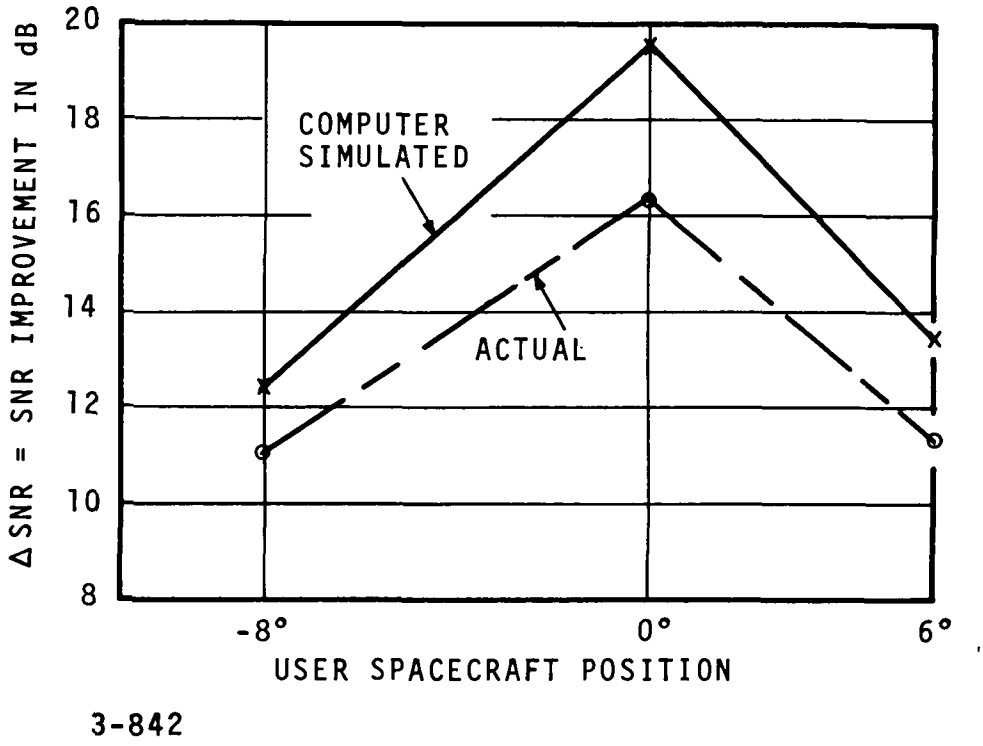

FIGURE 3-10. SNR IMPROVEMENT: ATLANTIC SCENARIO

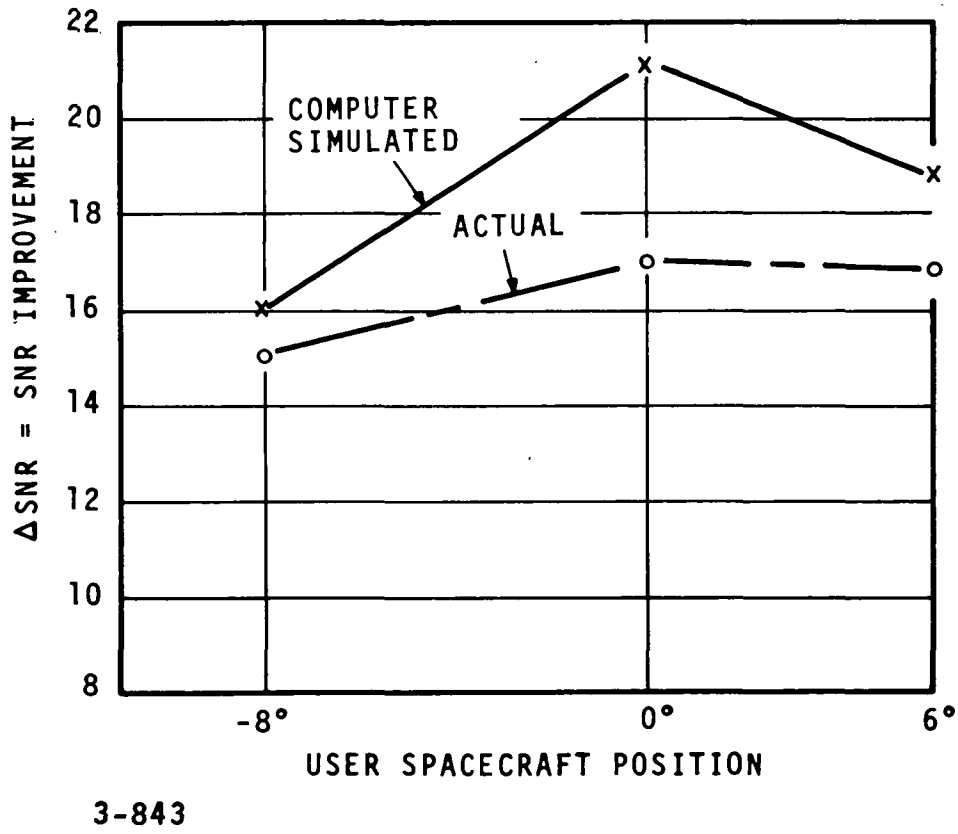

FIGURE 3-11. SNR IMPROVEMENT: PACIFIC SCENARIO

the element spacing selected within the range of 4 λ to 9 λ, the adapted S/I ratio at five locations of the desired signal was measured. The results of these adaptive tests are tabulated in Table 3-6. (The resultant S/I ratio for a F-FOV system has been included for reference purposes.)

With the amount of mutual coupling and the magnitude of grating lobes an unknown factor for the array plus the effects of operating in the near field, no decision concerning an optimum element spacing could be made merely on the basis of these recorded results. Although it would require further testing and perhaps element redesign to determine the optimum element spacing for the adaptive array, it would appear that for the elements employed in these tests a spacing of 5 λ is appropriate.

TABLE 3-6. S/I FOR F-FOV AND VARIOUS ARRAY DIAMETER AGIPA's

Signal location (degrees):	-8	-4	0	+4	+8
F-FOV	0.7	1.2	1.5	0.7	-1.0
4 λ AGIPA	15.5	15.9	17.5	13.1	9.2
5 λ AGIPA	11.7	15.0	18.0	13.1	10.2
6 λ AGIPA	7.2	14.1	16.2	13.5	9.4
7 λ AGIPA	6.2	10.8	12.7	13.0	10.6
8 λ AGIPA	4.9	9.8	10.8	12.5	11.8
9 λ AGIPA	8.5	10.7	10.2	10.5	11.3

NOTES: Signal horizontally polarized

10 jammers in Atlantic scenario, randomly polarized

3.4 NULL STEERING ARRAY PATTERNS

Figures 3-12 through 3-17 depict the effect on the antenna array pattern nulls due to the adaptive nature of the AGIPA system. The procedure for obtaining these array patterns was always the same. The desired signal was located at boresight and an interfering jammer signal was moved about

on the same axis as the signal. Each time after relocating the jammer, the system was allowed to adapt and an array pattern recorded.

Figure 3-12 shows the effect on the placement of the nulls of the array when the jammer is only slightly removed from the natural nulls of the five-element array. Although the pattern in Figure 3-12 appears at first sight to be still symmetrical about boresight, careful inspection of the placement of the nulls reveals a slight shifting of the array pattern to accommodate placing a null on the jammer.

As the offending jammer was relocated further from boresight into areas normally illuminated by the main side lobe of the array, the array patterns became less and less symmetrical. Figures 3-13 and 3-14 depict the situation where the jammer has been relocated to -9 degrees and -15 degrees on the horizontal axis, respectively. In both instances, the normally symmetrical array was deformed in order to place a null on the interfering jammer.

The effect of moving the offending jammer well into the un-adapted beamwidth of the main beam of the array is displayed in Figure 3-15. Here the jammer has been located at -4 degrees horizontal and the array pattern shows the shifting necessary to place the jammer into a null.

The resultant array patterns from first placing two jammers on the same side of boresight (signal location), and second, from placing the two jammers unsymmetrically on either side of boresight are depicted in Figures 3-11 and 3-17, respectively. In Figure 3-16, the two jammers have been located at +4 and +10 degrees on the horizontal axis and the array pattern shows a general distortion and shifting of the array to reduce jammer strength. In Figure 3-17, where the jammers have been relocated to -5 and +4 degrees on the horizontal axis, it may be seen that the resultant main beam has been reduced in beam width to null jammers this close to the desired signal.

The conclusion that may be drawn from an inspection of Figures 3-12 through 3-17 is that the AGIPA system will shift array patterns, distort symmetry, adjust beamwidth, or in other ways steer nulls so that the jammer strength with relation to the desired signal is always minimized.

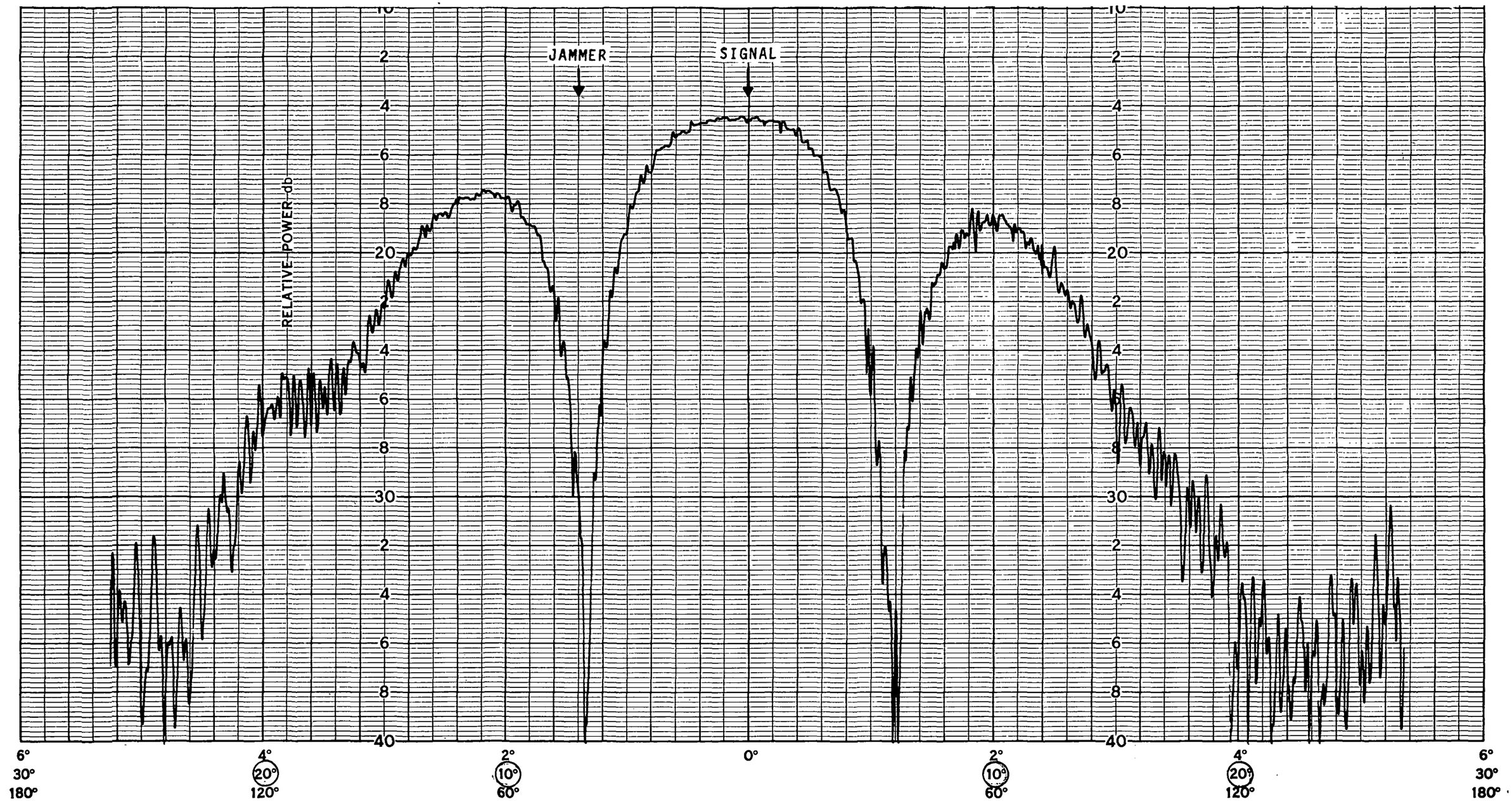

3-844

FIGURE 3-12. ARRAY PATTERN--JAMMER AT -7 DEGREES HORIZONTAL

FIGURE 3-12

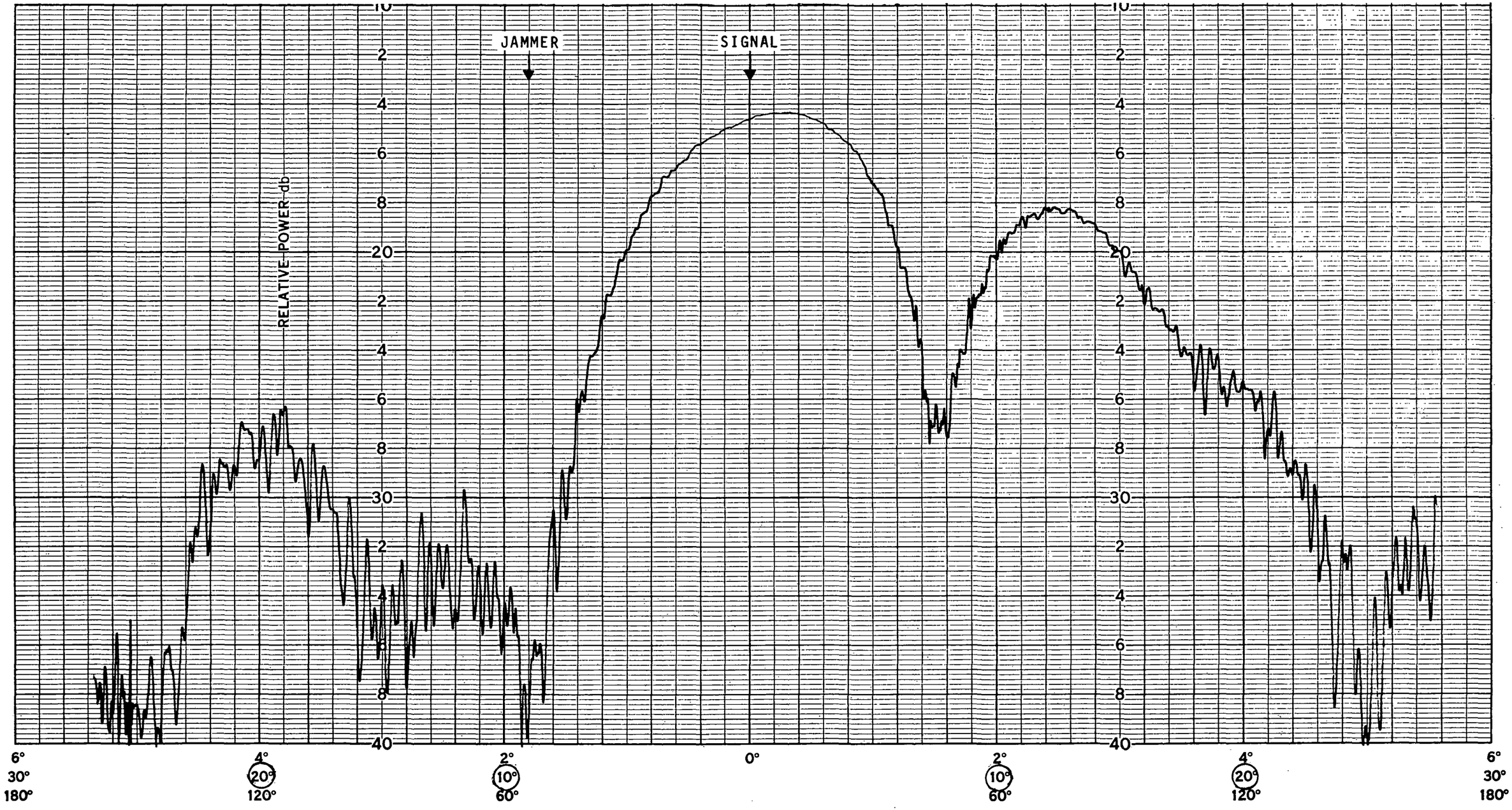

3-845

FIGURE 3-13. ARRAY PATTERN--JAMMER AT -9 DEGREES HORIZONTAL

FIGURE 3-13

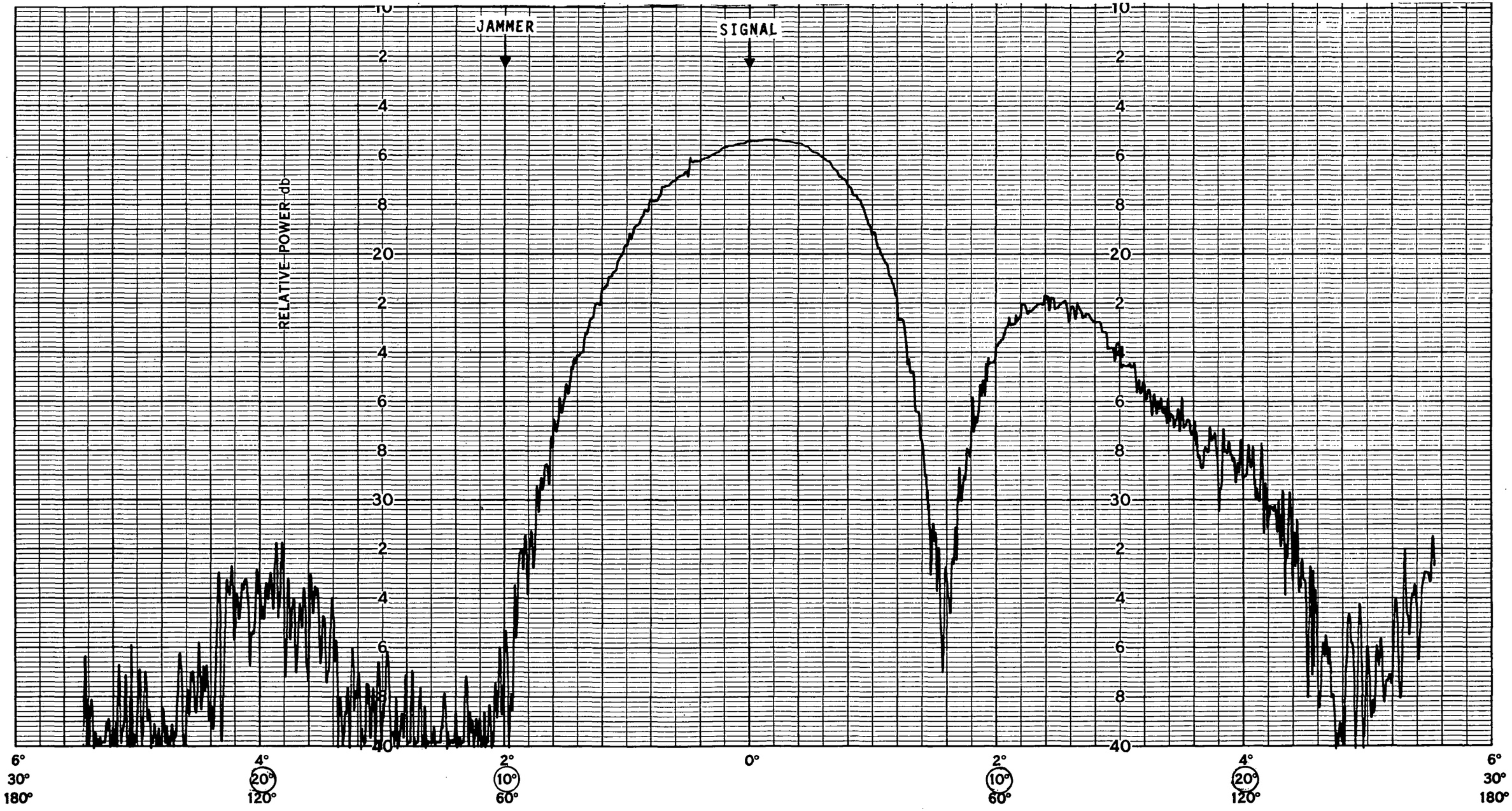

3-846

FIGURE 3-14. ARRAY PATTERN--JAMMER AT -15 DEGREES HORIZONTAL

FIGURE 3-14

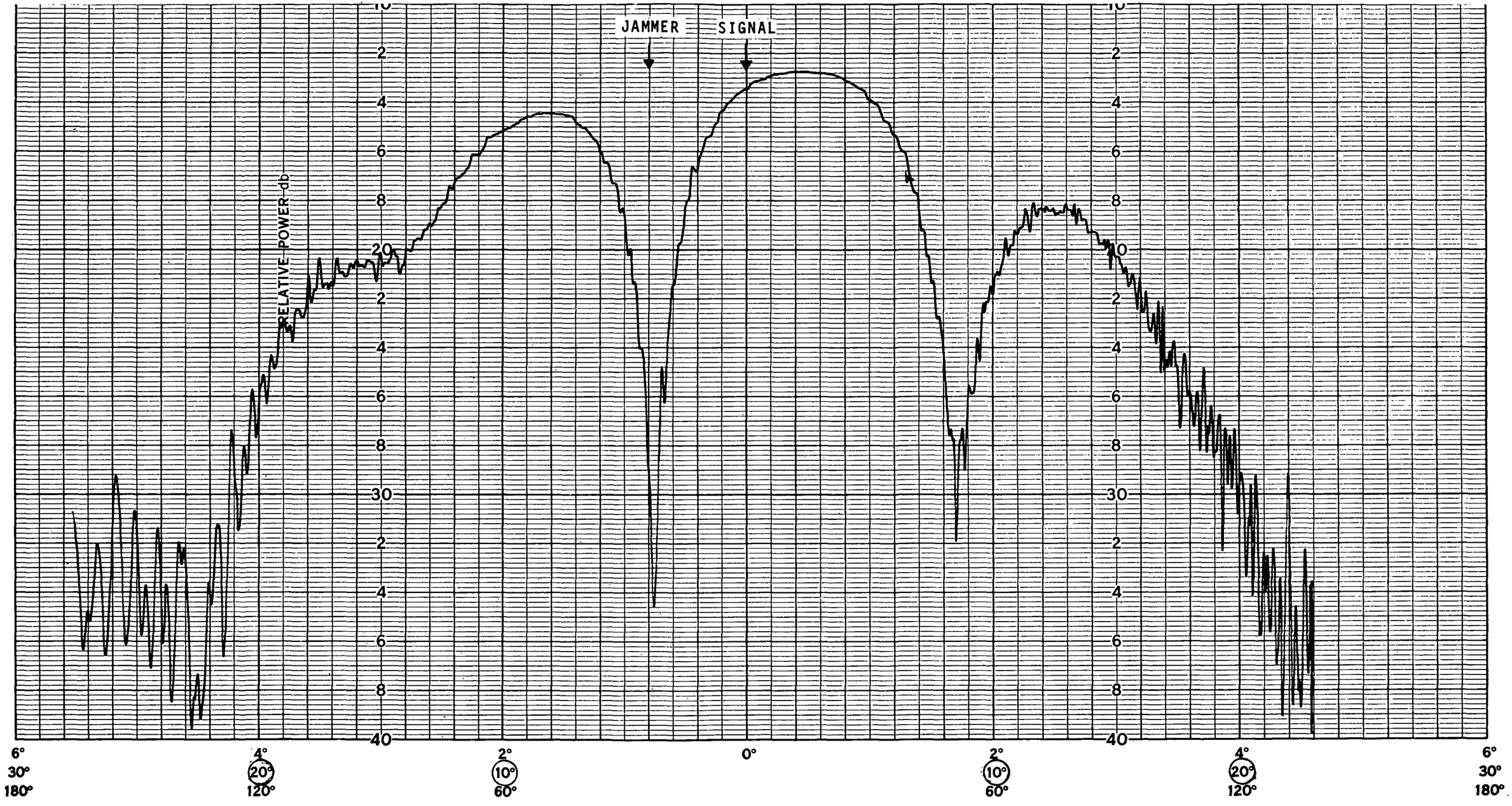

3-847

FIGURE 3-15. ARRAY PATTERN--JAMMER AT -4 DEGREES HORIZONTAL

FIGURE 3-15

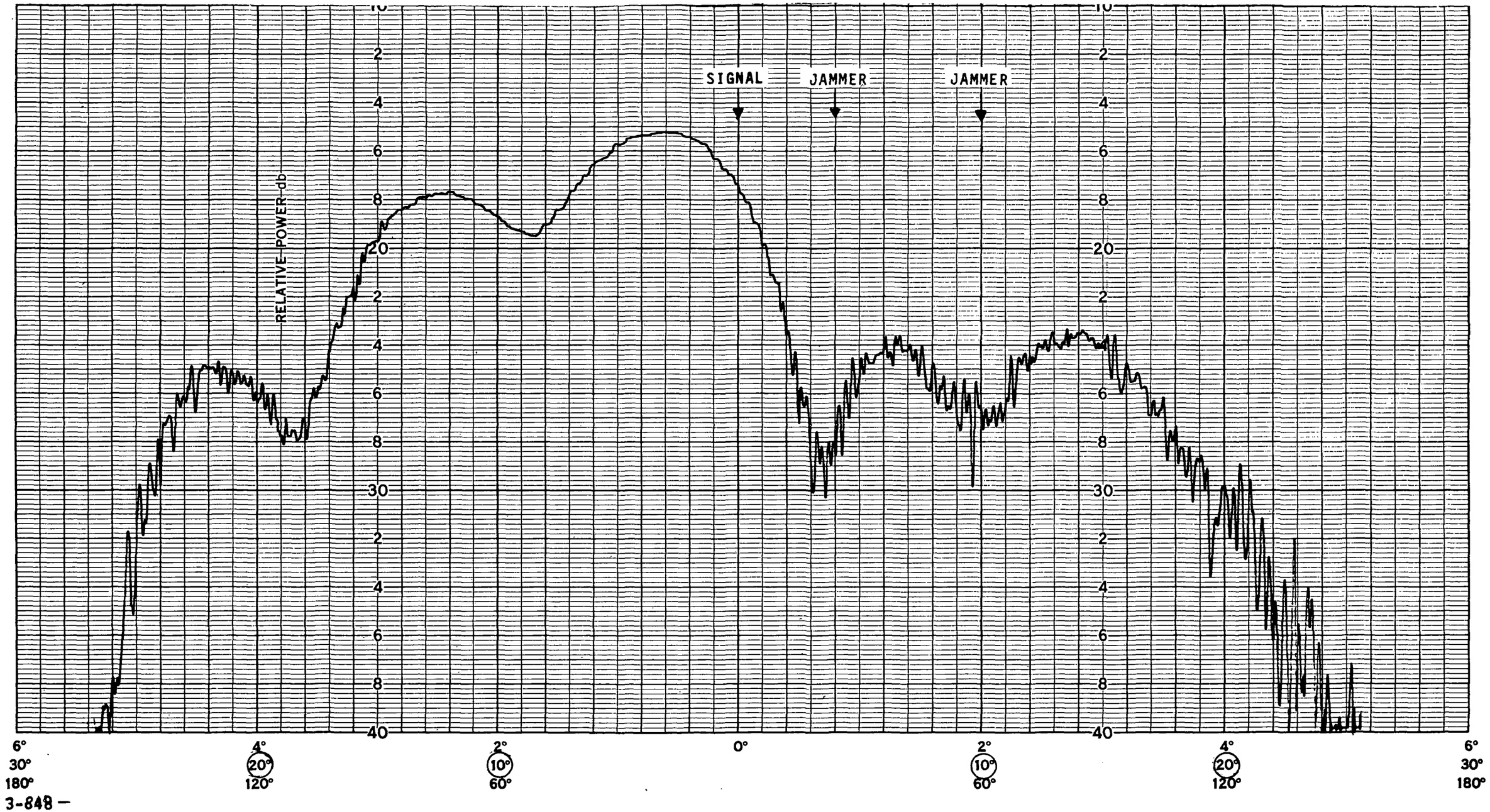

FIGURE 3-16. ARRAY PATTERN--TWO JAMMERS AT 4 AND 10 DEGREES HORIZONTAL

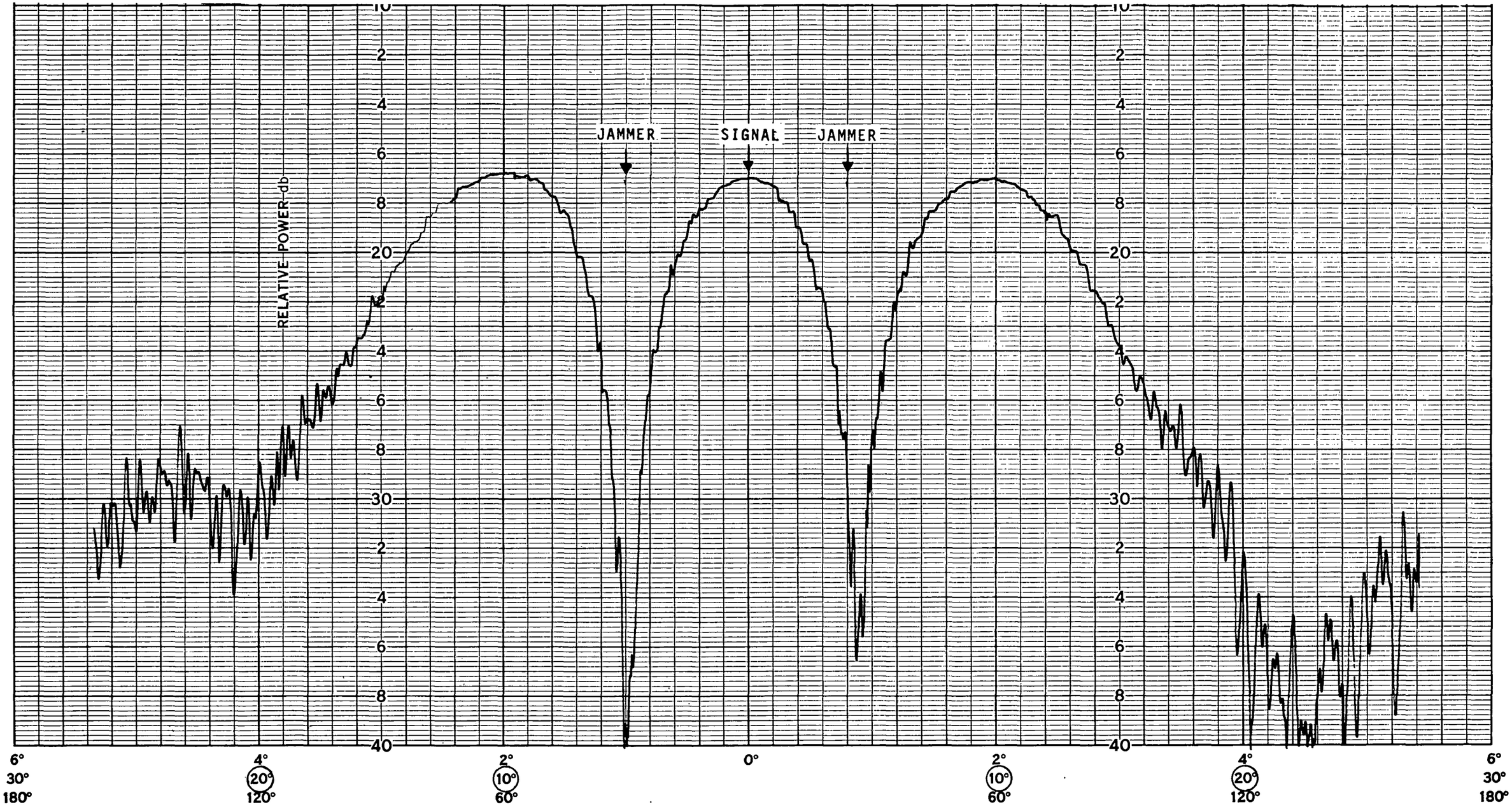

FIGURE 3-17. ARRAY PATTERN--TWO JAMMERS AT -5 AND 4 DEGREES HORIZONTAL

FIGURE 3-17

4.0 SPECIFICATIONS/SIZE/COST OF OPERATIONAL AGIPA/TDRS-LDR/LINK

An effort is made in this section to state the specifications, size, and cost of an operational AGIPA system on a per-user basis. Generally speaking, most specifications for an operational AGIPA/TDRS-LDR/Link cannot be stated independent of the remainder of the TDRS system. However, the conclusions of the TDRS configuration in conjunction with Tradeoff Study NAS5-21705 and the results of this AGIPA feasibility program, some general specifications and estimates of size and cost can be made.

The following paragraphs detail the specifications required for the TDRS/LDR link beginning at the TDRS with the specifications for the array elements.

4.1 ANTENNA SPECIFICATIONS

The array antennas used in this feasibility study were selected with minimum cost as a goal. The antennas used were not designed to meet TDRS requirements. However, the following specifications are intended to meet the TDRS design requirements for the LDR receiver array elements.

Frequency	136 to 138 MHz
Polarization	Orthogonal linear
Isolation between polarizations	20 dB minimum
Input VSWR	1.2:1 maximum
Peak gain per element	11.4 dBi above linear isotropic
Peak gain for array	18.4 dBi above linear isotropic
Half power beam width (element)	45 degrees (approximate)
Half power beam width (array)	8 degrees (approximate)
Beam Squint	±3 degrees (approximate)

Size of element	
Erected - diameter	7.2 feet (approximate)
- height	3.6 feet (approximate)
Stowed - diameter	2.5 feet (approximate)
Erection technique	Electric motor driven stem unit

4.2 TDRS/GS LINK

The space/ground link of the operational TDRS system must be capable of relaying the individual channels of the AGIPA array to the ground station. Because the adaptive processing of the data and interference signals occur at the ground terminal, it is vital to the system performance that a minimum of channel degradations occur in the TDRS/GS relay link. Each channel of the five element array contains information concerning the phase and amplitude of the desired signal relative to that of the RFI jammers.

This information, vital to the systems performance, is contained within each of the ten 2 MHz band-pass channels. The system design for the return segment of the ground link must be based upon the transmission of these ten channels with as little degradation as possible. The final amount of CNR degradation is a function of both the CNR for the user/TDRS link and the CNR for the TDRS/GS link. Considering the LDR return link, the requirements are based upon providing a CNR = 9.9 dB (that is, $P_e = 10^{-5}$) at the GS. To determine the CNR_{GS} which must be maintained on the TDRS/GS link, and to calculate the amount of degradation caused by the tandem link, , the expression applied is:

$$CNR_F = \frac{CNR_{TDRS} \cdot CNR_{GS}}{CNR_{TDRS} + CNR_{GS} + 1}$$

where:

CNR_F = final carrier to noise ratio

CNR_{GS} = CNR generated on TDRS/GS channel

CNR_{TDRS} = CNR received from the user in the TDRS receiver bandwidth

The degradation in carrier-to-noise ratio is $\Delta CNR = CNR_{TDRS} - CNR_F$. These parameters are plotted in Figure 4-1. This relationship determines the TDRS/GS link requirements. If 30 dB of spread-spectrum processing gain is assumed, a CNR = -20.1 dB is required per channel. Note that combining the ten channels at ground station yields an additional 7.0 dB of processing gain. The final required CNR for each channel, therefore, must be no less than -27.1 dB for the LDR link to remain above the required 9.9 dB threshold. To permit a maximum degradation in CNR of 1 dB, the curve of Figure 4-1 is entered at -26.1 dB and we obtain a CNR_{GS} = 6.0 dB.

Thus, for a minimum signal strength on the TDRS user return link, a CNR_{GS} = 6.0 dB is required. If the TDRS/GS link is specified for this level of CNR, then the link will be more than adequate for the higher carrier-to-noise ratio's expected on the LDR return link.

4.3 AGIPA GROUND STATION PROCESSING EQUIPMENT

The AGIPA portion of the ground station processing equipment, which begins with the output of the TDRS/GS link demultiplexer and ends with the adapted array output to the data demodulator, may now be defined. Figure 4-2 is a block diagram of the ground portion of a single user. The estimated size, cost, and processing time for the operational AGIPA equipment is predicated on the following assumptions:

- The equipment will be fabricated to best commercial practices
- Minimal documentation

- The ground processing equipment will be identical in scope and similar in requirements to that employed by the AGIPA feasibility model
- There will be one correlator per channel. That is, instead of a single time-shared correlator as employed in the feasibility model, there will be ten correlators utilized; one per channel
- The more rapid computing floating point processor unit will be assumed for all computation times and system costs.

The projected size, estimated cost, and processing time for four alternative systems is tabulated in Table 4-1. Most of the information found in Table 4-1 is a result of the cost, speed, and complexity tradeoff analysis computed in Appendixes A and B. The four alternative schemes are compared in Appendixes A and B and reflect variations in the number of users serviced per computer. These schemes vary from one computer per user to forty users per computer. The processing time per step is a function of both the computer usage and the computer model assumed. The Nova 820 is a slightly quicker computer than the Nova 1220. These two computers have been selected as representative of the models presently available and capable to contain a Floating Point Processor Unit integral to their main frame.

The projected size of the 40-user AGIPA system is estimated in terms of the number of standard six-foot high equipment racks (Bud Model E-2005 or equivalent) necessary to hold the systems. Based on the present size of the feasibility model and taking into consideration that no effort was expended in miniaturizing the hardware, it is estimated that any one user could be contained within a single, 4-inch high, 23-inch deep, standard 19-inch wide equipment rack drawer. The two alternative computer models selected, the Data General Nova 1220 and the Data General 820, both occupy 10-1/2 inches of a standard 19 inch equipment rack. On the basis of the number of users (40) and the number of computers employed to service these

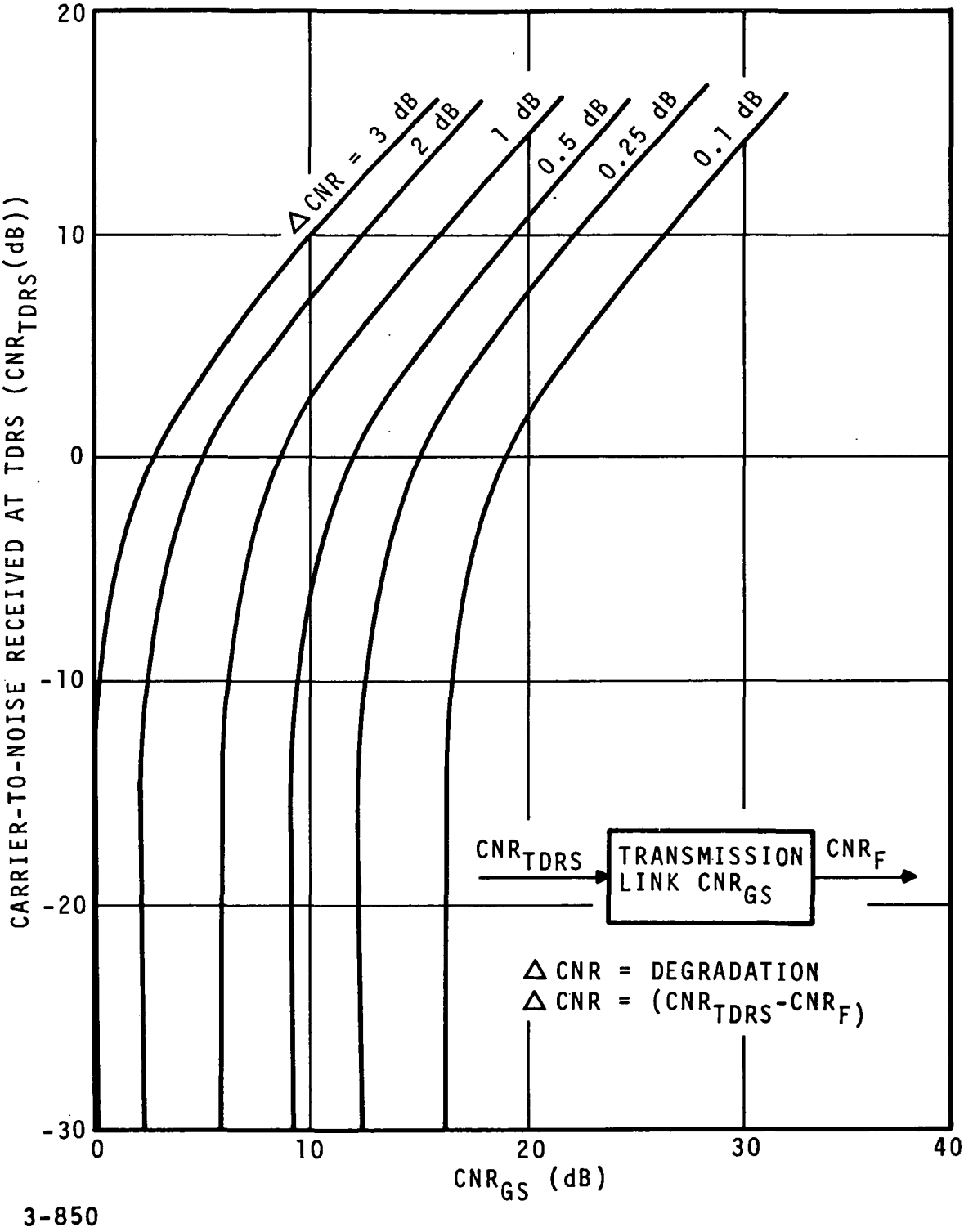

FIGURE 4-1. CNR REQUIREMENTS IN TANDUM LINK AS A FUNCTION OF CNR DEGRADATION THROUGH TDRS

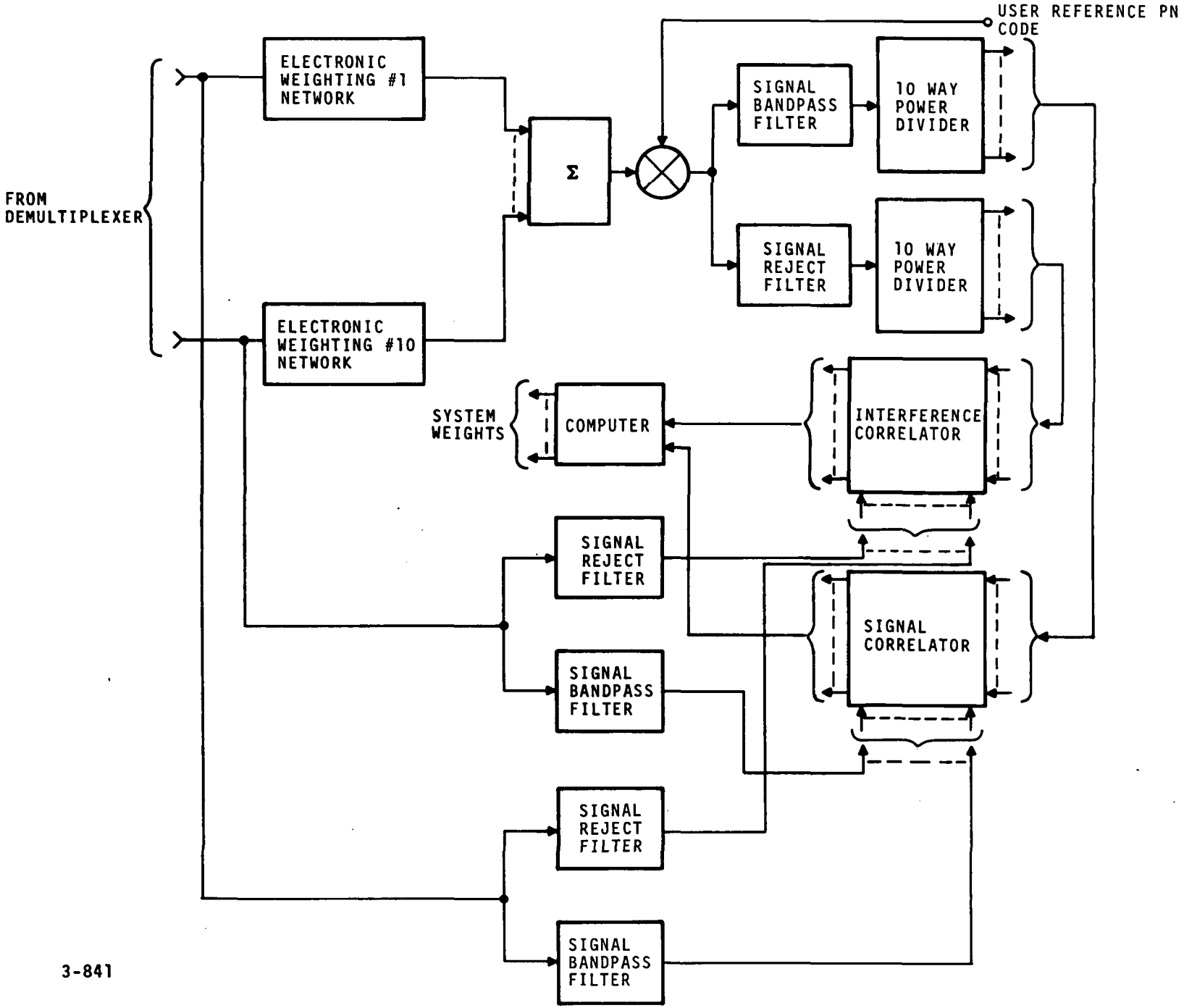

FIGURE 4-2. AGIPA GROUND STATION PROCESSING EQUIPMENT, BLOCK DIAGRAM

TABLE 4-1. SIZE, COST, AND PROCESSING TIME

Users/ Computer	Computer	Processing Time/Step (ms)	Minimum Quantity Standard Equipment Racks Required	Cost/ User*	Remarks
1	Nova 1220	49	10.5	$55 k	Inefficient use of computers Large amount of racks required Possibly more expensive Minimum software changes Most flexible
4	Nova 1229	49	7.5	$48 k	Optimum use of computers 10-four channel multiplexers required
5	Nova 820	46	4.5	$47 k	Rapid Processing Optimum use of equipment 8-five channel multiplexers required Additional software required
40	Nova 820	360	3.5	$45 k	Very slow Complex multiplexer required Complex additional software required

* Includes computer spares but is exclusive of multiplexer costs, G&A, fee, field installation, or system integration.

users for the 12 alternative schemes of Table 4-1, the quantity of standard 6-foot equipment racks was computed.

The estimated per user costs tabulated in Table 4-1 do not reflect the additional cost incurred by the time shared multiple users for either the necessary multiplexers or the supplementary software required to implement the multiple users per computer scheme. When these costs are not considered, the five users per computer scheme appears to be the favored approach. The five users per computer scheme has the most rapid processing time, is less expensive than the single user per computer scheme, and employs only a moderate number of equipment racks. The single computer per 40 users scheme, although the least expensive technique, has such a slow processing time that the moderate cost savings over the five user per computer scheme could not justify the increased processing time.

If the costs for a multiplexer and the required additional software can be kept below $40,000 each ($8000 per user), then the five users per computer scheme would remain the favored approach. However, if these costs increased or if a system was envisioned where there would be substantially less than 40 users, and the efficiencies of the five users per computer scheme could not be realized, then the single user per computer with its flexibility and lack of complexity could easily become the favored approach. The costs tabulated in Table 4-1 on a per-user basis are for a 40 user AGIPA system only. As mentioned previously, they do not include either the multiplexer or software necessary for the multiple users per computer schemes, nor do they include field installation, the fee, G&A, or the necessary on-site system integration or maintenance.

APPENDIX A
AGIPA TRADEOFF ANALYSIS

This appendix investigates the ground station processing equipment and computing equipment in particular for 40 simultaneous users. Tradeoffs are made between cost, speed, and complexity, and are used to recommend a specific configuration. The AIL feasibility model, constructed for a single simulated user, is used as a model for the system processing equipment.

The tradeoff analysis shows that a computer-sharing technique will provide a cost savings in computer hardware, while permitting processing for each user at the same rate as if each had its own computer. A configuration of eight Nova 820 computers, with each computer servicing five users is recommended.

The cost of the recommended computer system is approximately $75,000. A nonshared computer system would cost close to $300,000. At the other extreme, a single computer, costing approximately $10,000, would be capable of processing all 40 user signals, but with a significant penalty in speed.

Processing Time

The AGIPA feasibility model system employs a Nova 1200 computer. The following improvements are proposed to achieve optimum processing speed:

Build 10 correlators
Add floating point hardware
Streamline software for input/output conversions

The expected processing time with these improvements can be broken down to be:

Inputs, computation, and outputs:	12 ms
Settling time for filters:	37 ms
Total time per step -	49 ms

Approximately 75 percent of the total time is spent waiting for filters to settle. This time could be used profitably performing other computations. There is sufficient time for computation for three other users (3×12 ms) while the first user's filters are settling. With a program alternating the computer among four users, they can all be processed at the same speed as if they had individual computers.

Data General Corporation, the manufacturer of the computer used in the feasibility program, also manufactures compatible machines with faster hardware execution times. The improvement for the AGIPA application is not proportional to the increase in machine speed, since only one model of Floating Point Processor is available. However, the Nova 800 series contains a high speed data channel, which would decrease computation time to an estimated 9 ms. Then, the filter waiting time becomes 80 percent of the total time, enabling each computer to service five users at maximum speed.

Table A-1 contains a tradeoff of processing time versus various configurations of Nova 1220 or 820 computers. The number of users per computer is also shown. The Nova 1220 and 820 models are used in the tradeoff because they have sufficient memory and interfacing capability for this application at the lowest cost.

Table A-1 shows that the processing time is essentially equal for 10 or more Nova 1220's or 8 or more Nova 820's. Using fewer than these numbers of computers results in a drastic increase in processing time.

TABLE A-1. PROCESSING TIME VERSUS COMPUTER CONFIGURATIONS

Computers	Computer Type	No. of Users per Computers	Processing Time/Step (ms)	Remarks
40	Nova 1220	1	49	Inefficient use of computer
20	Nova 1220	2	49	Inefficient use of computer
10	Nova 1220	4	49	Best use of computer
8	Nova 820	5	46	Best use of computer
5	Nova 1220	8	96	
5	Nova 820	8	72	
4	Nova 1220	10	120	
4	Nova 820	10	90	
2	Nova 1220	20	240	
2	Nova 820	20	180	
1	Nova 1220	40	480	
1	Nova 820	40	360	

Therefore, the optimum number of computers for fast processing is 10 Nova 1220's or 8 Nova 820's.

Reliability

The Data General Reliability Report on Nova Line Computers gives a MTBF of 5600 hours for a Nova 1200 and 4800 hours for a Nova 820, both with 8K memory. These figures do not include the Floating Point Processor, which would add fractionally to the failure rate.

The failure rate of a computer does not depend on the number of users it services. The total number of computer failures in a 40-user system will be lower for a shared-computer system, as there are fewer computers.

An analysis of the recommended 8-computer system was made using a binomial distribution of failures, as each machine's failures are independent. For a period of 560 hours for Nova 1200's or 480 hours for Nova 820's, the probability of six of the eight computers continuing to operate is 0.962. Therefore, if no repair work were possible for 20 days, two spare computers would be sufficient 96.2 percent of the time. In fact, most failures can be quickly repaired by replacement of a printed-circuit board. If we use 24 hours as the mean time to repair, the probability of six of the eight computers continuing to operate is 0.9999. This means that two spare computers will be sufficient for the installation if repair service is provided, as there is less than one chance in 10,000 of a third failure in the 24-hour period.

The reliability of any one channel is not changed regardless of whether or not it shares a computer. Clearly, the shared-computer system increases the probability of five channels being out of service, for the case when a spare computer is not available. However, the probabilities derived above make this situation rare. The need to provide repair service exists regardless of the number of computers used. Therefore, the recommended system should achieve excellent reliability, with two spare machines serving as back-ups. A regular program of preventive maintenance should also be provided, as and adjunct to the repair service.

Data Loss

With the recommended computer configuration providing optimum processing time, as detailed above, the AGIPA hardware for each user will be able to track its signal at all times and provide optimum signal to interference ratios and error rates consistent with the antenna array geometry and the RFI environment. In such a case, the only additional data loss would occur at the time of hardware failure.

Signal processing hardware failure could be quickly identified by computer controlled tests. These tests could be initiated manually or automatically at the occurrence of loss of lock. The one user whose processing unit failed would be lost until new hardware were to be switched in. If this were done within one minute, the user's computer could continue to track the user, as it traverses less than one degree per minute.

Computer failure would probably manifest itself in one of two ways: the computer would generate meaningless weights, resulting in loss of lock; or, the computer would cease its processing, resulting more gradually in loss of lock. Also, power failure is possible. A simultaneous loss of lock for all users serviced by one computer will point out that computer as the source of failure. Data from all its users would probably be lost until a backup computer were switched in and could acquire each new user. The switching can be accomplished in a few seconds after the computer failure is recognized.

Cost Considerations

The various machine configurations have been priced according to the Data General Corporation price list dated 1 August 1972 and Data General Corporation OEM Discount Agreement Form 202 dated April 1972. The machine configurations consist of:

Nova 1220 or 820 central processor with 8K core memory
Floating Point Processor
Interface for AD converter
Turnkey console

The various quantities of machines qualify for increasing discounts, according to the OEM schedule. Table A-2 lists the total cost for each of the configurations considered in TableA-1. Quantities of spare computers are also listed, in approximate proportion to the results of the section on Reliability above. The cost of computers and spares is also listed.

TABLE A-2. COMPUTER COSTS

Computers No.	Computers Type	Cost ($)	No. Spares	Total Cost ($)
40	Nova 1220	291, 060	8	349, 272
20	Nova 1220	152, 145	4	182, 574
10	Nova 1220	81, 585	2	97, 902
* 8	Nova 820	75, 306	2	90, 465
5	Nova 1220	44, 651	2	59, 425
5	Nova 820	49, 511	2	65, 893
4	Nova 1220	35, 721	2	50, 935
4	Nova 820	39, 609	2	56, 479
2	Nova 1220	18, 742	1	26, 791
2	Nova 820	20, 782	1	29, 707
1	Nova 1220	9, 922	1	18, 742
1	Nova 820	11, 002	1	20, 782

* Recommended System

Multiplexer costs have not been considered. Appendix B will show how a shared-computer system results in a reduction of multiplexer hardware, compared with a 40-computer system.

Selected Approach

The recommended configuration for the 40 users consists of eight Nova 820 computers, each processing five of the users. As shown above, processing time considerations allow the sharing of a computer among five users with no penalty in speed.

Figure A-1 shows a cost versus speed tradeoff for various configurations of machines. The recommended system is seen to have both the

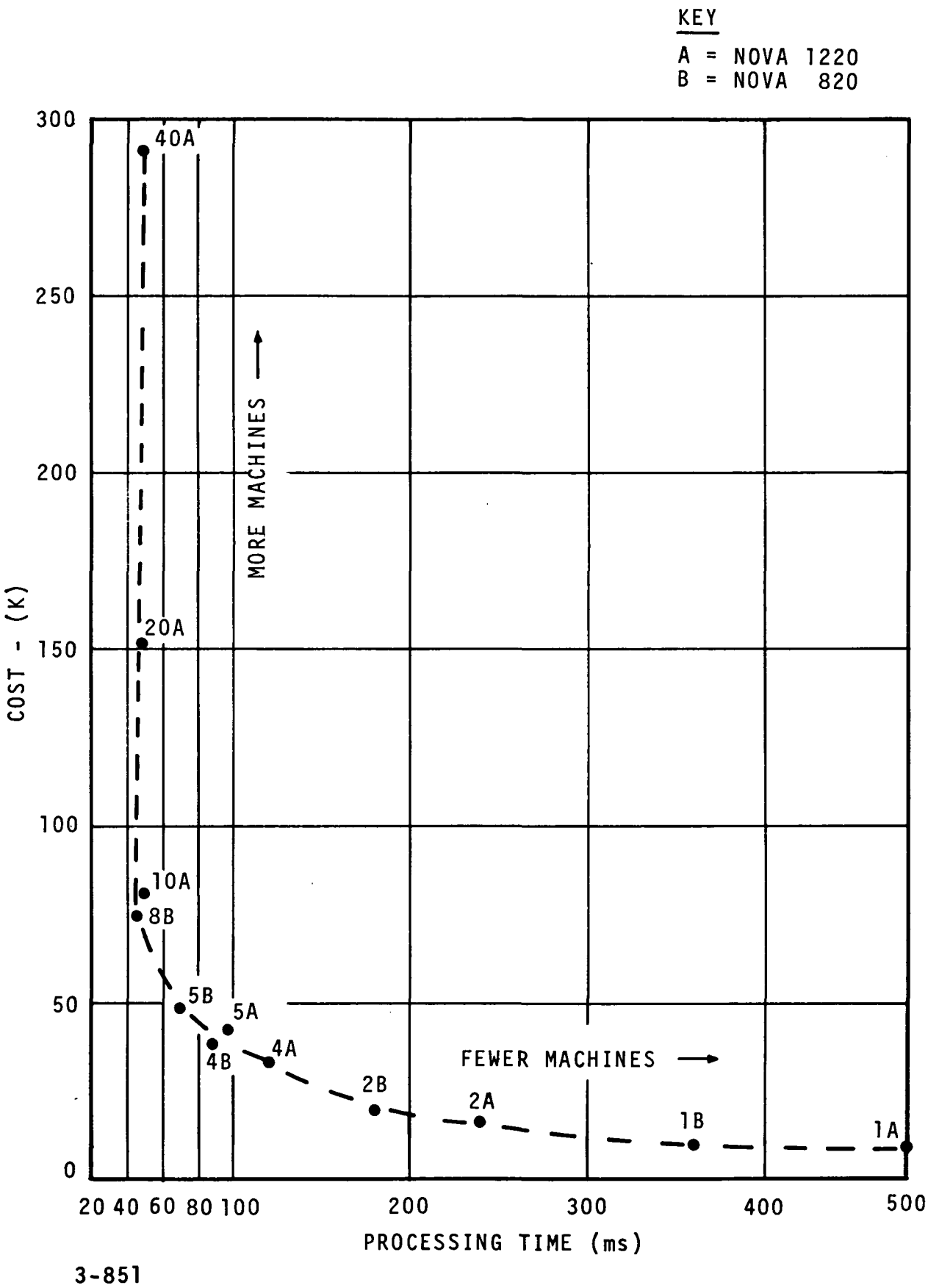

FIGURE A-1. COST VERSUS SPEED TRADEOFF

lowest cost and fastest processing time for the alternatives shown. The use of more machines does not improve processing speed. The use of fewer machines saves money, but at a drastic penalty in processing speed.

The cost of backup computers, which was list in Table A-2, does not affect the shape of the curve in Figure A-1. With 2 backups, the cost of the recommended system is $90,465.

APPENDIX B
SHARED-COMPUTER AGIPA SYSTEM

Functional Description

The increased number of inputs to a shared-computer system can be accommodated by a straightforward extension of the analog multiplexing system now used for input. Figure B-1 shows the detail of a multiplexer for each AGIPA signal processing unit. The inputs to this multiplexer are the X-signal, Y-signal, X-interference, and Y-interference from each correlator, and the signal and interference detector outputs. This totals 42 inputs, and requires two levels of standard eight-input multiplexers. Each multiplexer is switched by a counting-decoding circuit, which is stepped by a control line from the computer.

Figure B-2 shows the outputs of five AGIPA processors multiplexed once again for reading into a single ADC. This scheme, which can also be expanded, enables one computer to read in the 210 analog inputs required for five users. The analog multiplexer and the few logic circuits required for control are the only additions required for input to a shared computer. On the other hand, this method only uses one ADC per five users, while a nonshared system would required five ADC's for five users.

For output, a decoder circuit enables one channel to receive data, as shown in Figure B-3. The clock and data are sent to all five users, but only affect the desired user. The decoder is the only addition to the shared system, while a nonshared system would require a separate output logic circuit for each user.

The shared system, then, is of nearly the same complexity as a nonshared system. Increases in hardware are offset by decreases, as

described above. The resulting cost differential is negligible compared to the computer cost, and has not been evaluated in detail.

Programming Changes

The program for a shared computer will be virtually unchanged. The only additions will be a counter to determine the user being processed and longer lists to store pertinent data. Immediately after output of new weights for one user, the program will read input data for the next user. As detailed above, in "Processing Time," there is time to process four other users while a fifth is waiting for its measurable voltages to settle. The result is an efficient use of computer power, with no delay in processing speed for the five users controlled by each computer.

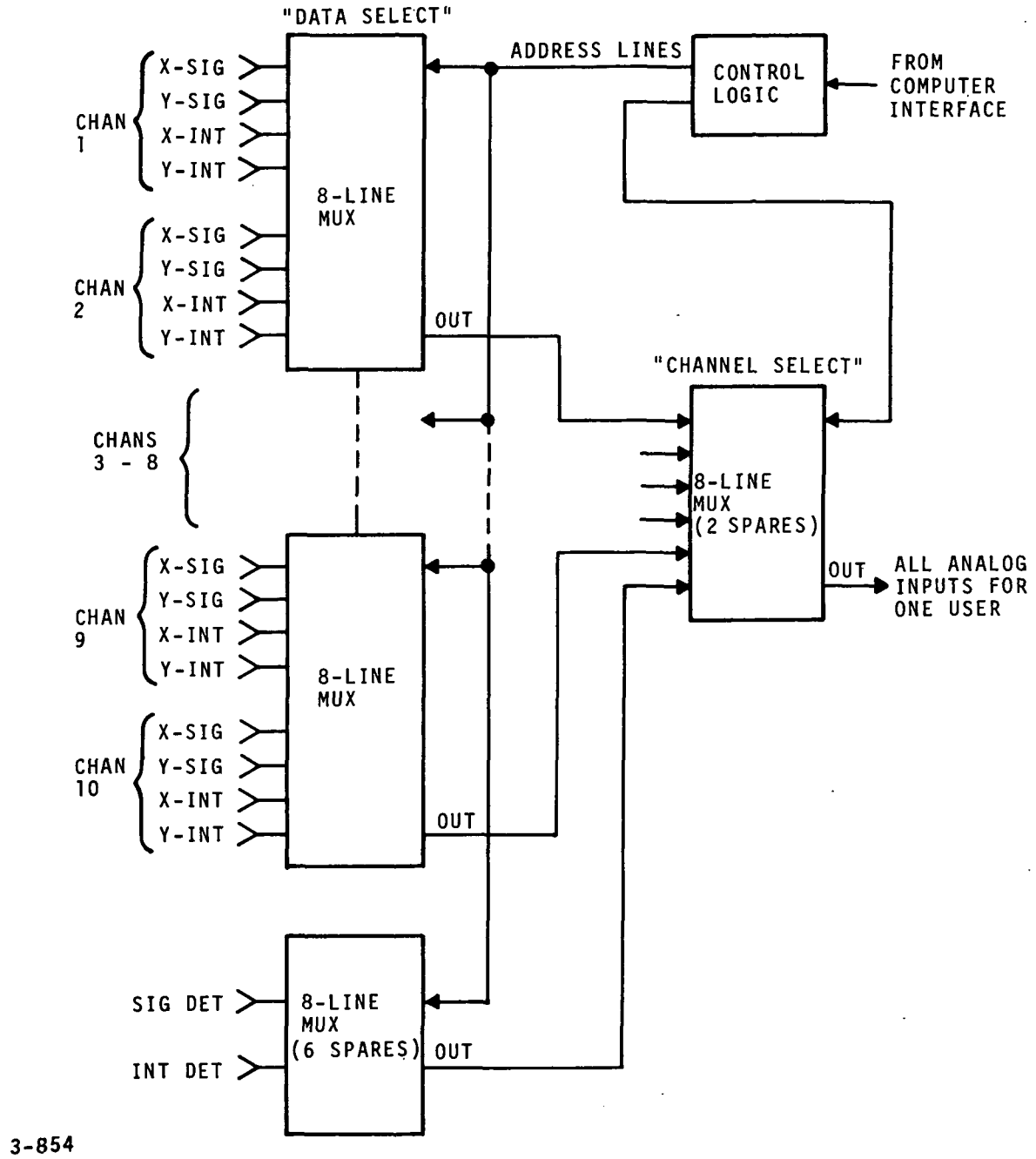

FIGURE B-1. MULTIPLEXER ASSEMBLY FOR AGIPA SIGNAL PROCESSING UNIT

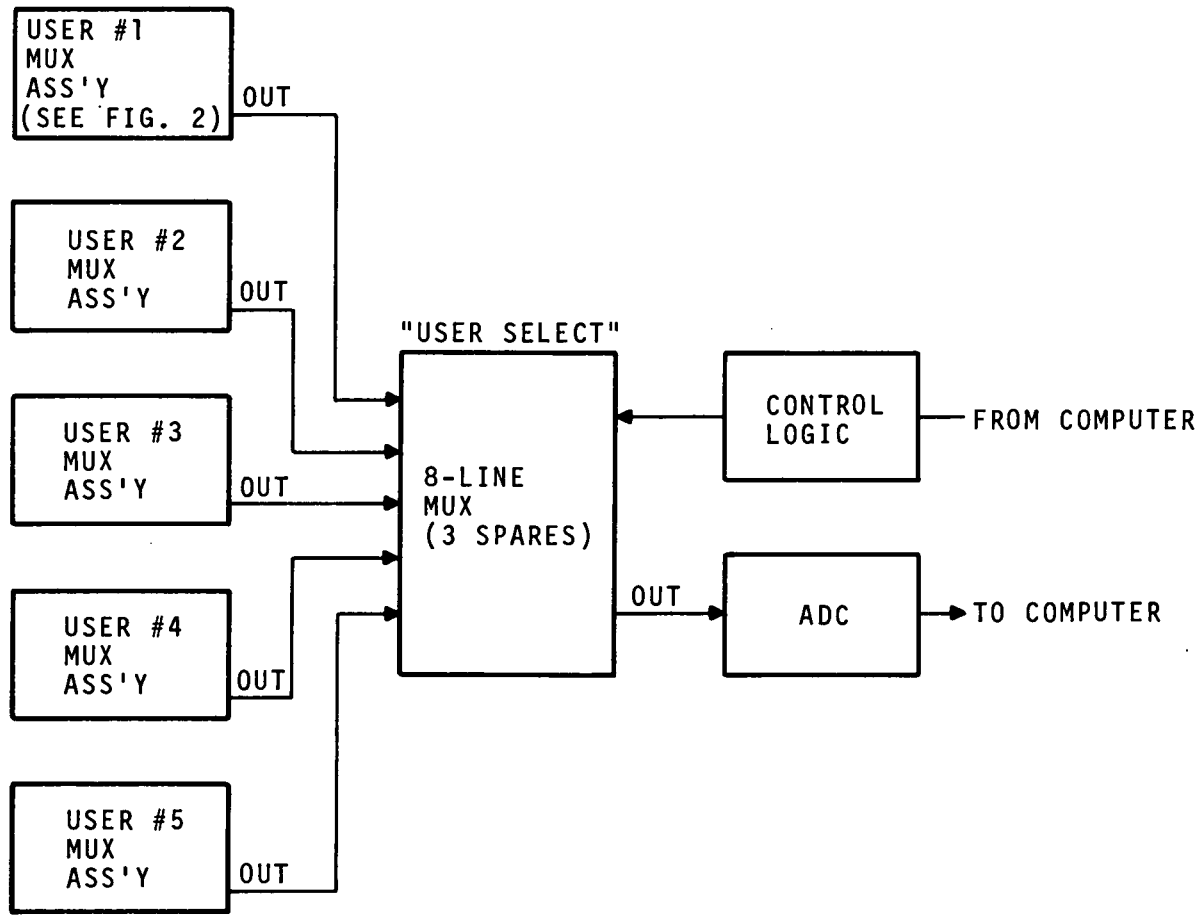

FIGURE B-2. MULTIPLEXER FOR SHARED COMPUTER INPUT

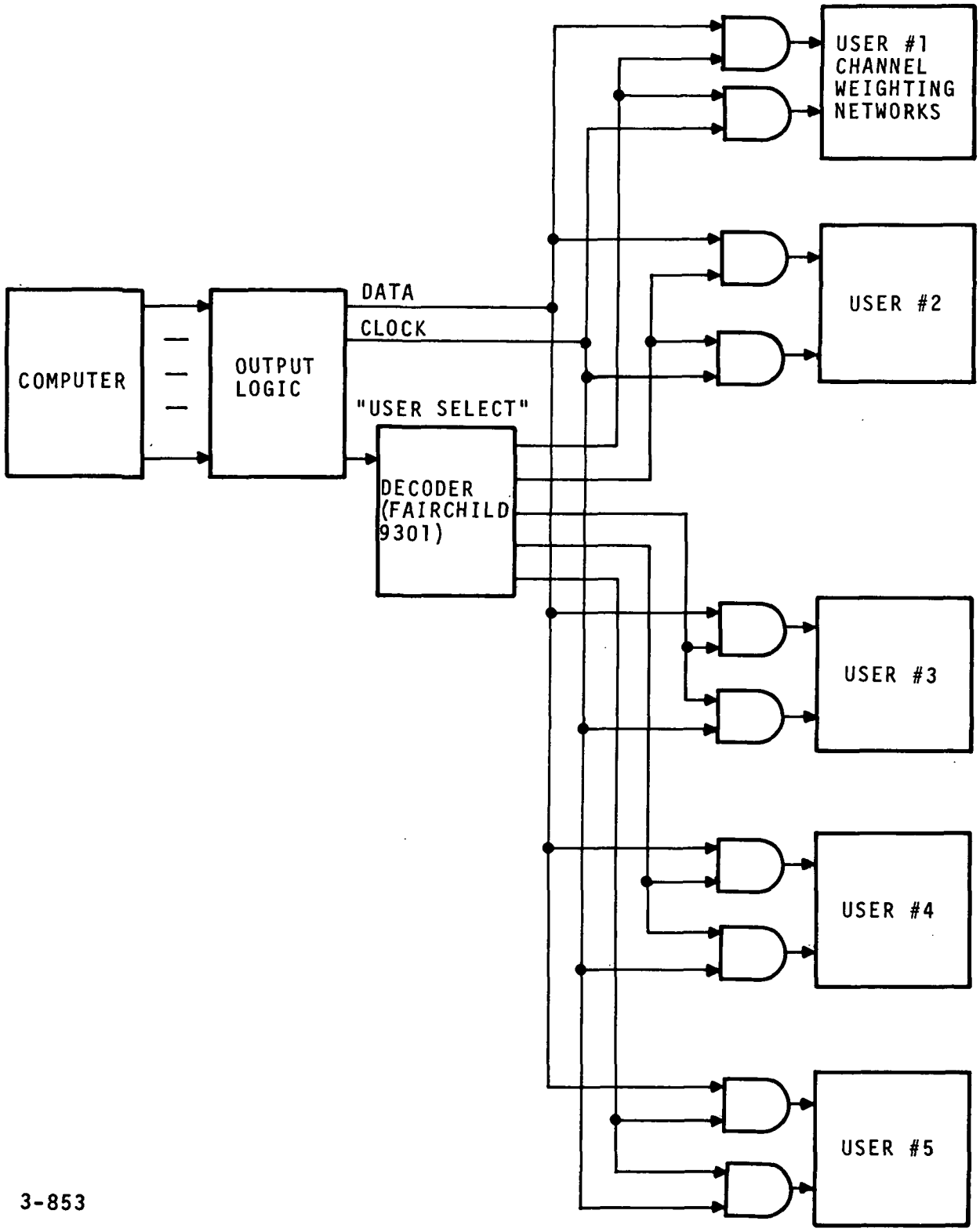

FIGURE B-3. DATA MULTIPLEXER FOR COMPUTER OUTPUT TO MULTIPLE USERS

APPENDIX C

ADDITIONAL TESTING OF GOLD CODE MODULATION TECHNIQUES

September 1973

J. M. Smith (Project Engineer)

W. B. Denniston (Engineer)

Modification Number 2

Dated 13 August 1973

INTRODUCTION

Upon receipt on 13 August 1973 of Modification Number 2 to NASA Contract NAS-5-21653, AIL proceeded to build the necessary hardware to evaluate the performance of the pseudo-random sequences which are being considered for application in the S-Band Multiple Access Link of the Tracking Data Relay Satellite. The results of the tests are contained in this appendix as directed in the contract modification.

The specific parameters which were evaluated related to the amount of degradation introduced into the system by restricting the RF spread spectrum bandwidth occupied by a received pseudo noise coded signal and the measured isolation between signals encoded by unique pseudo-random sequences (Gold codes).

To perform the tests, several components developed for the AGIPA system functioned as test instrumentation simplifying the tests and minimizing the amount of new hardware required.

The following sections describe the tests, the method employed for obtaining the test data, and a comparison of the measured results with theoretically predicted data.

This appendix is organized as follows:

Section 1.0: General Test Description

Section 2.0: Test One Description and Results

Section 3.0: Test Two Description and Results

1.0 GENERAL TEST DESCRIPTION

Test one, the first part of this two part testing program, was devised in order to measure the degradation in processing gain resulting from channel band limiting of a pseudo-random encoded data signal. Figure C-1 is a simplified block diagram of the equipment configuration necessary to implement test one.

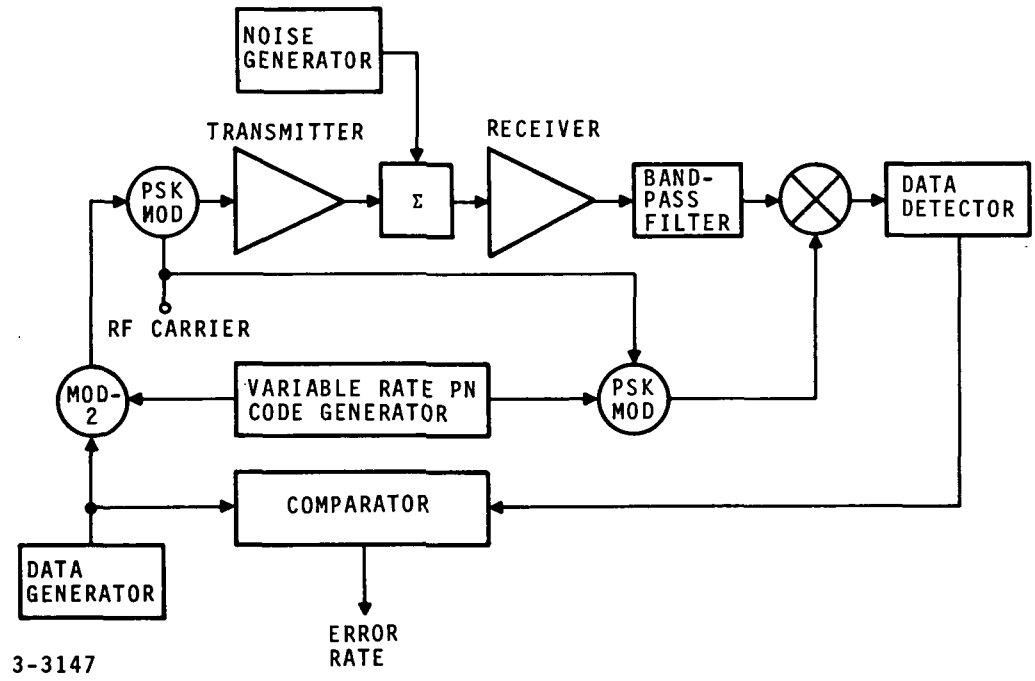

FIGURE C-1. SIMPLIFIED BLOCK DIAGRAM TEST ONE

A low frequency data stream is modulo-two added to the output of a variable rate pseudo-random code generator and the resultant signal employed to PSK modulate an RF carrier. The biphase modulated signal is summed along with an artificially generated noise signal and the aggregate result is channelized through a fixed bandwidth narrow band-pass filter. A similarly encoded carrier signal, employed as a reference, effectively

removes the code and the data is subsequently detected and compared on a bit-by-bit basis with the original data stream. By maintaining the channel bandwidth fixed and varying the code generator chip rate, the degradation in processing gain, as measured by the data stream error rate, may be determined as a function of the channel bandwidth-to-code chip ratio.

For the second test, the objective was to measure the isolation between two pseudo-random Gold codes. Figure C-2 is a simplified block diagram depicting the basic test layout for test two. The test setup shown in Figure C-2 is similar to that required for test one with the addition of a second Gold code generator. For this test the chip rate was maintained constant, but the selected sequence of the two code generators and the phase relationship of their outputs were made variables.

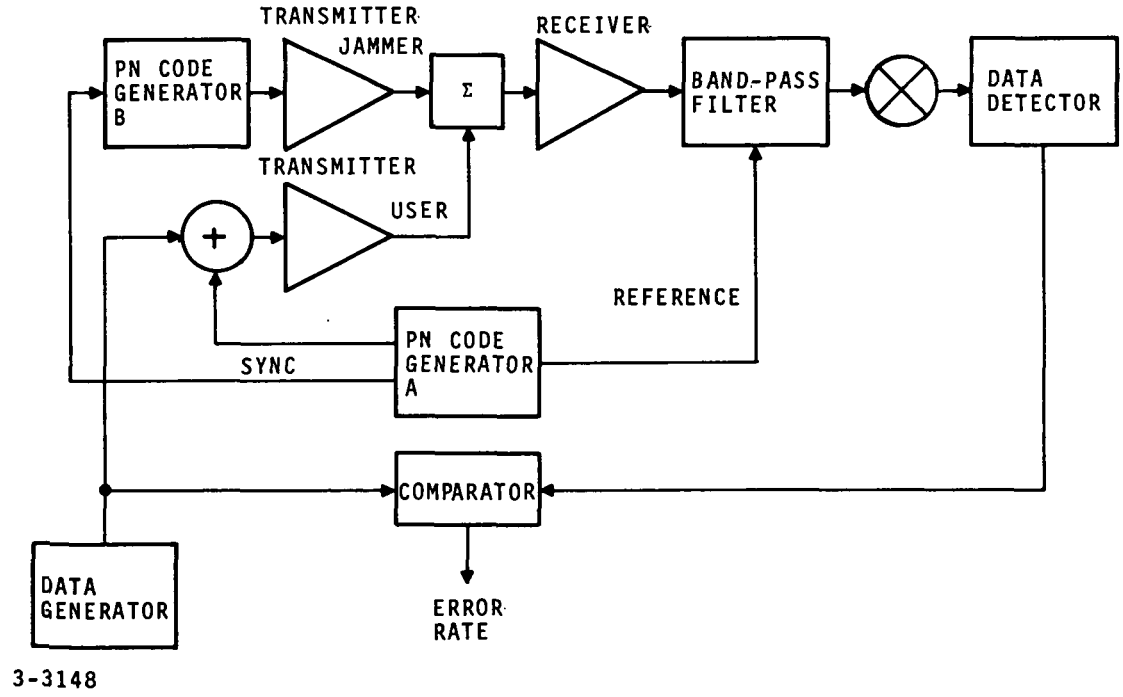

FIGURE C-2. ISOLATION TEST OF PN CODED SIGNALS

The output of code generators "A" and "B" are both employed to PSK modulate identical frequency RF carriers. Both modulated signals are summed and fed to the test receiver. The reference signal at the receiver is an RF carrier modulated by a code sequence identical to that of code generator "A." The reference signal will have a high cross correlation value with its like received code, Code A, and a low cross correlation value with the received Code "B" modulated signal. It is the objective of this test to record the degree of rejection of, or isolation between, the dissimilar sequences.

2.0 TEST ONE DESCRIPTION AND RESULTS

2.1 TEST ONE DESCRIPTION

To measure the error rate as a function of bandwidth-to-chip rate ratio (BW/CR), the filters in the receiver main line and reference (LO) line were fixed at 4.5 MHz while the chip rate of the pseudo-random code was varied from 0.5 to 5.0 MHz. The upper limit was determined by the maximum rate available from the code generator while the lower limit was selected because lower chip rates did not cause any further improvement in the error rate.

Figure C-3 is a block diagram of the actual setup used for this test. The error rate is determined by the bit error rate tester (BERT) at the lower left of the figure. The BERT generates a 1.0-kbs pseudo-random data stream which is modulo-2 added to one output of the code generator. The code generator can generate any one of 8191 sequences, all belonging to the family of sequences called Gold codes. The Gold code length is 8191 bits and the chip rate is controlled by the variable rate clock frequency. The encoded data PSK modulates a 137-MHz carrier and subsequently is summed with RF noise. The noise is generated by a high gain 137-MHz IF strip. The power level of both signals is individually controlled by variable attenuators.

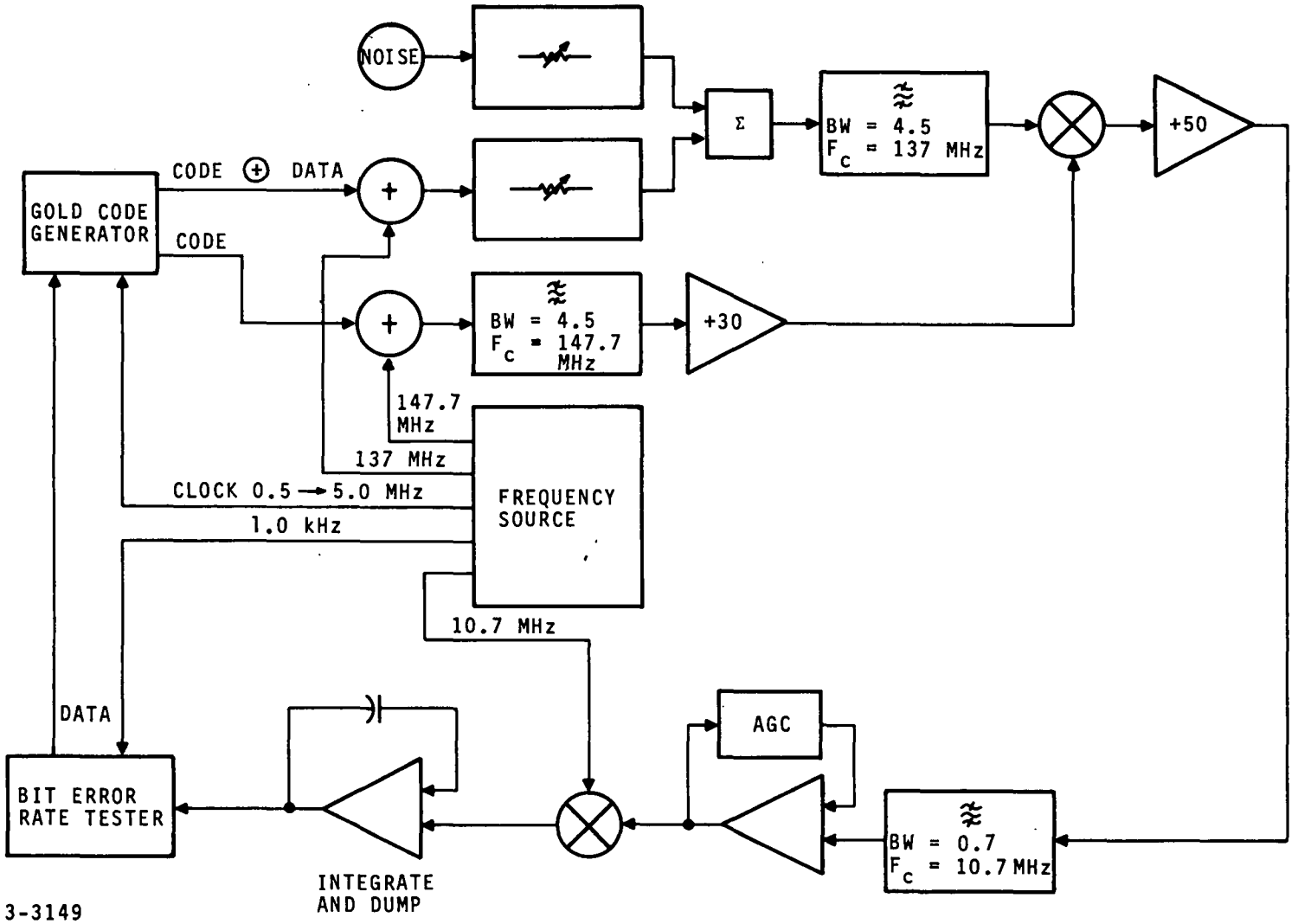

FIGURE C-3. BLOCK DIAGRAM OF BW/CR VERSUS ERROR RATE TEST

The spread spectrum user signal and the noise are filtered by the receiver band-pass filter which has a noise bandwidth of 4.32 MHz. Figure C-4 plots band-pass characteristics of this filter. The filter is a five-pole Tchebycheff with a 0.5-dB ripple.

The 137-MHz filtered output is then mixed with a 147.7-MHz reference signal. The reference signal is produced by the code generator's other output (that is, PN code only) which is employed to PSK modulate a 147.7-MHz carrier. In the receiver the two signals are multiplied and the resultant is a data modulated 10.7-MHz carrier.

This signal is amplified and filtered by a 700-kHz filter to reduce the wideband noise power going to the AGC controlled amplifier. The AGC amplifier output is downconverted by a coherent 10.7-MHz carrier thus giving the data at baseband. The data is then detected by an integrate and dump circuit, which decides on the presence of a one or zero, and then compared in BERT with the generated data stream to determine the number of errors accumulated over a preset period of time.

2.2 TEST ONE RESULTS

The first step taken during testing was to plot a reference curve at 0.5 MHz or a BW/CR of 8.64 which plots error rate versus the signal attenuation. Reference was then made to an ideal curve for a DPSK signal with a coherent reference to determine the absolute noise level and the error rate was plotted versus signal-to-noise ratio for BW/CR = 8.64. The error rate was then retaken at a fixed signal level for BW/CR = 8.64 and then recorded at the other four chip rates. The data recorded at BW/CR = 8.64 established the noise level at that time. Data taken at the other chip rates was accepted as long as a monitor of the noise level did not show any change. Data was taken in this manner at a number of signal power levels; Figure C-5 plots the results.

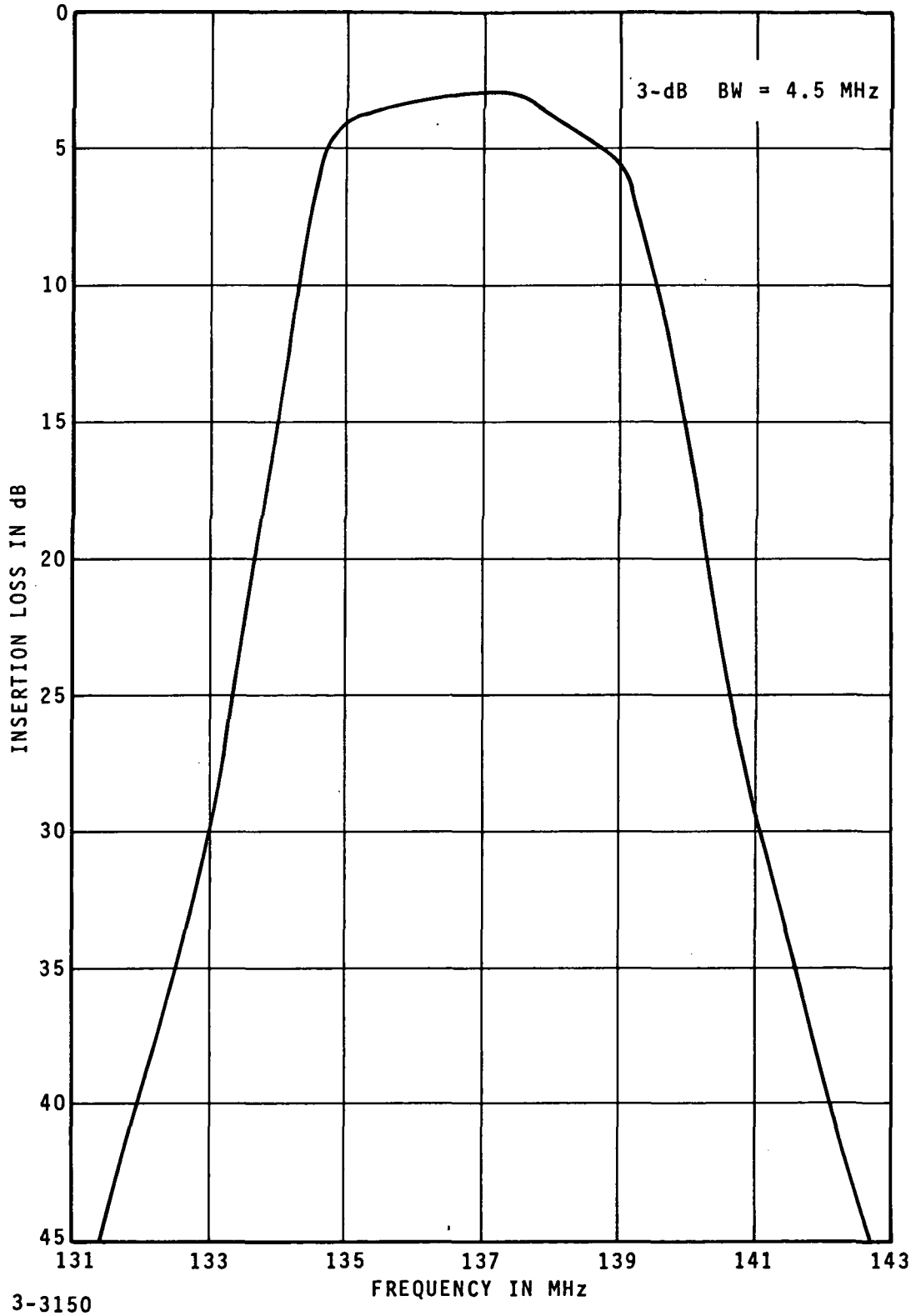

FIGURE C-4. 137-MHz BAND-PASS FILTER

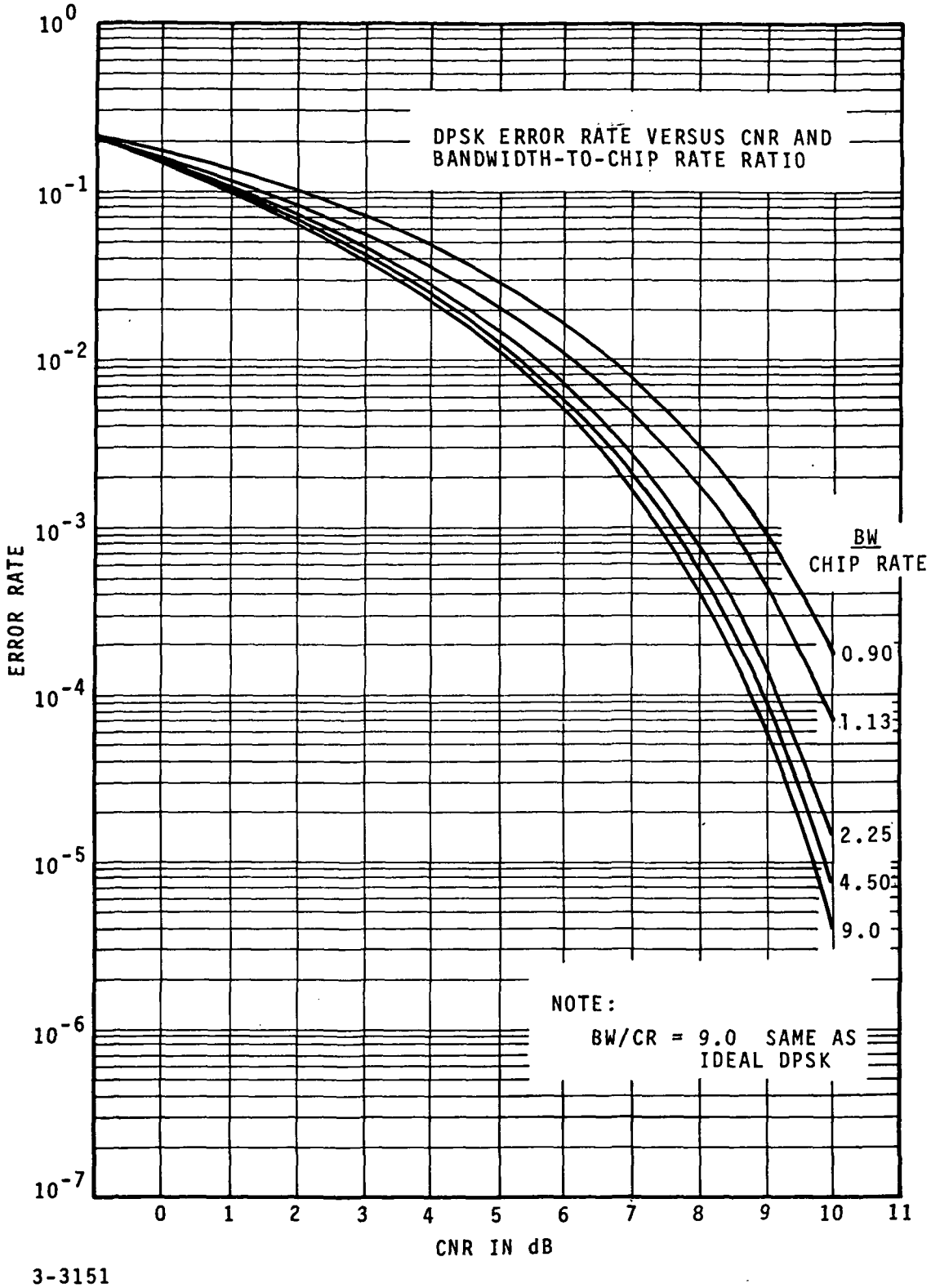

FIGURE C-5. EFFECTS OF BANDWIDTH REDUCTION

The curves show a definite degradation with decreasing BW/CR. The lowest curve taken at BW/CR = 8.64 follows an ideal curve while, in contrast, the lower BW/CR ratios reflect an increasing error rate. Figure C-6 plots an expansion of the low error rate portion of the curves and the degradation is more obvious. Figure C-7 is a plot of the degradation versus BW/CR ratio taken from the curves in Figure C-6. From this curve it can be seen that the degradation at a BW/CR = 1.5 is 0.57 dB, while for BW/CR = 1.0 the ratio has risen sharply to 1.2 dB.

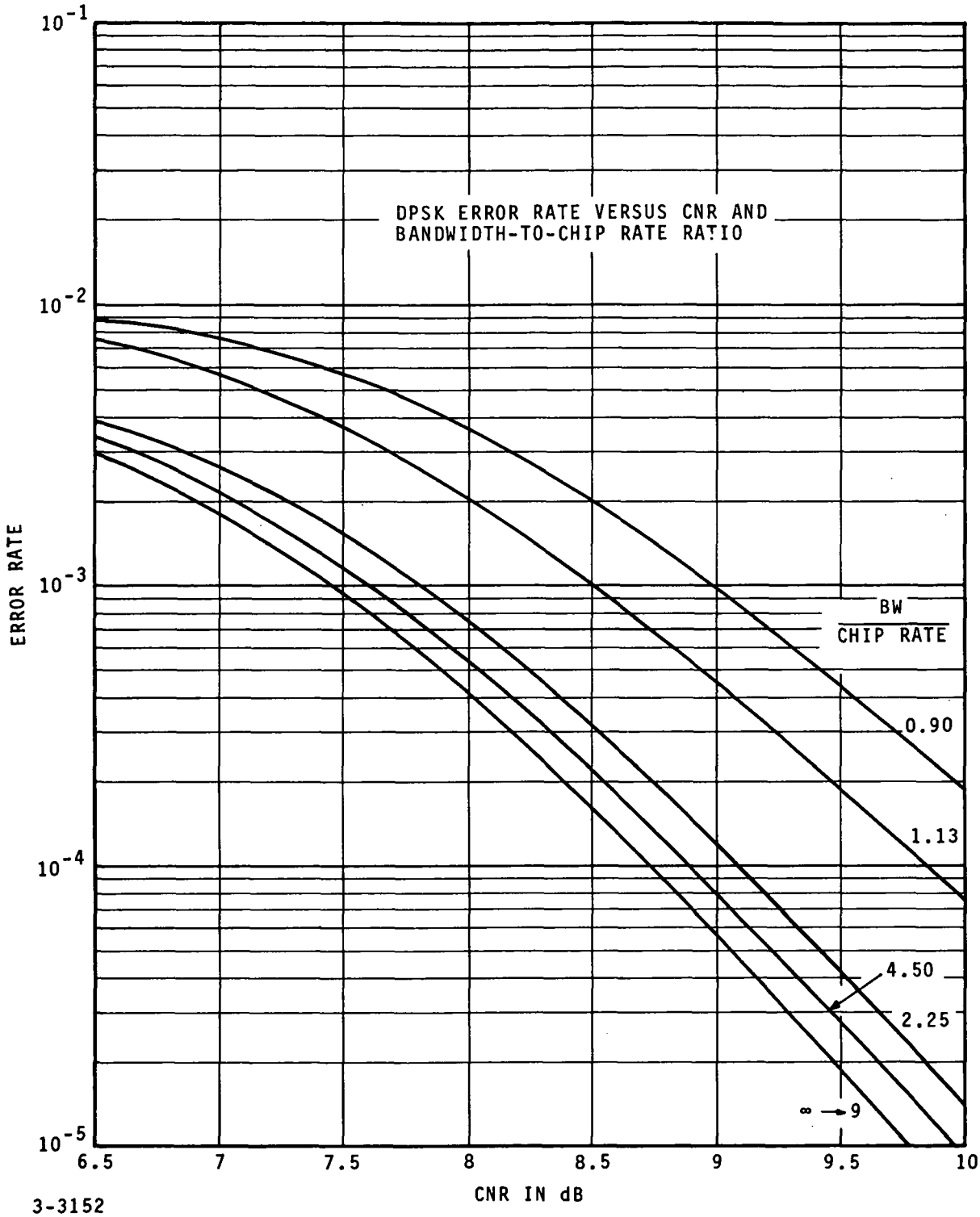

FIGURE C-6. EXPANDED PORTION OF FIGURE C-5

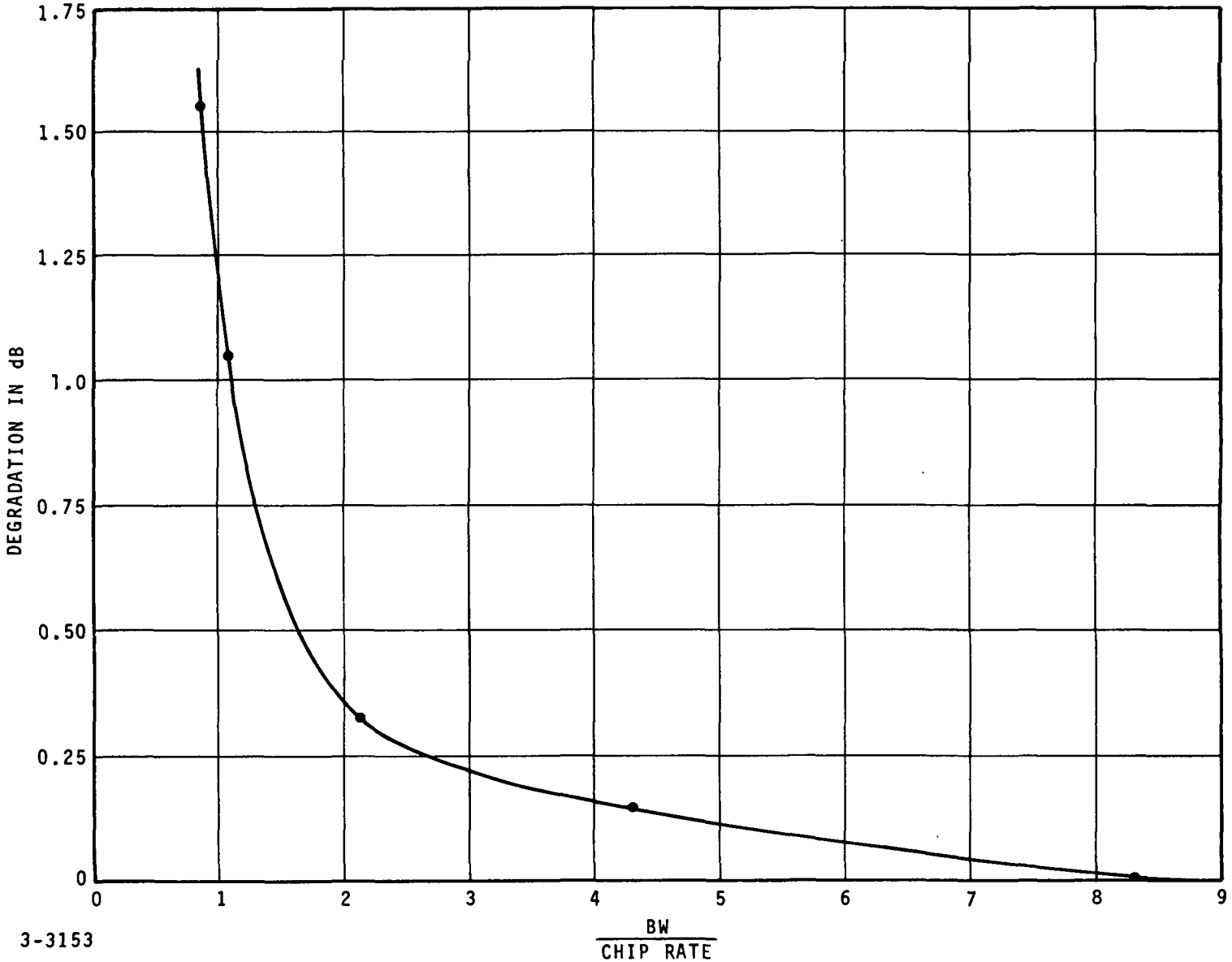

FIGURE C-7. DEGRADATION VERSUS BANDWIDTH-TO-CHIP RATIO FOR SPREAD SPECTRUM DPSK

3.0 TEST TWO DESCRIPTION AND RESULTS

3.1 TEST TWO DESCRIPTION

For this test the setup shown in block form in Figure C-8 was used. The second Gold code generator was employed to generate a sequence different from that generated by the lower generator in the figure. The cross correlation between the codes was calculated by a computer simulation of the two Gold code generators and the multiplying process. This allows the amount of noise generated to be compared with the cross correlation of the codes used. The signals were controlled in amplitude by the variable attenuators and then were coupled together along with thermal noise before being filtered by the 4.5-MHz filter. Since BW/CR = 2.16 (that is, chip rate fixed at 2 MHz, noise bandwidth at 4.32 MHz) the degradation to processing gain is shown (Figure C-7) to be 0.32 dB. The filtered signal is mixed with a 147.7-MHz reference signal which is modulated as in test one, with the same code as the desired signal. The desired signal is despread and its data now phase modulates the 10.7-MHz resultant. The added thermal noise and the cross correlation products between the reference and undesired PN code are also included with the 10.7-MHz signal. At this point a 1.0-kHz crystal band-pass filter limits the data channel bandwidth. This filter is employed to determine the RF processing gain in a data bandwidth of 1 kHz. Figure C-9 shows a plot of the filter characteristic. This plot shows the filter bandwidth to be 975 Hz with a center frequency 62 Hz below 10.7 MHz. The filtered signal is amplified by an AGC amplifier and downconverted to baseband with a coherent 10.7-MHz signal. An integrate and dump circuit detects this signal and indicates the presence of either a 1 or 0 to the bit error rate tester. The tester compares the transmitted and received signals and accumulates the number of errors during the preset number of data bits.

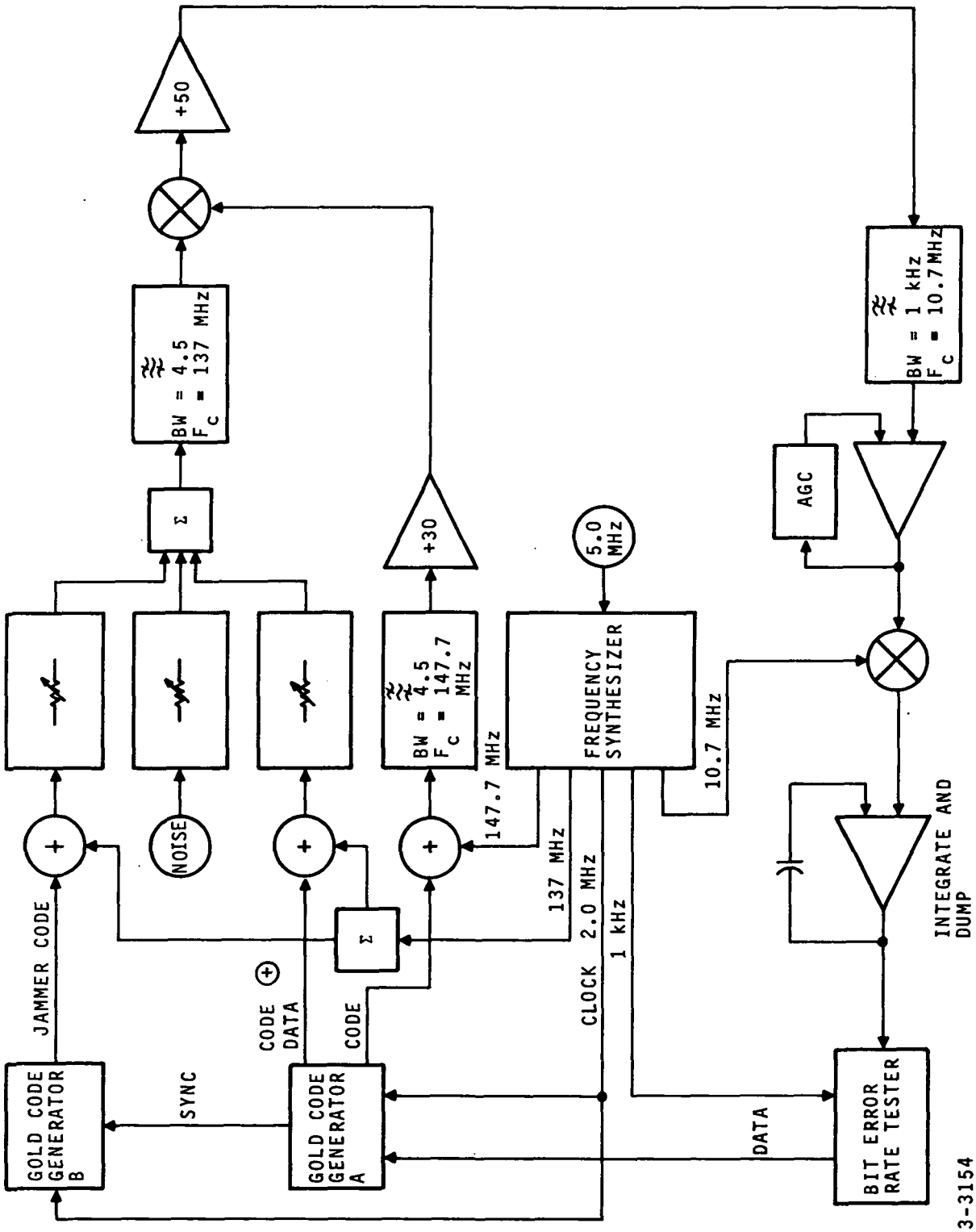

FIGURE C-8. BLOCK DIAGRAM OF PN ISOLATION TEST

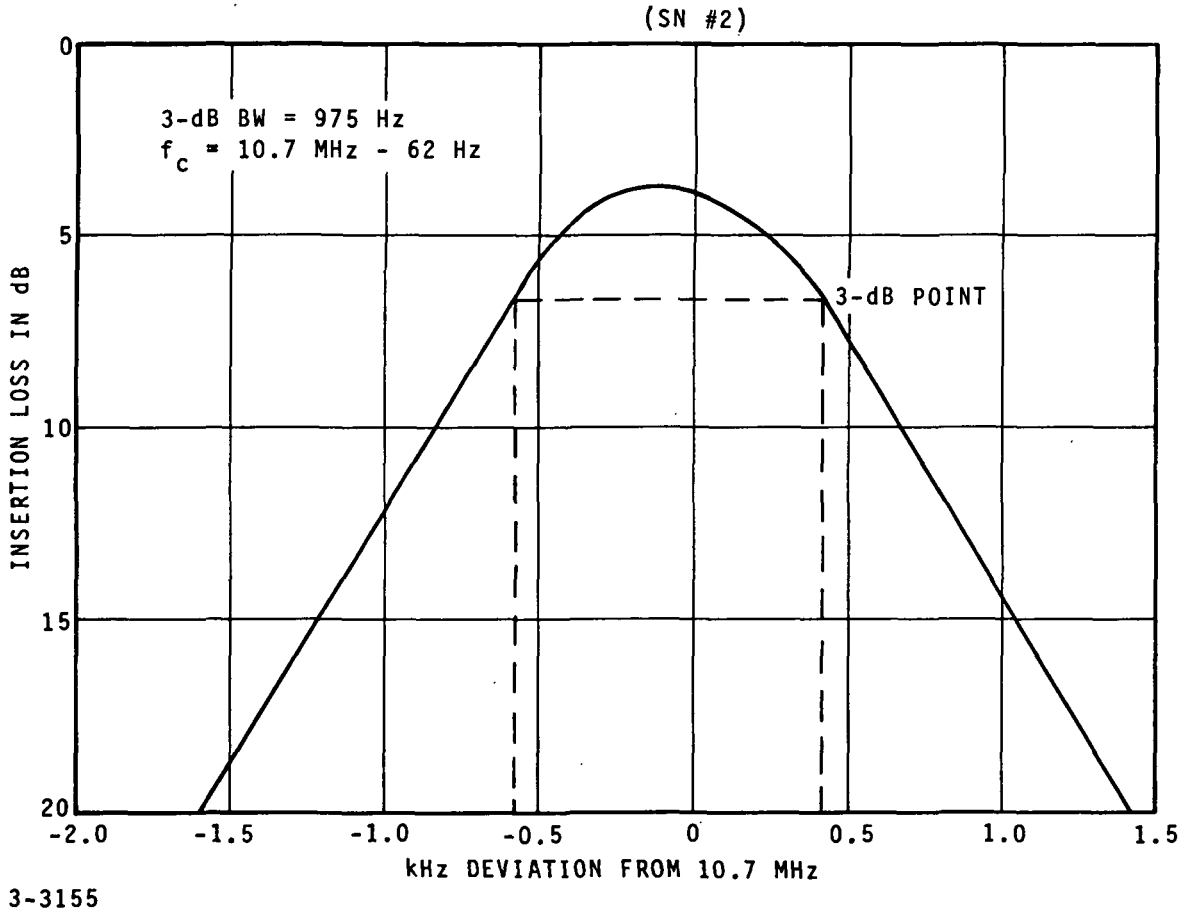

FIGURE C-9. 10.7-MHz CRYSTAL FILTER

A Gold code is generated by the modulo-2 addition of the outputs of two preferred pairs of maximal length code registers. The A register runs continuously through its 8191 steps and then repeats after reaching a state of all 1's. At this point the B register is loaded in accordance with the setting of a bank of thumbwheel switches. The B register continues through its 8191 bit sequence commencing with the loaded state. In this manner the relationship between the two registers is altered and a new Gold code results. The taps of the registers employed in these tests were prewired to:

$$A = A1 \oplus A4 \oplus A6 \oplus A9 \quad A10 \oplus A13$$

$$B = B1 \oplus B3 \oplus \overline{B4} \oplus B13$$

A front panel switch allowed the Gold code of the jammer code generator to be delayed by one bit with respect to the desired code.

3.2 TEST TWO RESULTS

To first determine the extent to which hardware limitations might influence the test findings, the PSK modulators were checked. A 500-kHz square wave was employed to modulate the RF carriers. The jammer, the signal, and the reference modulators all suppressed the carrier by 35 dB.

The actual processing gain of the system was then measured by comparing the resultant power of a CW signal to a coded signal through the 1.0-kHz bandwidth crystal filter at 10.7 MHz. The processing gain equaled 31.6 dB. It should be noted here that the noise bandwidth of the 10.7-MHz crystal filter is equal to 1530 Hz. A reduction in processing gain of approximately 1.8 dB is incurred with this filter when results are compared to an ideal 1000-Hz band-pass filter. To take the final test measurements it was necessary to find a pair of codes with high cross correlation properties. The code generators were set to produce the same code in phase and a reference

power at 10.7 MHz was noted. Then the code of the reference generator was changed by shifting the starting point of the B register. Meanwhile the A registers of the reference and jammer generators were still in phase and producing the same code. The various Gold code pairs produced what appeared to be the same value of processing gain (34.6 ±0.75 dB) regardless of the selected B register starting point. The phase of the jammer code was then delayed by one bit and a wider range of power variation resulted which showed a processing range of 27.3 dB to as great as 39 dB. Each code pair produced a different value of isolation. The code pair which resulted in the least isolation (27.3 dB) was selected to be used in the final tests. This pair was 00004_8 for the jammer and 00107_8 for the desired signal.

For the final test the signal and jammer power were measured with a wideband power meter to determine the signal-to-jammer ratio. The signal and noise error rate was recorded to determine the carrier-to-noise ratio (CNR) in the data bandwidth of 1.0 kHz. The jammer was subsequently added and the resulting error rate was recorded; Figure C-10 shows the results. The figure is referenced by the bottom ideal curve generated by the chip-rate-to-bandwidth ratio tests. The five curves cover a range of signal-to-jammer power ratios of -10.7 to -25.7 dB. The spread of the curves shows that the errors generated by a stronger jammer are less affected by the presence of noise. As the jammer power is reduced the curves approach closer and closer to the ideal noise-only curve.

These curves show that once the isolation between a pair of codes is known, the resulting error rate is easy to calculate. As an example consider the case where the carrier-to-noise ratio is 6 dB and the carrier-to-jammer ratio (CJR) is -15.7 dB. With an isolation of 27.3 dB the jammer power in the data bandwidth should be 11.6 dB below the signal. If this

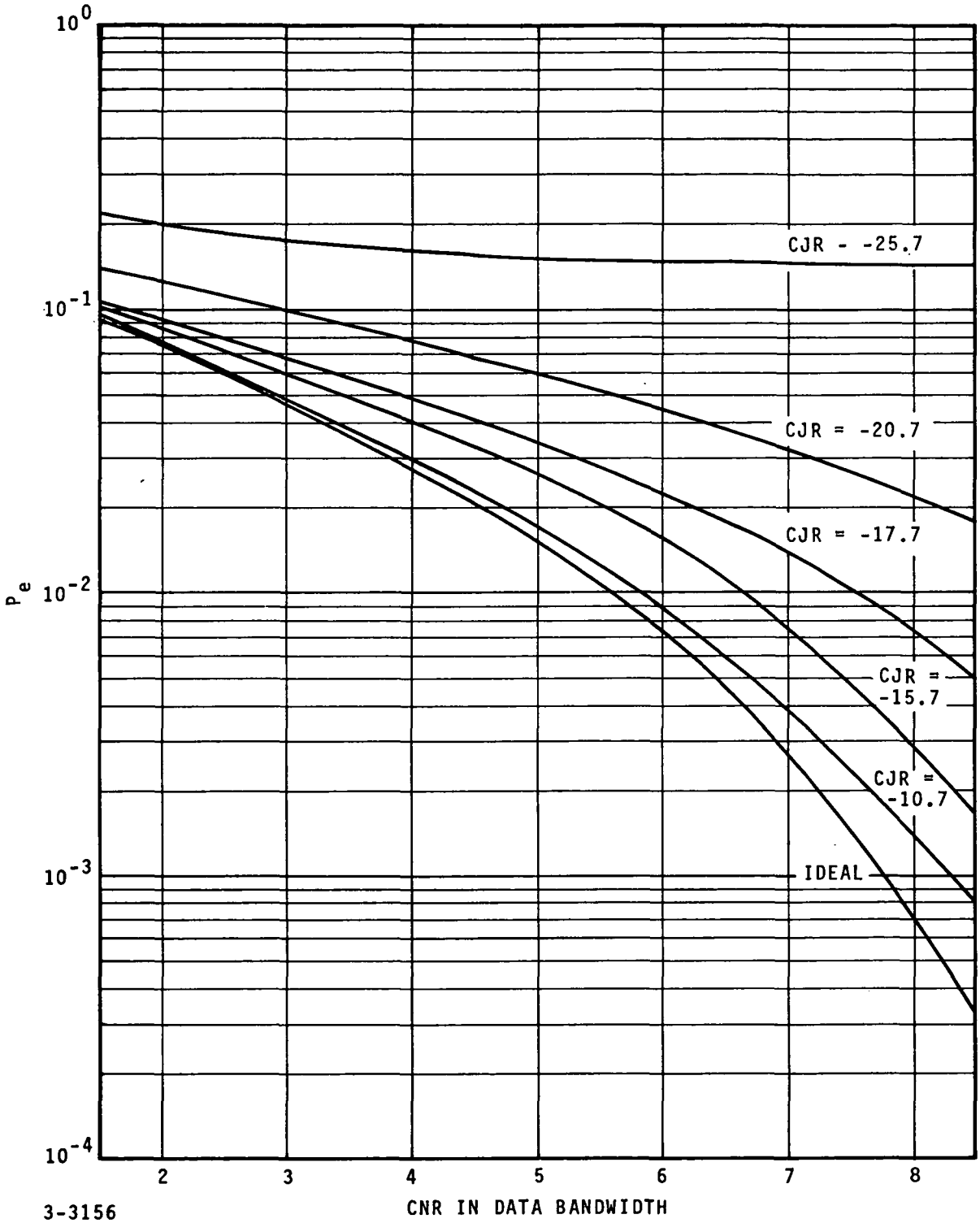

FIGURE C-10. ISOLATION BETWEEN CODES

amount of RF power is added directly to the noise power, the sum will be 4.95 dB below the carrier. It may be seen (Figure C-10) that the error rate corresponding to a CNR of 4.95 dB is the same as that measured for a -15.7-dB CJR and a 6-dB CNR.

Figure C-11 is an extrapolated version of Figure C-10. The end points of the -25.7-dB and -20.7-dB curves were measured with no noise present.

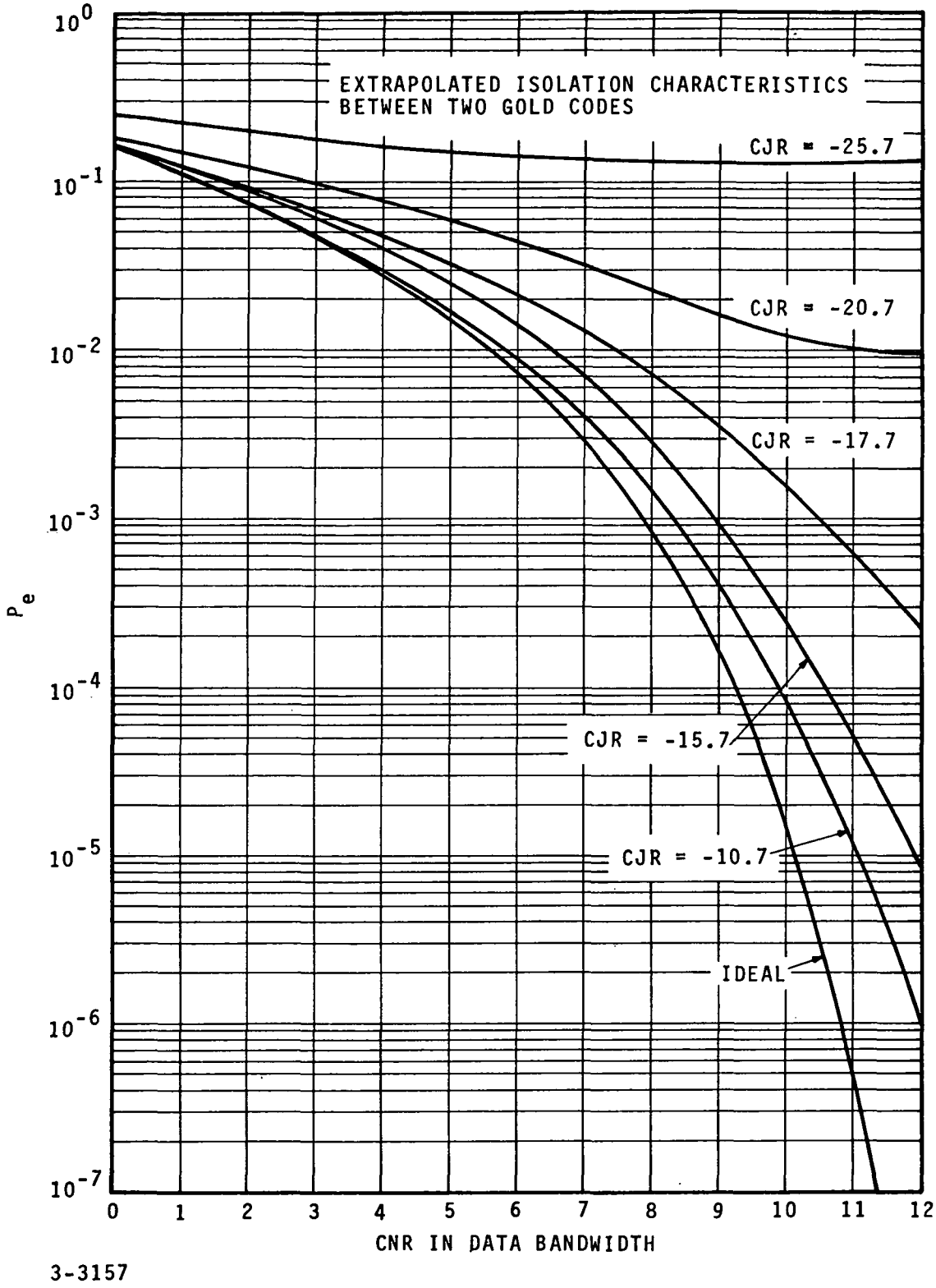

FIGURE C-11. EXTRAPOLATED CURVES OF FIGURE C-10